ISSN 2667-9787
ISSN 2720-8087 (online)
Reviewed Scientific Journal

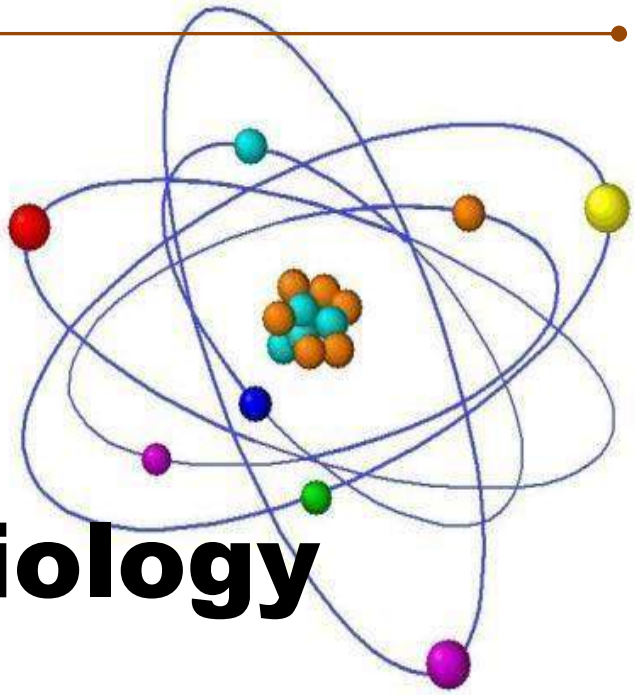

# Radiobiology and Radiation safety

The journal "Radiobiology and Radiation Safety" publishes scientific articles reflecting the results of studies of radiation and nuclear effects and various issues related to radiation safety problems

Vol.3,№4
2023

**Editorial office:** 14 Levan Gotua St, Rooms-913; 931, Tbilisi, Georgia, 0160

**Tel:** (+995) 032 237-03-00/911

**E-mail:** radiobiologia2020@gmail.com

**Website:**https://radiobiology.ge

# TABLE OF CONTENTS

# GAMMA-IRRADIATION INDUCES THE NUCLEAR AND NUCLEOLAR CHANGES IN PLANT MERISTEMATICCELLS: AN ULTRASTRUCTURAL AND OPTICAL TOMOGRAPHY APPROACHES

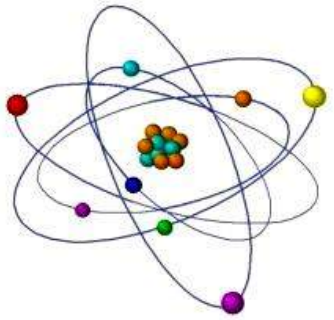

**[1]Tchelidze P., [2]Ivanishvili N*.,[2]Gogebashvili M.**

[1] Carl Zeiss Education and Scientific Center, New Vision University, Georgia
[2] I. BeritashviliCenter of Experimental Medicine, Laboratory of Radiation Safety Problems,Georgia

*Corresponding author: nazikoivanishvili@gmail.com

ABSTRACT: *The ultrastructural analysis combined with optical tomographic approach performed by means of serial semithin sections has been utilized to study 3D nuclear and nucleolar changes induced by acute γ-radiation of onion (Alllium cepa L.) root tips. To discriminate dose-dependent nuclear/nucleolar reaction at the photonic and electron microscope levels we utilized medium (2.5 Gy) and high (5.0 Gy) doses of irradiation. .$^{137}$Cs was used as a source of γ-radiation. Our results are indicative to profound micro- and ultrastructural changes related to morphological signs of the radiation induced inhibition of entire nuclear/cell metabolism. Therefore, the nucleolar reaction fits perfectly all requests to be served as reliable criterion of plant cells and tissues functional state in postradiation period. Additionally, the intensity of developing postradiation nuclear/nucleolar damages correlates with the dose impact. Most likely these alterations are strictly doze-dependent.*

**Key words:** γ-radiation, plant cell, nuclear and nucleolar changes

INTRODUCTION The problem of the anthropogenic load on biosystem is assumed to be the key issue of the environmental deteriorations. In living organisms, the radiation induced cellular disorders are the most dangerous. Therefore, there is an acute need forreliablemorphological criteriato dismantle the radiation pathologies in cells and tissues. Traditionally the cell nucleus is considered as the most radiosensitive cellular site due to: i) its large size, and ii) localization of genetic material, while its precisely arranged spatial structure is highly sensitive to overall functional disturbances [1]. In this context the specific (chromonemal) organization of a plant cell nucleus presents especially interesting link between structure, functional activity and restoration capacity of the irradiated cell and tissue.

Importantly, that among morphological features of plant nucleus the large sizes of nucleolus, caused by extremely high dose of ribosomal genes as well as its peculiar ultrastructure depicts itself as rather attractive [2-14]. The nucleolus is a highly dynamic compartment inside the non-random 3D architecture of the cell nucleuswith key function of ribosome biogenesis. Posed as a derivate of the chromosomal nucleolus organizer regions (NORs) the interphase nucleolus in plant [3-15] and animal [15-32] objects appears in light and electron microscopes in form of the most prominent/largest and complex nuclear component. It's well documented that nucleolar micro- and ultrastructure reflect post-mitotic spatial distribution of three major processes involved in ribosome biogenesis, i.e. transcription of ribosomal genes (r-genes), processing of newly synthesized rRNA (pre-rRNA) and assembling of preribosomal particles [16, 17, 19-31]. The nucleolus emerges as a result of compact folding of active r-genes into the structure ranging from one to several micrometers. As a consequence, rRNA synthesis and processing/assembling machineries acquire the strict territorial pattern in the form of five sub-compartments or nucleolar components (NCs). Thusthree basic NCs,

i.e. fibrillar centres (FCs), together with r-gene expression products in the form of dense fibrillar component (DFC) and granular component(GC)are regularly seen in animal and plant objects. Meanwhile, transcriptionally active nucleolar DNA adopts by folding into FCs non-nucleosomal conformation, the inactive part retains nucleosomal organization. Correspondingly, the nucleolus also contains nucleolus-associated DNA domains (naDNA) or intra- and peri-nucleolar condensed chromatin (ICC and PCC, respectively) linked to interstices or nucleolar vacuoles (NV). Furthermore, DFC and GC correspond to early and late processing subcompartments [16-31].

The sensitive nuclear response to changes in ribosomal genes r-genes activity could be of particular interest. Because the function of ribosomal r-genes is ultrastructurally embodied into specific nucleolar organization its changes offer a key to the visualization of their r-genes expression *in situ* [3, 15, 17, 19, 22, 23, 27, 30, 31]. Therefore, the ultrastructure of the nucleolus in highly proliferative plant tissues in response to the less studied action of physical factors (radiation, in particular) looks like very prospective. Hence, the value of the electron microscope (EM) visualization of radiation-induced nuclear/nucleolar damages is obviously high. Indeed, the functional state of the whole cell metabolism that directly depends on the ribosome biogenesis level in postraditionaly damaged plant cell could be easily traced according ultrastructural changes of the prominent nucleolar organization.

Here we propose a plant model focused on the dose-dependent spatial nuclear/nucleolar changes in radiation damaged meristematic cells (*Alllium cepa L.*) root tip. Since the activity of r-genes and related molecular events linked to the ribosome biogenesis is morphologically expressed in quantitative parameters and topography of NCs their rearrangement has been studied in the course of inhibitory effect of the acute γ-radiation. In order to demonstrate 3D nuclear/nucleolar reaction at the resolution of light microscope (LM) we addressed to the optical tomography (8) using 1μm serial semithin sections.

## MATERIAL AND METHODS

For onion bulbs irradiation the following technique has been applied. The meristem cells of 1cm onionroot tip has been used as an object for LM and EM observations. Before irradiation, the water sprouted onion bulbs were incubated at the room temperature for 24h. The exposure of plants to γ-irradiation was performed by means of “Gamma-capsule” apparatus, equipped with a holder for $^{137}Cs$ as a source of γ-rays and producing 1.2 Gy/min. The samples were treated within the appropriate time period in order to reach 2.5 Gy and 5.0 Gy doses. Then bulbs were kept growing at the same conditions for additional 24h before fixation. The same zones of normal and irradiated root type meristeme have been used in further LM and EM examinations. Plant tissue processing for EM (fixation, dehydration and embedding) was carried out according to routine technique. The fixation procedures were done at 4°C, whereas the dehydration and impregnation were performed at room temperature. For fixation, onion root tips were immersed in 2.5% glutaraldehyde (Merck, USA) diluted in PBS (Gibco, USA). Then the tissue samples were postfixed with 2% $OsO_4$ (Merck) solution diluted in the same buffer. Both, fixation and postfixation were performed for 24h. After dehydration in gradual series of acetone (Merck) and impregnation with acetone and Epon 812 (Embed Kit, EMS) mixture tissue samples were embedded in Epon and polymerized at 60°C for 48h. Tissue blocks were sectioned using glass knives and “Reichert-Young Ultracut” ultramicrotome. Ultrathin sections were counterstained by conventional contrasting procedure using lead citrate by staining sections mounted on Maxtaform Mesh 200 copper grids. Contrasted ultrathin sections were observed and registered with “Hitachi 300” (Japan) EM.

The optical tomography has been performed using 50-100 serial semithin sections (1μm

thick) placed onto polylysin-coated Super Frost slides (Menzel Glasser, USA). The following conditions allow the proper serial sectioning as well as the collection of series on the slide (28). First of all, it is necessary to trim under low magnification of ultramicrotome stereomicroscope the epoxy resin block to obtain the appropriate size of a pyramid and produce ~1x1 mm sections, so that cross sectioned root tip must be completely positioned within the section plane. Moreover, it is necessary to change the knife as often as it possible, in order to prevent scratches as well as other damages usually produced by a glass knife. In order to avoid sticking of section to the knife edge we used high speed cutting mode.Right after producing short series or single section that float in knife bath ribbons of 2-4 serial sections as well as separated single sections can be easily picked-up and than transfered (grouped or one by one) to the slide surface using Magic Loop (EMS, USA). Under low magnification microscope control the series of semithin sections could be accurately mounted on slides. Importantly, that the working surface of pick-up loop must be rinsedin 96% alcohol every time before use. To maintain precise serial consequence the cutting must be stopped after a suitable number of sections have been accumulated in the bath in the form of short ribbon or single sections. In this way each slide can be covered by the more or less oriented rows consisting of 10-20 semithin sections. In order to follow precisely the serie we have numberd each section right after they have been placed on the slide and dried. To perform this, firstly we checked in phase contrast microscope whether serial sections were arranged and labeled in proper way using super fine permanent pen. After drying sections became firmly attached to the polylysin-coated glass surface, that allows their further staining with commercial (ready to use) 1% aqueous solution of Toluidine Blue (EMS, USA). Following extensive washing with water or differentiation using $70^0$ ethanol can be also safely performed due to firm adhesion of sections to the polylysin coat.

After the staining the serial semithin sections were examined and imaged in 512x512 pxl format using Carl Zeiss Axiolab Microscope. Under low magnification the suitable zones have been selected for further imaging and 3D reconstruction. The contrast and the brightness of the recorded images were finally adjusted by means of ImageJ software. For 3D reconstruction and modelling of onion root tip meristeamatic cells the basic method described by Chelidze and coauthors [19] has been used. The contours of the cell, nucleus and nucleolus were outlined directly on the screen of PC monitor using digitizer, and then “extracted” from entire images. The resulting files were exported to “AutoCAD” (AutoDesk, USA) software, and the contours of cell, nucleus and nucleolus were matched by color gradation, with following layer-by-layer assembling and triangulation of primary volumes. At the final stage the reconstructed volumes were rendered and rotated using “3D Studio Max” (AutoDesk, USA) software in order to select most appropriate foreshortenings of resulted 3D models.

## RESULTS

The following EM images (Fig. 1) visualize nuclear and nucleolar morphology in control cells. On random sections nuclei display all ultrastructural characteristics that are common for many plant species, including onion root tip meristematic cells [4-14]. Nuclei appear as having smooth, round-shaped contours of nuclear membrane and typical for plants chromonemic organization of chromatin. Large nucleoli are prominent not only because their big sizes but also due to extremely dense package of NCs. They are positioned in central or close to central regions within the nuclear volume and can reach reach up to 4-6 μm in diameter. At low magnifications it is clearly visible that nucleolus usually occupies nearly two thirds of nuclear volume. According ultrustructural composition nucleoli of onion root tip meristematic cells may be related to highly active group of compact nucleoli, characterized by

complete absence of reticular network or nucleolonema, and tight package of DFC and GC specifically organized to yield the "core-cortex" composition (Fig. 1, d,e; see also 15) In similar manner, compact nucleoli presented in the object under the test exhibit the predominance of GC that indicates the intensive production of pre-ribosomal particles. Indeed, in all our samples GC was especially well developed (Fig. 1, d,e). Typically for compact nucleoli, GC was localized on the nucleolar periphery while the DFC occupied central region of the nucleolus. Importantly, that to one more specific feature of plant cell the permanent presence within the nucleolus of profound light zones could be attributed. These light intranucleolar zones are clearly visible even at low magnifications (Fig. 1; arrows). One can identify mentioned light zones as FCs (Fig. 1, a-e; arrows) or nucleolar vacuoles (Fig.1, c; upper nucleolus). Since the fibrillar network of FC is made up by undercondensedrDNP clusters with non-nucleosomal conformation the pale staining interior of FC is sharp contrast with the condensed nucleosomal chromatin inside relatively small intersticies or large NVs. Hence, light zones we observed in onion root tip can be definitely attributed to FCs due to less condensed package of the DNP fibrils. Meanwhile, the small discrete foci or more elongated and twisted fibers of condensed chromatin are especially well distinguishable within FCs due to their sharp contrast against light, fibrillar background constituted of ~10 nm fibrils with homogenous appearance. These, so called heterogenous FCs (hFC) according Medina and coauthors (4, 9, 10; see Fig. 1, d,e) are also among the most specific nucleolar features described in plant cells, while no evidences exist in regard to presence of hFC in animal objects.

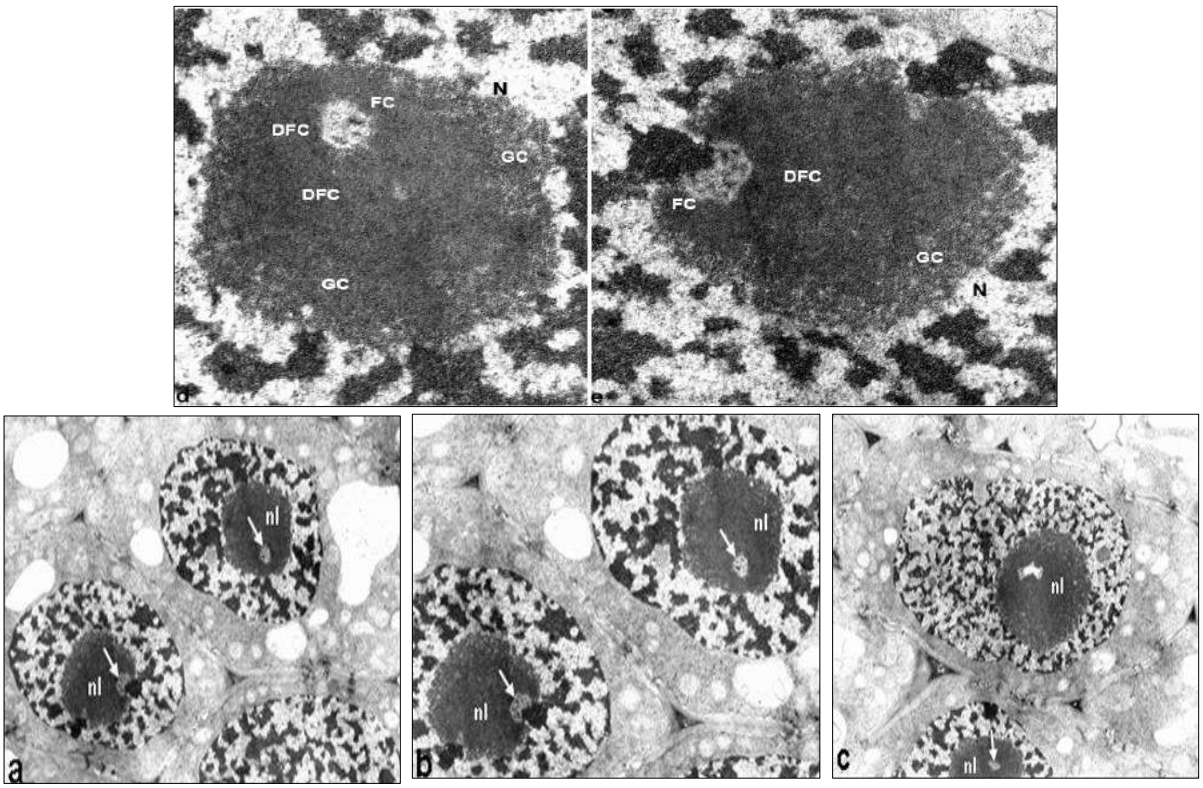


**Fig.1. Ultrastructural organization of the normal meristematic cell from onion root tip. Note the large compact with well recognizable FC (arrows). At higher magnification the DFC and GC are organized in "core-cortex" fashion. Magnifications: a – 6.000; b – 8.500; c – 7.300; d,e – 20.000**

3D models demonstrating the overall spatial organization of the reconstructed whole cell as well as nuclear/nucleolar volumes in control meristematic cell of onion root tip are displayed on Fig.2 Rotation and tilting of models at different angles reveals strongly polygonal cellular borderlines (Fig.

2,a,b) whereas nucleus is characterized by elliptical shape with smooth surface. As it was alreadymentioned the smooth nuclear outlines were presumed by analysis of random ultrathin section, being finally reproduced by means of 3D models (Fig. 2,c-f). In addition, analyzing 3D models by rotation and tilting it became obvious that large nucleolus takes nearly one third of the nuclear volume.

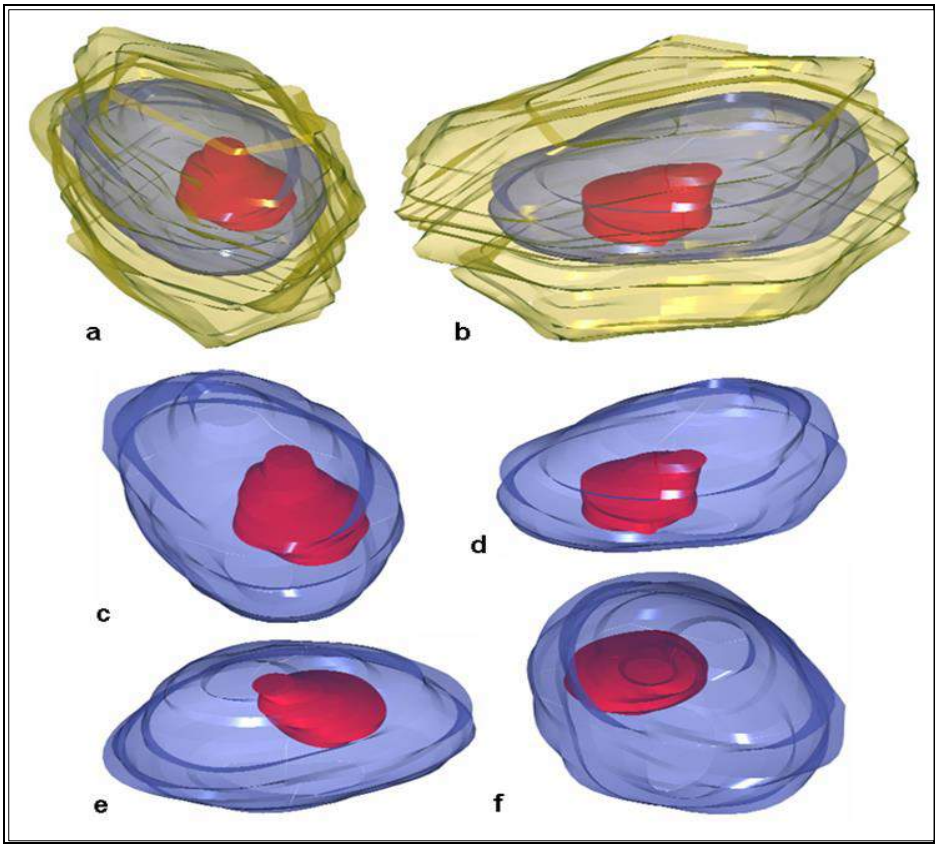


**Fig.2. 3-D models demonstrating the global organization of onion root top meristematic cell as revealed by the optical tomography. Note the polygonal shape of the meristematic cell. Nucleolus occupies around one third of nuclear volume.**

Exposure of root meristematic cells to the dose of 2.5 Gy provokes drastic ultrustructural reorganization in the global intracellular arrangement. Thus after 24h of irradiation, significant damages were observed, which are more distinctly reflected in the ultrastructure of nucleus and nucleolus (fig. 3). In fact, these changes cover all meristematic cells we have investigated. Obviously, such an influence leads to dramatic cessation of r-genes expression that is distinguished by the morphological alterations of the nucleolus known as nucleolar segregation (3, 17,24, 30-32). Within observed postradiational period nucleoli shift to the nuclear periphery and their sizes decrease sharply (Fig. 3). On the EM images they look like very dense and round-shaped bodies 1-1.5 μm in diameter which are almost completely consisted of DFC which is sharply delineated from the FCs (Fig. 3, a) while territories occupied by GC are visibly reduced. Thus on Fig. 3, a, it became clear that territories occupied by GC are visibly reduced that witnessed of rRNA processing cessation or even blockage. At the same time GC was also clearly separated from DFC. Usually, FCs are localized on nucleolar periphery and contact with the blocks of peri-membrane condensed chromatin blocks (Fig. 3, a,b). Moreover, meristematic cell response to radiation is also evidenced by changes of nuclear envelope. At the low magnification it was clearly visible that nuclei lose their regular round contours while the nuclear envelope permanently revealing quite deep invaginations (Fig. 3, b).

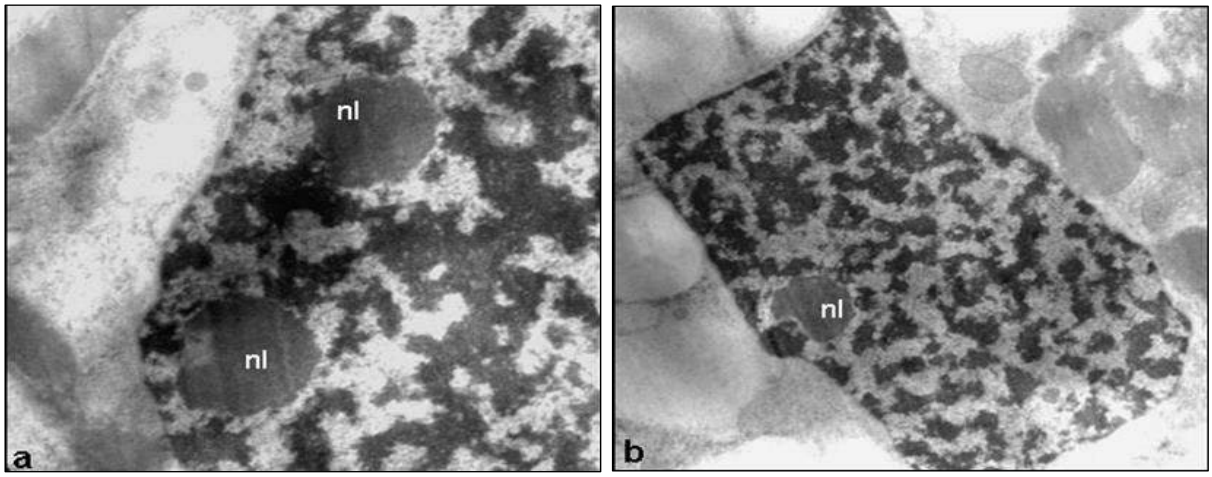


**Fig. 3. Segregated nucleoli (Fig. 3,a) appeared as a result of the exposure of onion root tip cells atthe dose of 2.5 Gy. Note the drastic nuclear deformation on Fig 3,b. Magnifications: a – 16.000; b – 12.000.**

All these ultrastructural peculiarities which certainly are indicative to the effect of radiation were well pronounced on corresponding 3D models (Fig.4). First of all, deep deformations of the cell wall arose as consequence of irradiation making cellular borderlines largely irregular (Fig. 4, a-c). At appropriate angles the profound deformations of nuclei could be distinctly visualized by rotation and tilting of corresponding 3D models (Fig. 4, d-f). Moreover, such approach made it largely clear that nucleolar territory is dramatically reduced and nucleoli are shifted toward the nuclear envelope.

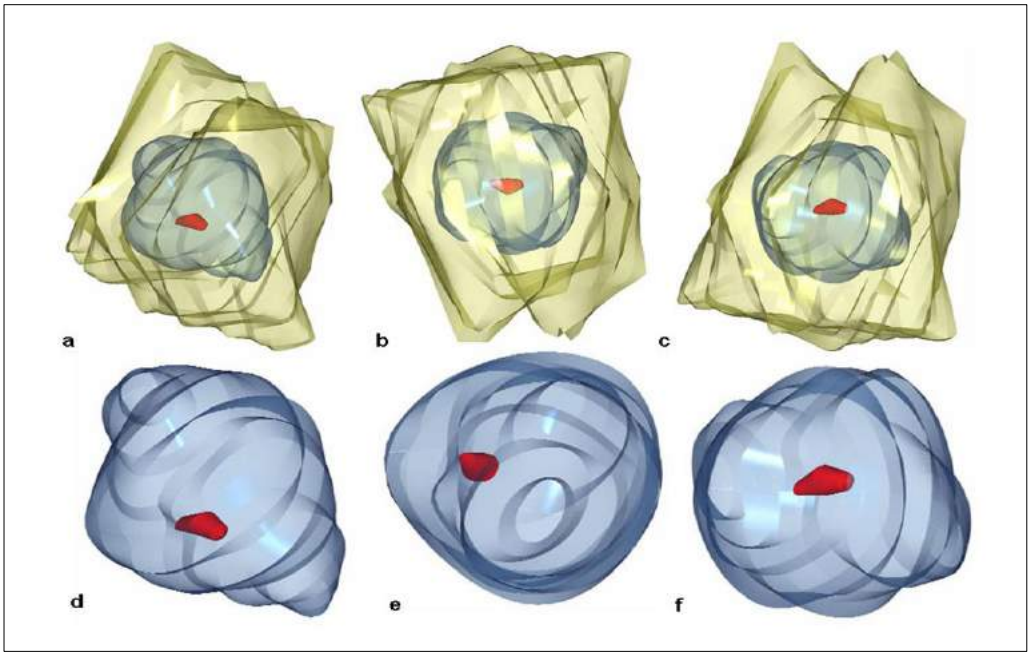


**Fig. 4. The deep structural changes e.g. cellular and nuclear deformations are clearly visible during rotation of 3-D models. Nucleolar volume reduces dramatically wile the nucleolus is localized in the peripheral regions of nucleus.**

In parallel to the dose enhancement the strong destructive events are observed in majority of meristematic cells. Thus by the treatment of onion roots at a doze of 5.0 Gy morphological signs of nuclear inactivation became much more pronounced (Fig. 5, a-c). For example, the most strictly depicted changes were regarded to the deep nuclear disorganization that was revealed on EM images

as peculiar deformation causing strange shape of nuclei (Fig. 5, c). Beside nuclear pathologies the intensive structural changes of nucleoli that are extremely "non-canonic" were also obvious. Also, the extensive decrease in number of nucleoli containing more or less evident FCs has been noticed. In contrast, the great number of irradiated cells reveals instead FCs the large blocks of intranucleolar condensed chromatin (Fig. 5, a,b).

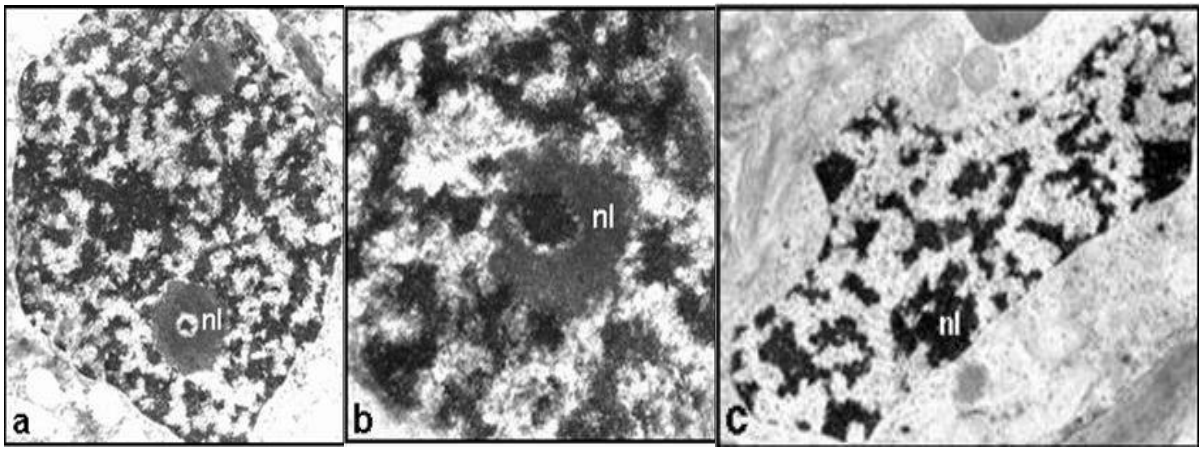


**Fig. 5. Peculiar structural alterations arose in onion root tip meristem after exposure of plants at the dose of 5.0 Gy. Note massive blocks of condensed chromatin within the nucleoli (Fig. 5, a,b). Fig. 5,c demonstrates the extremely deformed nucleus with peculiar shape. Magnifications: a – 12.000; b – 18.500.**

On the other hand, the nucleoli with clearly expressed and typical heterogeneous FCs are rare. All cellular as well as nuclear and nucleolar pathologies described in objects that were irradiated by high dose were more demonstrable when we utilized the option allowing the rotation of 3D models (Fig. 6).

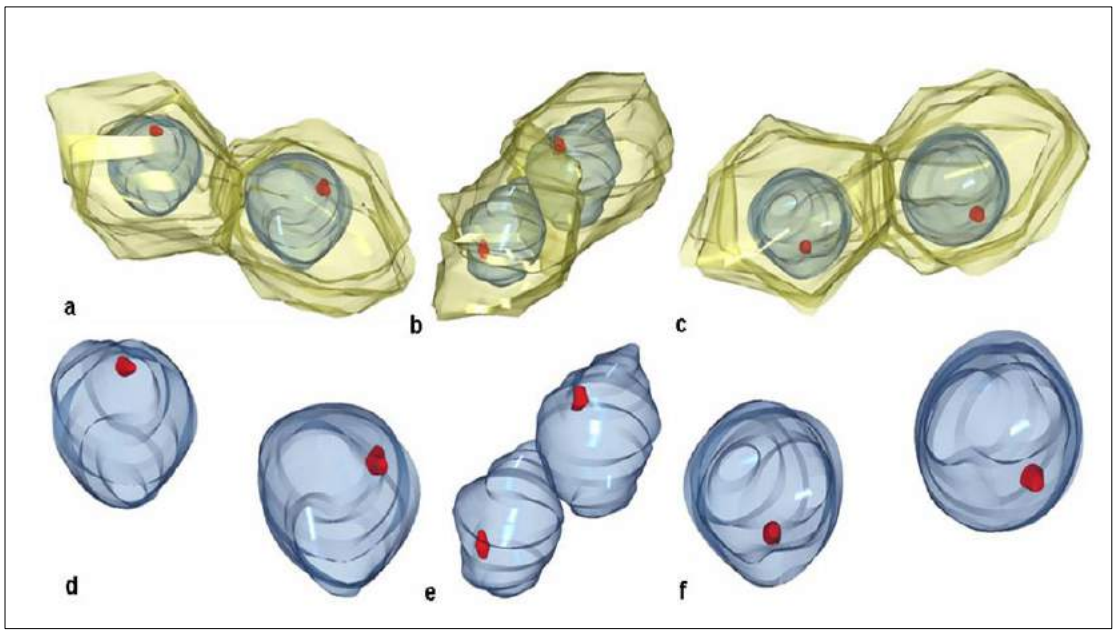


**Fig. 6. Rotation of 3-D models makes cellular and nuclear damages clearly visible. Note the cellular and nuclear deformations at the angles presented in Fig. 6,b and Fig.6,e. Nucleoli are reduced in size and shifted to the nuclear periphery.**

DISCUSSION

For many years, the nucleolus has appeared as a paradigm for the study of molecular and structural organization of active genes, of their transcription and of their processing. To understand how the different players of the transcriptional and processing nanomachineries are organized within NCs, many efforts have been devoted to the analysis of the nucleolus within living or fixed cells in animal and/or plant objects by using cellular imaging [20, 21, 27, 30-38]. Therefore, over the past 25 years the nucleolus has become recognised as the unique model to study the spatial organization of actively transcribing mammalian genes in functional and dynamic association with overall structure and metabolism of interphase cell.

The precondition for current investigation was the ability of FCs and DFC to move and fuse within a crowded nucleolar volume, revealed by classical EM studies on artificial inactivation of r-genes including the experiments where Actinomycin D (AmD) was first used as a chemical inhibitor of nucleolar processes [39, 40]. Since these experiments up to now AmD has been acknowledged the best studied, RNA polymerase I inhibitor inducing typical rearrangement of NCs, known as nucleolar segregation [30-33]. Corresponding ultrastructural changes of the nucleolus and linked inactivation dynamics under influence of chemical inhibitors were extensively documented in mammalian and human cells. However, same issues were less broadly studied in plant objects. By contrast, it is still unknown how physical factors, such as temperature, electromagnetic and γ-irradiation etc., considered as potential inhibitory agents disturbing the cellular metabolism by interfering with giant array of r-gene sequences will be reflected in 3D nuclear/nucleolar structural hierarchy. Meanwhile, it remains much more problematic to realize, which molecular as well as nano- and ultrastructural mechanism underlying territorial rearrangement of nuclear domains induced by physical factors. In respect to the influence upon any living systems γ-irradiation represents the most dangerous and quite realistic treat among all physical factors produced by the modern technological world.

Our hypothesis was based on presumption that during inhibitory action of γ-irradiation on r-genes level the dynamics of NCs rearrangement may develop via same mechanism as those caused by chemical inhibitors, thus yielding classical pattern of the nucleolar segregation. Correspondingly, we consider rapidly proliferating meristematic plant cells which nucleoli comprise high dose of r-genes, reflected in extremely big nucleolar size, as reliable experimental target. Accordingly, to address the γ-irradiation induced ultrastructural reorganization of the nucleus and nucleolus, we focused on postradiation displacement/spatial redistribution as well as ultrastructural appearance of FCs, DFC and ICC, being resorted to two complementary approaches. To identify the NCs and specify their rearrangement within the composition of normal and altered plant nucleoli we firstly applied conventional EM analysis. Secondly, to follow the changes in shape and sizes as well as spatial displacements of nuclei and nucleoli within cellular and nuclear volumes, respectively we resorted to 3D reconstruction using LM images obtained on serial semithin sections. These approaches allowed us to demonstrate precisely both the postradiation reshuffling of NCs in the form of non-canonic nucleolar segregation andintranuclear movement of the nucleolus inside nuclear volume. Undoubtedly, the results obtained are indicative to specific changes which are related to morphological signs of the radiation induced inhibition of entire cell metabolism. Hence, the responses of extremely sensitive nanostructural machineries involved in ribosome biogenesis are of particular importance. In fact, the nuleolar reaction fits perfectly all requests to be served as adequate criterion of plant cells and tissues functional state in prostradiation period. It is important to underline that intensity of developing postradiational nuclear/nucleolar damages correlates with the dose impact. Therefore, these alterations are certainly doze-dependent whereas general ultrastructural appearance after irradiation is indicative

of inhibited cell in which both nuclear processes and nuclear r-genes activity were artificially ceased or arrested.

Importantly, that current findings open exciting rout to analogous experiments in animal cells and tissues. Thus interpreting specific nucleolar reaction visualized in our plant object it's important to be reassured regarding specific character of the nucleolar reaction. Indeed, because of quite profound differences in ultrastructural appearance between the segregated nucleolus of irradiated plant cells and those in chemically inhibited animal objects, it's still hard to say whether peculliary altered ultrastructure observed in our experiments should be attributed to the specific postradiation reaction of the r-genes machineries. Definitely, in order to answer the question whether postradiation changes defined in plant meristematic cells are of universal character, next experimental series should be aimed on animal cells and tissues. Such an approach will help us to clarify if physical factors will produce in animal cell changes similar to the nucleolar reaction of the plant meristem or postradiation damage of r-genes will generate classical segregation of NCs.

As it was mentioned above one more specific expression of the nucleolar reaction was increase of chromatin condensation inside heterogeneous FCs. Arguably, heterogeneous FCs may occur as a result of condensation of ribosomal chromatin inside FCs (or on their periphery), that gives the rise to nucleosomal structure of inactivated part of rDNP-fibers**.** Most probably at high irradiation doses the further inactivation of r-chromatin takes place, resulting in massive condensation of rDNP fibrils. Nevertheless, all above described nucleolar changes are well known from literature and unambiguously indicate the inactivation of rRNA genes transcription and ribosome biogenesis.

In conclusion, we would emphasize: it's quite possible that cellular, nuclear and nucleolar changes visualized here, may be considered as specific morphological properties of postradiation death. Hence, functioning of r-genes and linked nucleolar modifications in postradiation conditions increasingly deserves further investigations.

REFERENCES

[1]. Jean-Pierre Pouget. Basics of radiobiology. Nuclear Medicine and Molecular Imaging, 2022, Volume 1 (Cover date: 2022), Pages 30-51

[2]. Long, E. O. & David I. B. (1980). Repeated genes in euckariotes. Ann Rev Biochem, 49, 727-764.

[3]. Hadjiolov, A. (1985) The Nucleolus and ribosome biogenesis, in Cell Biology Monographs (Alfert, M., Beerman, W. and Goldstein, L. ed.), Springer –Verlag, Wien, New York, pp. 1-263.

[4]. Risueno, M. C. & Medina, F. J. (1986). The nucleolar structure in plant cells. *Revis Biol Cell*, 7, 1-154.

[5]. Motte, P., Deltour, R., Mosen, H. &Bronchart R. (1988). Three-dimensional electron microscopy of the nucleolus and nucleolus-associated chromatin (NAC) during early germination of Zea mays L. *Biol Cell*, 62, 65-81.

[6]. Highett, M. J., Rawlins, D. J. & Shaw, P. J. (1993) Different patterns of DNA distribution in Pisum sativum nucleoli correlate with different levels of nucleolar activity. *J. Cell Sci*, 1993, 104, 843-852.

[7]. Shaw, P. J., Boven, A. F., Wells, B., Highett, M. J. & Jordan, E. G. (1996). The organization of nucleolar activity in plants. *J. Microsc*, 181, 178-185.

[8]. Rawlins, D. J. & Shaw, P. J. (1999). Three-dimensional organization of ribosomal DNA in interphase nuclei of Pisum sativum by in situ hybridization and optical tomography. *Chromosoma*. 99, 143-151.

[9]. Medina, F. J., Cerdido, A. & de Carcer G. (2000). The functional organization of the nucleolus in proliferating plant cells. *Eur J. Histochem*, 44, 117-131.

[10]. Saez-Vasques, J. & Medina, F. J. (2008). The plant nucleolus. *Adv Bot Res*, 47-1-46.

[11]. Shang, G, Wang, F, Hao, S. & Jiao, M. (2009). Dynamic changes of nucleolar DNA configuration and distribution during the cell cycle in Allium sativum cells. *Micron*, 449-454.

[12]. Kim S. H. (2009). Plant nucleolar dynamics. *J. Plant Biol*, 52, 193-201.

[13]. Stepinski, D. (2010). Organization of the nucleoli of soybean root meristematic cells at different states of their activity. *Micron*, 41, 283-288.

[14]. Stepinski, D. (2014). Functional ultrastructure of the plant nucleolus. *Protoplasm*, 251, 1285-1306.

[15]. Chelidze, P. & Zatsepina, O. (1988). Morphofunctional classification of the Nucleolus. *UspehiSovr. Biologii,* 105**,** 252-268 (in Russian).

[16]. Sheer, U. &Weisenberger, D. (1994). The nucleolus. *CurrOpin Cell Biol*, 6, 354-359.

[17]. Thiry, M. &Goessens, G. (1996). The nucleolus during the cell cycle, in *Molecular Biology Intelligence Unit* (Landes R.G ed.). Springer-Verlag, Heidelberg, 1-144

[18]. Heliot, L., Kaplan H., Lucas L., Klein C., Beorchia, A., Doco-Fenzy, M., Menager, M., Thiry, M., O'Donohue, M.F. &Ploton, D. (1997). Electron tomography of metaphase nucleolar organizers regions: Evidence for a twisted-loop organization. *Mol Biol Cell***,** 8, 2199-2216.

[19]. Chelidze, P., Dzidziguri, D. &Tumanishvili, G. (1998). Increased Functional Load on Mouse Kidney Proximal Tubule Epithelial Cells Causes Changes in Nucleolar 3-D Architecture. *J. Cell and Tissue Res,* 292,411-426.

[20]. Scheer, U. & Hock, R. (1999). Structure and function of the nucleolus. *CurrOpin Cell Biol*, 11, 385-390.

[21]. Cheutin, Th., O'Donohue, M.-F., Beorchia, A., Vandelaer, M., Kaplan, H., Defever, B., Ploton, D. &Thiry, M. (2002). Three-dimensional organization of active rRNA genes within the nucleolus. *J. Cell Sci*, 115, 3297-3307.

[22]. Cheutin, T., Misteli, T., and Dundr, M. (2003). Dynamics of nucleolar components, in *The Nucleolus* (Olson, M.O., ed.), Plenum Publesher, pp. 44-57.

[23]. Mosgoeller, W. (2003). Nucleolar ultrastructure in vertebrates, In: *Nucleolus* (Olson, M.O., ed.), Plenum Publesher, pp. 1-11.

[24]. Ploton, D.,O'Donohue, M.-F., Cheutin, T. &Thiry, M. (2004). Three-dimensional organization of rDNA and transcription. In: *Nucleolus* (Olson, M.O., ed.), Landes Bioscience, 154-169.

[25]. Misteli, T. (2005). Concepts in nucleolar architecture. *BioEssays*, 27, 477-487.

[26]. Thiry, M. and Lafontaine, D.L. (2005). Birth of a nucleolus: The evolution of Nnucleolar compartments. *Trends Cell Biol*, 54, 194-199.

[27]. Derenzini, M., Pasquinelli, G., O'Donohue, M.-F., Ploton, D. &Thiry, M. (2006). Structural and functional organization of ribosomal genes within mammalian cell nucleolus. *J. Histochem Cytochem*, 54, 131-145.

[28]. Tchelidze, P., Kaplan, H., Beorchia, A., O'Donohue, M.-F., Bobichon, H., Lalun, N., Wortham, L., Ploton, D. (2008). Three-Dimensional Reconstruction of Nuclear Components by Electron Microscope Tomography. *In: Methods in Cell Molecular Biology (R. Hanckock ed*.), 436, 137-158.

[29]. Tchelidze, P., Chatron-Colliet, A., Thiry, M., Lalun, N., Bobichon, H. &Ploton, D. (2009). Tomography of the cell nucleus using confocal microscopy and medium voltagwe electron microscopy. *Critical Reviews in Oncology/Hematology*,69,2, 127-143.

[30]. Tchelidze, P., Benaassarou, A., Kaplan, H., O'Donohue, M.-F., Lucas, L., Terryn, C., Rusishvili, L., Mosidze, G., Lalun, N. &Ploton D. (2017). Nucleolar sub-compartments in motion during rRNA synthesis inhibition: Contraction of nucleolar condensed chromatin and gathering of fibrillary centers are concomitant. PLoS ONE, 12, 1-37.

[31]. Michel, J., Nolin, F., Wortham, L., Lalun, N., Tchelidze, P., Banchet, V., Terryn, C. &Ploton, D. (2019). Various Nucleolar Stress Inducers Result in High Distinct Changes in Water, Dry Mass and Elemental Content in Cancerous Cell Compartments: Investigation Using Nano-Analytical Approach. Nanotheranostics, 2019, 3, 179-195.

[32]. Tchelidze, P., Kaplan, H., Terryn, C., Lalun N., Ploton, D. &Thiry, M. (2019). Electron Tomography Reveals Changes in Spatial Distribution of UBTF1 and UBTF2 Isoforms within Nucleolar Components during rRNA Synthesis Inhibition. Journal Struct Biol, 208, 1–23.

[33]. Shav-Tal, Y., Blechman, J., Darzacq, X., Montagna, C., Dye, BT. & Patton. J.G. (2005). Dynamic sorting of nuclearcomponents into distinct nucleolar caps during transcriptional inhibition. Mol Biol Cell, 2005, 16, 2395–2413.

[34]. Boisvert, F. M., van Koningsbruggen, S. N., Navascues, J. & Lamond A. I. (2007). The multifunctional nucleolus. Nat Rev Mol Cell Boil, 2007, 8, 574–585.

[35]. Sirri, V., Urcuqui-Inchima, S., Roussel, P. & Hernandez-Verdun, D. (2008). Nucleolus: the fascinating nuclear body. Histochem Cell Biol, 2008, 129, 13–31.

[36]. Pederson T. (2010). The nucleus introduced. Cold Spring HarbPerspect Biol, 2010, 10, 1–16.

[37]. Hernandez-Verdun, D, Roussel, P, Thiry, M, Sirri, V. & Lafontaine, D. (2010). The Nucleolus: structure/function rela-tionship in RNA metabolism. WIREs RNA, 2010, 1, 415–431.

[38]. Tafforeau, L, Zorbas, C, Langhendries, J. L., Mullineux, S.-T., Stamatopoulou, V. &Mullier, R. (2013). The complexity of human ribosome biogenesis revealed by systematic nucleolar screening of pre-rRNA processing factors. Molecular Cell, 2013, 51, 539–551.

[39]. Reynolds, R. C., Montgomery, P. O. & Hughes, B. (1964). Nucleolar "caps" produced by actinomycin D. Cancer Res, 1964, 24, 1269–1277.

[40]. Simard, R., Langelier, Y., Mandeville, R., Maestracci, N. & Royal, A. (1974). Inhibitors as tools in elucidating the struc-ture and function of the nucleus. In: Busch H, editor. The Cell Nucleus. New York: Academic Press, 1974, 447–487.

# GONADAL DYSGENESIS AS A MARKER OF GENOMIC INSTABILITY IN POPULATIONS OF *DROSOPHILA MELANOGASTER* FROM DIFFERENT OF RADIATION FACTOR IMPACT REGIONS OF UKRAINE

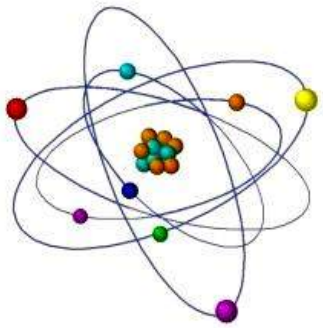

***Kravets A.P, Sokolova D.A.**

Institute of cell biology and genetic engineering of National Academy of Sciences, Ukraine

*Corresponding author: kaplibra@gmail.com

ABSTRACT: *To investigate the differences of the gonadal dysgenesis frequency as an indicator of the activation of mobile elements through natural populations of Drosophila melanogaster, selected from Ukrainian regions with different radiation impact. Follow-up study of the dynamics of this indicator under chronic exposure in laboratory conditions for 10 generations. The study was conducted in two stages. The first one included trapping of insects in regions with different radiation load with subsequent assessment of both the time of maturation and the index of the gonadal dysgenesis through the first (F1) generation, obtained in laboratory conditions. At the second stage, the dynamics of this indicator was investigated for the F1- descendants of each ten consequent generations, which were developed both with and without additional gamma-exposure. Differences of the gonadal dysgenesis frequency as an indicator of the activation of mobile elements were revealed in F1 - descendants of natural populations of Drosophila melanogaster, selected from regions of different radiation impact. Under conditions of additional low rate chronic irradiation in laboratory conditions for 10 generations, significant differences in changes in the level and dynamics of this indicator were established depending on the accumulated dose of Drosophila populations from the city of Netishyn (Khmelnytskyi NPP) and Magarach city. There were no signs of adaptation.*

*The discrepancy between the real and expected biological effects has reflected the difference in the intensity of the radiation background, which was traditionally determined by the gamma - emitters and did not take into account the wide range of other genotoxic elements from nuclear power emissions. A complex, non-monotonic type of frequency dynamics of gonadal dysgenesis could be determined by the interaction of radiation damage, protection and recovery.*

***Key words***: Drosophila melanogaster; radiation, gonadal dysgenesis, genomic instability

## INTRODUCTION

Genetic and radiobiological studies of the last decades have shown that the most important effect of radiation exposure with low intensity is the emergence of genomic instability and its transmission through generations. Forms of manifestation and distant consequences of genomic instability are equally diverse (structural reorganization of the genome, activation of mobile elements, developmental violations, oncological diseases) as well as difficult to predict [1,2,3,4,5,6,7]. This phenomenon is investigated on various experimental models and has already been identified by some key features: the possibility of transgenerational transmission, the non-clonality of genome disorders, that is the instability of the reaction, which is determined by many components.

Scientific developments have established significance and threat of the induced genomic instability, but with hygienic (anthropocentric) normalization, this phenomenon is not taken into account due to its insufficient research [8]. Environmental regulation, which only forms its own principles, does not consider this phenomenon at all. No less difficult to predict the effects of radiation exposure is to take

into account radioadaptation - a phenomenon that undoubtedly extends to a set of processes that lead to genomic instability. The study of the morbidity structure of the population in areas of high radiation background leads to the conclusion that low-intensity radiation exposure is dangerous only as a "new" environmental factor and has no serious consequences for human health as a constitutive component of the environment for many generations [9]. The limit between the "new" and the constitutive has not yet been established, but this phenomenon indicates the importance of radioadaptive processes and the need to develop approaches to study the speed of their formation and results.

Before the effects of genomic instability were understood as a radiobiological phenomenon, they were discovered and studied by geneticists. The mobile elements were found in maize in the late 40s as the part of the genome, which was able to cleave and re-integrate again into the genome. Then it was indicated that almost all organisms, including humans, have had this jumping part of the genome [10]. It is now well established that up to 80% of spontaneous mutations are associated with the activation of mobile elements [11]. Also, it is indicated, that various stress effects, including radiation, lead to the activation of mobile elements [10].

*Drosophila melanogaster* is the most genetically investigated object. This species is radioresistant ($LD_{50}$ =1228 Gy for adult males and 1250 Gy for adult females) and synanthropic, it constantly accompanies human. As in the other prokaryotic and eukaryotic organisms, the Drosophila genome contains mobile elements of various types, the activation of which is effected with the environmental factors, including radiation exposure [11, 12]. This leads to genomic instability and increasing yield of mutations. The activation of mobile elements from P-, hobo- and I- families causes an increase in the frequency of gonadal dysgenesis, i.e. atrophy of one or both gonads of *Drosophila melanogaster*.

The study is devoted to the investigation of the level and dynamics of the gonadal dysgenesis frequency as a marker of mobile elements' activation through natural populations of Drosophila from Ukrainian regions with different radiation impact with follow-up study of the dynamics of the index under low-rate chronic exposure in laboratory for 10 generations.

## MATERIAL AND METHOD

The research was conducted on the natural Drosophila populations caught in the settlements of Ukraine with different radiation exposure. The insects from Netishyn were caught in 2014. The populations from Magarach, Pyriatyn and Lubny were received in 2014 from the collection of Taras Shevchenko Kyiv National University (Kyiv, Ukraine). Data on the radiation situation in Netishyn were obtained from the official website of Khmelnytskyi NPP. At the time of selection, the dose rate was 0,10 μGy/h. Accumulated dose through generations was approximately 0,02 Gy. Magarach, Pyriatyn, Lubny are settlements that are not included into the permanent radiological control zone due to the lack of enterprises related to radionuclide emission. According to official data, these regions like the entire Khmelnytskyi region belong to the "green" zone, for which the radiation background is ≤ 10 μR/h.

At catching used attraction of individuals with a fruit smell, with the subsequent placement into the test tubes with a nutrient medium. The study was conducted in two stages. The first one included the assessment of both the time of maturation and the index of the gonadal dysgenesis (GD) through the first (F1) generation, obtained in laboratory conditions. At the second stage, the dynamics of this index was investigated for the F1- descendants of each ten consequent generations, which were developed under laboratory conditions both with and without additional gamma-exposure with tree variants of the dose rate.

Exposure conditions. The source of prolonged exposure was the vessel with a solution of $^{137}CsCl$ located in the center of the tripod, with concentric slits for fixing test tubes with flies. The report presents the results obtained under exposure with different dose rate $1{,}2 \cdot 10^{-8}$, $0{,}3 \cdot 10^{-8}$ and $0{,}12 \cdot 10^{-8}$

Gy/sec. The flies were in glass vessels of 50 ml, the volume of the nutrient medium was 10 ml. Chronic exposure was conducted for 10 generations under room temperature + 21- + 23 $^0$ C.

Assessment of the frequency of gonadal dysgenesis**.** Gonadal atrophy was assessed in 50 individuals of each sex obtained from exposed parents. Gonadal dysgenesis was considered 0 if both gonads were complete morphologically, as 1 (GD (1)) if one gonad was underdeveloped or absent, and 2 (GD (2)) if both gonads were reduced or absent. From 4 tubes were selected both 50 males and females and evaluated the frequency of gonadal dysgenesis for each population.

The percentage of gonadal dysgenesis was calculated by the formula:

$$\%GD = ½\%GD(1) + \%GD(2)$$

Significance of differences between variants of the experiment was evaluated by parametric Student's t-test at 0,05 significance level.

RESULTS AND DISCUSSION

Estimation of the level of gonadal dysgenesis in F1-generation of insects immediately after moving to laboratory conditions indicated a significant difference in the index between populations from different radiation zones of Ukraine. Both males and females from Netishyn population demonstrated a 10 - 12-fold increase in the level of dysgenesis compared to the same rate in the populations from "clean" regions (Fig. 1).

The maturation period estimation (age of the first clutch) of the first generation of insects after the moving to laboratory conditions showed a significant maturation slowdown through the individuals of the Netishyn population (Fig. 2). Thus, the first stage of the study shows a significant difference in such important vital indexes as the maturation time and the yield of gonadal dysgenesis through populations from both "clean" regions and under constant low-intensity radiation exposure.

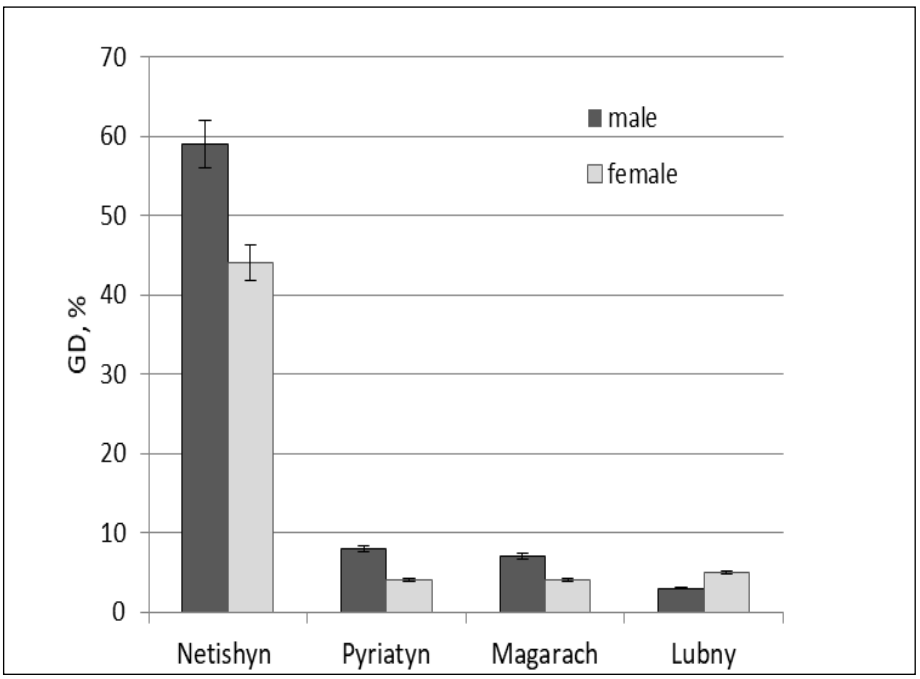


**Fig. 1. Initial gonadal dysgenesis (GD) yield through $F_1$-generation of populations from different regions of Ukraine**.

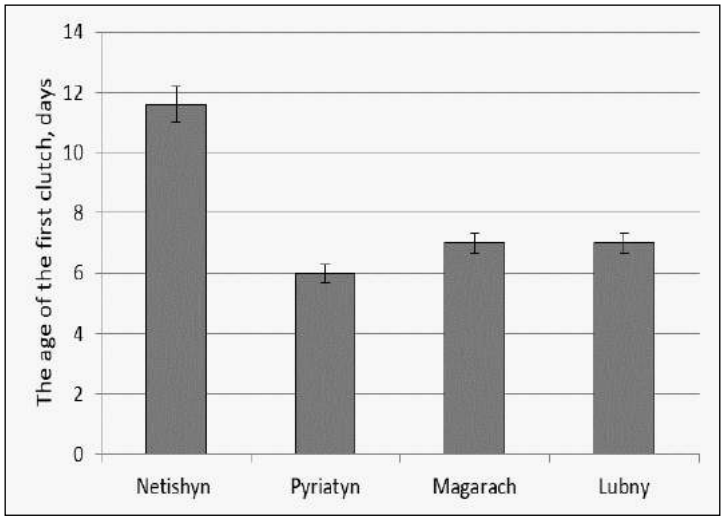


**Fig. 2. The age of the first clutch of the $F_1$- generation when moving individuals from different natural populations to laboratory conditions.**

The next study stage concerned the investigation of the GD dynamics through generations within populations from both areas with different radiation exposure without and with additional chronic gamma-exposure. Due to the technical limitations of the experiment, as well as the same level of both gonadal dysgenesis and maturation (Fig. 1, Fig. 2) within three populations from "pure" areas, in the second series of the experiment only Netishyn population and the population from Magarach were used. According to the data (Fig. 3) there is a big difference between the dynamic characteristics of GD frequency in generations without additional exposure. The Netishyn population demonstrated a clearly expressed oscillatory curve, while this index for the Magarach population had a relatively monotonous one. It is known that oscillatory dynamics is typical for systems with negative feedback and is an integral, final part of the homeostatic curve [13]. It shows a kind of over-regulation in the work of recovery processes. This phenomenon is well studied for technical and living systems under a single stress exposure. It is expected that the typical appearance of the homeostatic curve, which has one distinct pessimum and a series of fading oscillations on the ascending branch of the curve, will be significantly modified under constant stress exposure.

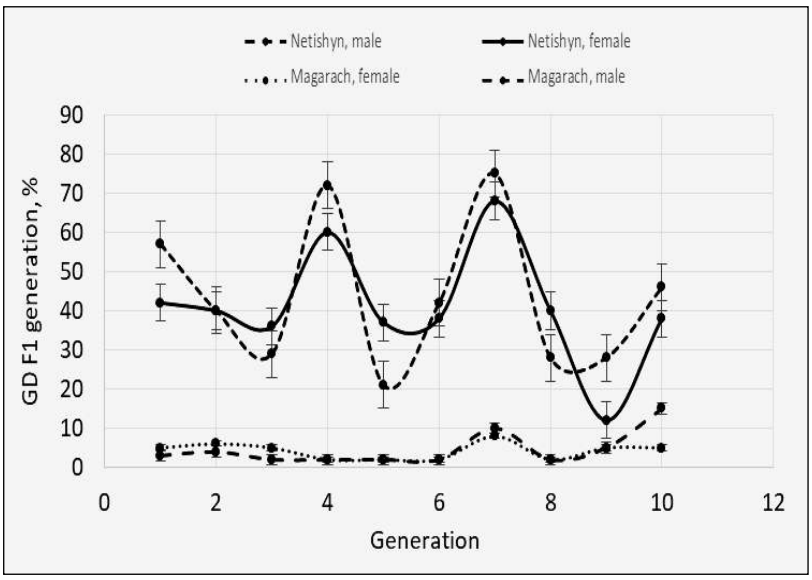


**Fig. 3. Dynamics of gonadal dysgenesis (GD) yield without additional chronic exposure**.

Similar oscillatory kinetics has been observed with another experimental model, the hybrid P - M system of the gonadal dysgenesis (the hybridization of Drosophila pure lines *Canton-S* without P-element and *radius incompletus (ri)* which includes the mobile element). Regular alternation of decrease and increase in the GD yield has been observed without additional exposure, so we can assume that the oscillatory dependence of the index is the result of chronic stress exposure of any nature. Additional chronic exposure of hybrid insects indicated changes in the oscillatory kinetics. There appeared a certain trend to both decreasing and increasing of the GD yield depended on the dose of additional exposure (Kravets et al. 2009).

Additional chronic exposure with the dose rate $0{,}12 \cdot 10^{-8}$ and $3 \cdot 10^{-8}$ Gy/sec led to the opposite reactions within both populations (Fig. 4, Fig. 5). The exposure of the first six generations of the Netishyn population indicated decreasing GD yield while maintaining the oscillation kinetics. Then, from the seventh generation, there was an increasing of the index followed by a decreasing with damped fluctuations. Increasing exposure of dose rate expanded a negative effect for the Magarach population. In Netishyn population a general dynamics of changes in both direction and GD yield was the same with slightly reduced increasing of the indexes for the seventh exposed generation (Fig. 5).

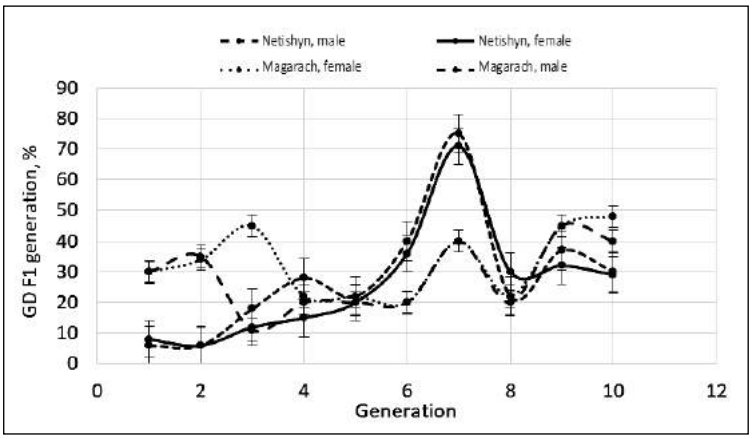


**Fig. 4. Dynamics of gonadal dysgenesis (GD) yield under additional chronic exposure with dose rate $0{,}12 \cdot 10^{-8}$ Gy/sec.**

Dynamic curve of GD yield for the Magarach population lost its monotony and for the fist – third generations exposed with the lowest dose rate has demonstrated a sharp increase of the index up to 30% for female and 45% for male.

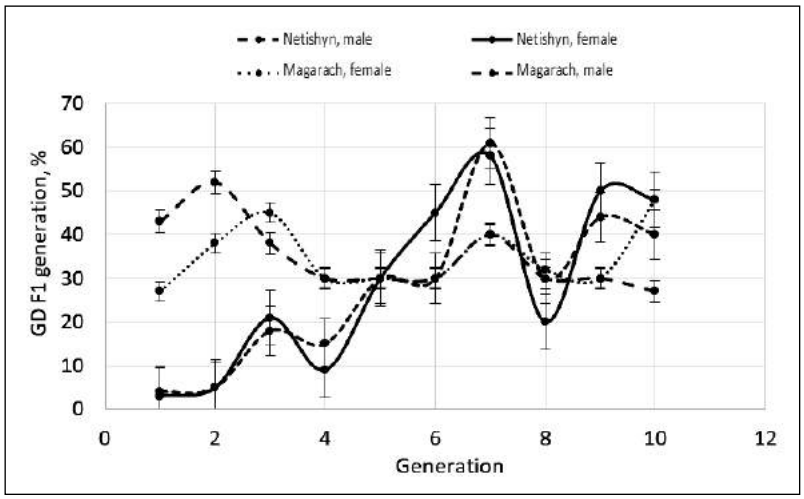


**Fig. 5. Dynamics of gonadal dysgenesis (GD) yield under additional chronic exposure with dose rate $0{,}3 \cdot 10^{-8}$ Gy/sec.**

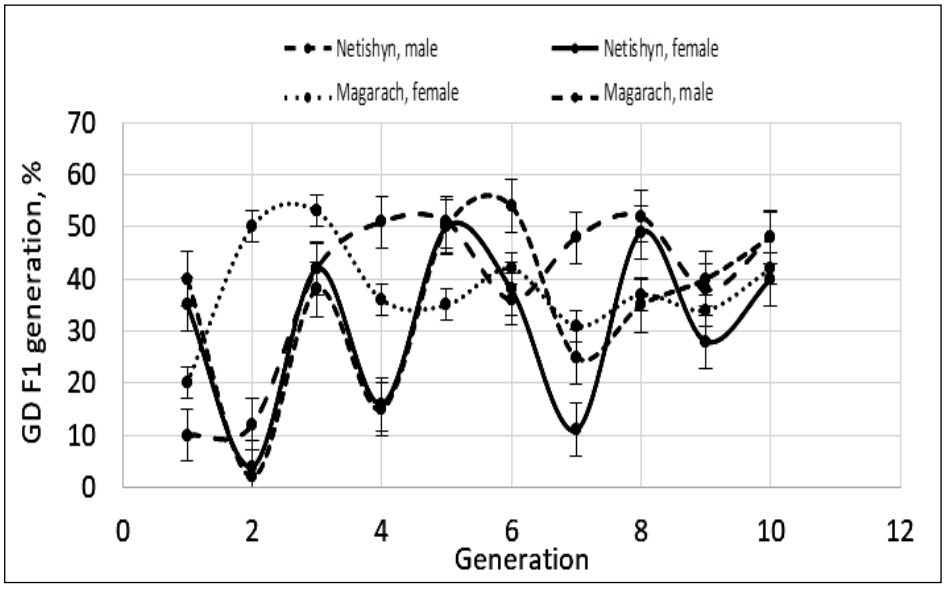


**Fig. 6. Dynamics of gonadal dysgenesis (GD) yield under additional chronic exposure with dose rate $1{,}2\cdot10^{-8}$ Gy/sec.**

Under increasing exposure dose rate up to $1{,}2\cdot10^{-8}$ Gy/sec the decrease compared to the control variant of the Netishyn population was disappeared, and dynamic curves of the GD yield became similar for the insects of both populations. The GD yield for the Netishyn population on average ranged from 2 up to 55%. For the Magarach one, the index was from 10 up to 53%.

The general dynamic type of dependence has become similar to the control one for the Netishyn population without additional exposure. Note that the study of small dose effects on different experimental models with their single or prolonged exposure has showed that dose curves have a complex non-monotonic nature, which differs significantly from the curves in the field of "large" doses [14,15,16].

The explanation of this phenomenon should take into account all currently known processes related to both the development of damage and the protective mechanisms of living things. Thus, a generalized explanation by Burlakova (1999) for single exposure dose curves in the field of small doses is based on the information about a complex system of damage development, induction and recovery processes. Within the system, each component has its own dose curve and turning-on "threshold". “Overlaying” of these dose curves causes complex nonmonotonic structure of the general curve "dose - effect" [14].

This idea has been developed by Kolomiytseva (2003) for the times of prolonged exposure when the effects have cumulative character and their appearance in time corresponds to the accumulative dose.

Interpretation of the results presented in this report should also include up-to-date information on the regulation of the mobile elements' activity. It is known that the activation of mobile elements induces a number of DNA protective mechanisms. The most important role in regulation of the activity of genome mobile elements is played by epigenetic mechanisms regulating gene expression. Inactivation of mobile elements is done by both switching the methylation of their sequences into *de novo* mode and activity of short non-coding RNA together with Argonaut protein complexes, which is a key component of the RNA interference [17]. A powerful defense mechanism is the reparative processes' activation, like a reaction to radiation damage [18]. Radiobiological study of the interaction of these two main mechanisms of mobile elements' activity regulation is just beginning. Right now, it allows us to approach the interpretation and preliminary estimates of the time of adaptive response

formation under exposure with certain doses and its absence under other one.

The most difficult to interpret the results is to explain the fact that according to the official data, all insect populations have originated from the regions belonging to the "green zone". One of the assumptions in the interpretation of this contradiction is related to the difference in the time of radionuclides' entry into the environment and their chemical composition, which determine both the natural radiation background in settlements of Poltavschina and Magarach and the technogenically changed in Netishyn. The generally accepted definition of radiation background intensity by gamma emitters [19] ignores a wide range of other radionuclides associated with NPP emissions and characterized with high genotoxic properties [20].

Exposure under ultra-low doses of technogenically-modified radiation background for tens of generations, as observed within Netishyn population, apparently has not become a constitutive factor forming a new stable pattern of genomic instability in generations which allows maintaining population density at the required level.

The effects of additional exposure with increased intensity (for example dose rate 0,12*10-8 Gy/sec) could occur with different stages. There are decreasing yield of genomic instability or its increasing up to the initial level with subsequent adaptive effect.

Thus, the data obtained on a simple experimental model show a complex interaction between the development of damage processes, on the one hand, and both protective and repair processes, on the other.

They also indicate the extreme complexity of interpreting the results of epidemiological studies and the uncertainty in predicting the effects of chronic exposure. The data show a significant discrepancy between the actual and expected radiation biological effects. Drosophila is an extremely radioresistant species with a high regenerative potential [21] and studying genomic instability on species with different radiosensitivity could provide an additional important information on the development of radiation safety standards for humans and biota.

Acknowledgment

The study was conducted in the framework of funding for research of the National Academy of Sciences of Ukraine №: III-3-18, "Methods and algorithms for minimizing environmental risks".

The authors are gratitude to Dr. I.A. Kozeretska and Ph.D. O.V. Protsenko, Taras Shevchenko Kyiv National University for both providing experimental material from Magarach, Lubny and Pyriatyn and discussing the results.

REFERENCES

[1]. Pelevina II, Gotlib VY, Kudriashova OV, Serebrianyi GG. 1996. Genome instability after exposure to low doses of radiation (in the 10-kilometer zone of the Chernobyl accident and in laboratory conditions). Radiat. Biol. Radioecology. 36 (4): 546-560.

[2]. Suskov II, Kuzmina NS. 2003. Polygenic realization of mutagenic effects in the body of people exposed to radiation in low doses. Radiat. Biol. Radioecology. 43 (2): 150.

[3]. Kuzmina NS, Suskov II. 2002. Expression of genomic instability in lymphocytes of children living under conditions of prolonged exposure to radiation factors. Radiat. Biol. Radioecology. 42: 735.

[4]. Dancause KN, Yevtushok L, Lapchenko S, Shumlyansky I, Shevchenko G, Wertelecki W, Garruto RM. 2020. Chronic radiation exposure in the Rivne-Polissia region of Ukraine: Implications for birth defects. American Journal of Human Biology. 22 (5): 667-674.

[5]. De Toledo SM, Buonanno M, Harris A, Azzam EI. 2017. Genomic instability induced in distant progeny of bystander cells depends on the connexins expressed in the irradiated cells. Int. J. Radiat. Biol. 93 (10): 1182-1194.

[6] Fang L, Li J, Li W, Mao X, Ma Y, Hou D, Zhu W, Jia X, Qiao J. 2019. Assessment of Genomic Instability in Medical Workers Exposed to Chronic Low-Dose X-Rays in Northern China. Dose Response. 17 (4): 1559.
[7]. Siama Z , Zosang-Zuali M , Vanlalruati A, Jagetia G C, Pau KS, Kumar NS. 2019. Chronic low dose exposure of hospital workers to ionizing radiation leads to increased micronuclei frequency and reduced antioxidants in their peripheral blood lymphocytes. Int. J. Radiat. Biol. 95(6):697-709.
[8]. [ICRP] International Commission on Radiological Protection publication 103. 2007. The 2007 recommendations of the ICRP. Published for the ICRP by ELSEVIER. 37:2-4.
[9]. Dobrzyński L, Fornalski K W, Feinendegen LE. 2015. Cancer Mortality Among People Living in Areas with Various Levels of Natural Background Radiation. Dose Response. 13 (3): 2391.
[10]. Golubovsky MD. 2000. Century of Genetics: Evolution of Ideas and Concepts. St. Petersburg: Borey Art.
[11]. Zainullin VG. 1996. Mutability of natural populations and laboratory lines of *Drosophila* under conditions of chronic irradiation in low doses of low intensity. Radiat. Biol. Radioecology. 36 (4):561-566.
[12]. Kozeretskaya IA, Protsenko AV, Afanasieva ES, Rushkovskyi SR, Chuba AI, Miusse TA, Meller AP. 2008. Mutation processes in natural populations of *Drosophila* and *Hirindo rustica* from the radioactively contaminated territory of Ukraine. Cytology and Genetics. 42 (4): 63-68.
[13]. Novoseltsev VN. 1978. Control Theory and Biosystems: Analysis of Protection Properties. Moskva: Nauka.
[14]. Burlakova EB. 1999. Features of the biological effect of small doses of radiation. Radiat. Biol. Radioecology. 39:26.
[15]. Kolomiytseva IK. 2003. Non-monotonicity of the dose-effect relationship in the region of low doses of ionizing radiation. Radiat. Biol. Radioecology. 43:179.
[16]. Kravets AP, Gatilova GD, Grodzinsky DM. 2008. Dynamics of the release of cytogenetic anomalies in the seedling meristem under chronic seed irradiation. Radiat. Biol. Radioecology. 48 (3): 208-219.
[17]. Law JA, Jacobsen SE. 2010. Establishing, maintaining and modifying DNA methylation patterns in plants and animals. Nature Reviews Genetics. 11: 204-220.
[18]. Yushkova E, Zainullin V. 2016. Interaction between gene repair and mobile elements-induced activity systems after low-dose irradiation. International Journal of Radiation Biology. 92 (9): 485-492.
[19]. Moiseev AA, Ivanov VI. 1990. Dosimetry and Radiation Hygiene Handbook. Moskow: Energoatomizdat.
[20]. Bazhenov AV, Buldakov LA, Vasilenko IY. 1990. Harmful chemicals. Radioactive substances. Leningrad: Chemistry.
[21]. Paithankar G J , Deeksha K , Patil R K. 2017. Gamma radiation tolerance in different life stages of the fruit fly Drosophila melanogaster. Int J Radiat Biol. 93 (4):440-448.

# EFFECT OF IONIZING RADIATION ON ATPASES

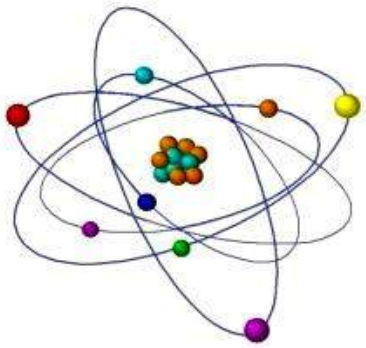

**[1]Chkadua G.N[*]., [1]Nozadze E.G., [1]Tsakadze L.G., [1]Shioshvili L.Sh, [1]Arutinova N. G., [1]Leladze M.V., [1]Dzneladze S.S., [1]Javakhishvili M.B., [2]Jariashvili T.I.**

[1]Laboratory of Membranology, I.Beritashvili Center of Experimental Biomedicine, Georgia
[2]Georgian National University

*Corresponding author: g.chkadua@biomedicine.org.ge

ABSTRACT*: Ionizing radiation (IR) has sufficient energy to ionize atoms by detaching electrons from them and promotes the generation of reactive oxygen species (ROS). ROS perform a multitude of signaling functions in different organisms from bacteria to mammalian cells. They were initially considered as a toxic byproducts of aerobic metabolism, but have now been acknowledged as important players in the complex signaling network of cells. Redox signaling is a result of a reversible, covalent modification of specific cysteine thiol residues in active and allosteric sites of proteins, which results in the alteration of protein structure and function. The Na,K-ATPase is activated with an "optimal redox potential range," where the increase of reactive oxygen species (ROS) levels beyond this "optimal range", are responsible for enzyme inhibition. Thus the effect of reactive oxygen species is expressed by biphasic action; stimulation by low doses and inhibition by high doses, which is a manifestation of a hormetic effect. This study was aimed to reveal the effect of IR treatment on the synaptic membrane fractions Na,K-ATPase and Mg-ATPase of the mouse brain. IR (1Gy and 5Gy) treatment of mice results in the alteration of the Na,K-ATPase and Mg-ATPase activity. Na,K-ATPase activity is increased during the initial 3 weeks, after 3 weeks enzyme activity is decreased, while Mg-ATPase activity only increased during the study.*

**Key words**: Na,K-ATPase, reactive oxygen species, thiol groups, ouabain, ionizing radiation.

## INTRODUCTION

As a result of wide use of nuclear energy sources (in particular uranium raw material mining and processing as well as nuclear catastrophes—such as Chernobyl and Fukushima) the level of background ionizing radiation is increased and people are exposed to natural sources of IR from the surrounding environment [1]; IR has sufficient energy to ionize atoms by detaching electrons from them [2] and promotes the generation of ROS. IR is also widely used in research, industry, and medicine [3–6]. Radiation therapy is an accepted therapeutic procedure in oncology. The effects of radiation therapy are achieved, by the production of free radicals. IR can present a health hazard when proper measures against excessive exposure are not taken. Therefore, the adequate determination of its deleterious effects on organisms is one of the essential problems of modern public health. Accidents at nuclear power plants cause severe body irradiation, which can lead to skin burns or acute radiation syndrome, whereas low doses of IR increase the risk of long-term effects, i.e., cancer [1]. IR causes cell damage to various organ systems and tissues [3, 6-8]. Radiation-induced increase in free radicals results in lipid peroxidation, leading to structural and functional damage to cellular membranes and membrane-associated proteins, including ion channels and transporters, which can contribute to the death and survival of irradiated cells [9].

IR-induced alterations may include a decrease in enzyme activity [10, 11] and a decrease in the membrane abundance of transporters. The damage to membrane organization and function is an initial step in cell death. During radiotherapy, formation of ROS in membranes would result in the damage of membrane bound transporters and enzymes. One of these enzymes can be Na,K-ATPase and Mg-ATPase. These ATPases have a crucial role in the maintenance of ion balance. The $Na^+$,$K^+$ pump is an electrogenic transmembrane ATPase, a member of the P-type ATPases family, that was discovered in 1957 by Skou [12]. Na,K-ATPase exchanges 3 sodium to 2 potassium, for the free energy of ATP hydrolysis. $Na^+$ and $K^+$ move against the concentration gradient, and the pump maintains the gradient of a higher concentration of sodium extracellularly and a higher level of potassium intracellularly. This concentration gradient is crucial for many processes within the cell. Na,K-ATPase also has an essential role in maintaining the resting membrane potential, regulating cell volume, and cell signal transduction. The physiological consequences of Na,K-ATPase regulation are important and play a crucial role in the adaptation of organisms to different conditions [13]. Many stimuli induce the specific modification of Na,K-ATPase and a change in Na,K-ATPase activity [14-17]. One of which is a group of chemically reactive molecules derived from the partial reduction of molecular oxygen, known as reactive oxygen species. These reactive species include oxygen-containing free radicals, such as superoxide anion radical ($O_2^{\bullet-}$) and hydroxyl radical (HO•), as well as hydrogen peroxide ($H_2O_2$). Due to their high reactivity, ROS are toxic to cells and damage a variety of macromolecules, including nucleic acids, proteins, and lipids [18]. Aside from their toxicity, ROS are important signaling molecules [19; 20]. The redox sensitivity of Na,K-ATPase was first shown in electric eels under a study of the effects of $H_2O_2$ [21]. This dual effect of p $H_2O_2$ was further demonstrated in other animal species, tissues, and with other species of ROS, such as hypochlorous anion, hydroxyl radicals, and superoxide. Despite the known effects of ROS on Na,K-ATPase, there is still a lack of information concerning the molecular mechanism of Na,K-ATPase alteration in the tissues after irradiation. Investigations of the enzyme properties in such condition enable us to understand the processes involved in the maintenance of ion homeostasis in tissues after IR.

## MATRRIAL AND METHODS

Experiments were performed on age- and weight-matched mice of both genders (10 weeks). The animals were subjected to one-time total-body IR procedure. One group (n=10) received 1Gy radiation, another group 5Gy radiation (n=8). Third group served as control, animals which do not received irradiation. After IR the mice were housed into different cages and observed.

Brain synaptic membrane fractions obtained from different group mice served as the investigation material. The synaptic membrane fraction was obtained using differential centrifugation; at 1.2-0.8 M concentration gradients of sucrose, according to de Robertis [22] recommendations.

Na,K-ATPase activity was measured as an ouabain sensitive part of total ATPase activity. Mg-ATPase was considered as the ouabain insensitive part. The total ATPase incubation medium contained 140 mM NaCl, 5 mM KCl, and 50 mM Tris-HCl buffer at pH 7.7. Mg-ATPase was determined by adding 1 mM ouabain into the medium, consisting of 145 mM KCl and 50 mM Tris-HCl buffer at pH 7.7. Protein concentration for the activity assay was 0.0044mg/ml. The samples were incubated at 37 $^oC$ for 15 minutes. ATPase activity was calculated according to the amount of inorganic phosphorus (Pi) (per mg protein and per hour), resulting from enzyme-induced ATP hydrolysis. The inorganic phosphorus levels were evaluated calorimetrically [23-

24]. Amount of protein was determined by the procedure of Lowry [25] using bovine serum albumin as a standard.

The experiments were subjected to statistical analysis. The following data is presented as an arithmetic means with a standard error. Differences between two groups were assessed using an unpaired two-tailed Student's t-test. A P value of $p < 0.05$ was considered statistically significant.

The rats experienced no suffering prior to decapitation. All experiments were approved by the animal care and use committee at the Ivane Beritashvili Center of Experimental Biomedicine

RESULTS

ROS are one of the redox signaling molecules produced by IR. The targets for this signaling pathway are cysteine (Cys) residues of proteins, where various thiol modifications also take place. To investigate the effect of IR on the Na,K-ATPase and Mg-ATPase, we have studied changes in enzyme activity after IR exposure. From the Fig.1, it is clear that IR at 1Gy activates the Na,K-ATPase system during 3weeks. Enzyme reaches maximal velocity at the 3 week mark and gradually decreases after 3 weeks.

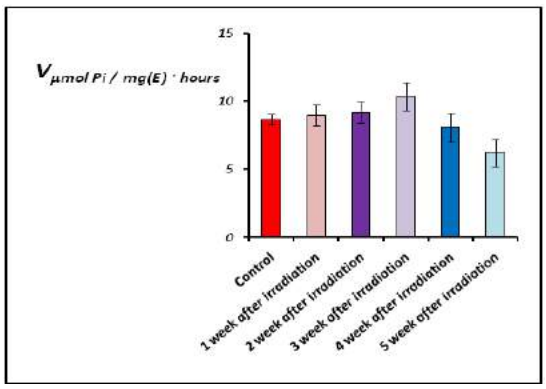


**Fig.1 Dependence of synaptic membrane Na,K-ATPase activity on IR (1Gy). The reaction medium was [MgATP]=1.69mM; [$Mg_f^{2+}$]=[$ATP_f$]=0.31mM.($P < 0.01$).**

In the case of high dosage of IR (5Gy), activity of Na,K-ATPase is again increased after 1week (Fig.2).

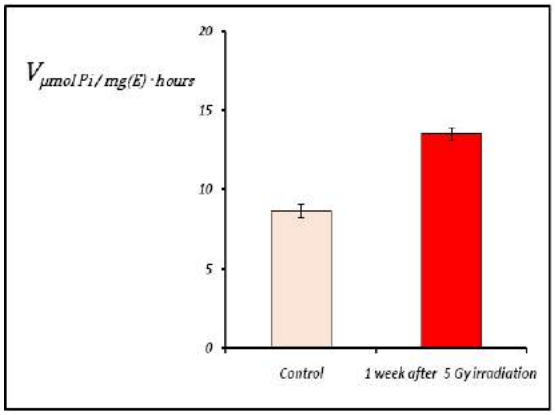


**Fig.2 Dependence of synaptic membrane Na,K-ATPase activity on IR (5 Gy). The reaction medium was [MgATP]=1.69mM; [$Mg_f^{2+}$]=[$ATP_f$]=0.31mM.($P < 0.01$).**

Activity of Na,K-ATPase after 1 week is higher in the case of 5Gy IR compared with 1Gy IR ( Fig. 3)

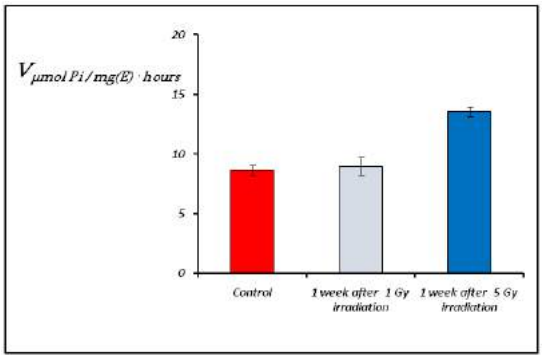


**Fig.3 Dependence of synaptic membrane Na,K-ATPase activity on IR. The reaction medium was [MgATP]=1.69mM; [$Mg_f^{2+}$]=[$ATP_f$]=0.31mM.($P < 0.01$).**

Different results were obtained in the case of Mg-ATPase study (Fig.4). After 1week Mg-ATPase activity was decreased, while after 2 weeks It's activity is increasing gradually during 5 weeks and does not undergo inhibition. (Fig.4).

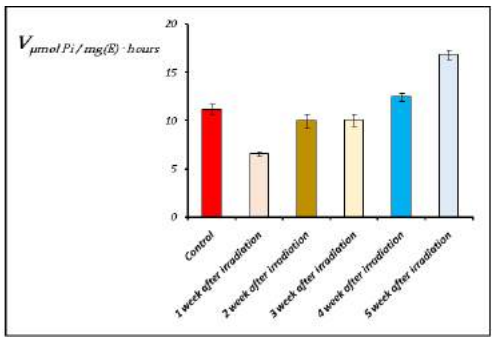


**Fig.4 Dependence of synaptic membrane Mg-ATPase activity on IR (1Gy). The reaction medium was [MgATP]=1.69mM; [$Mg_f^{2+}$]=[$ATP_f$]=0.31mM.($P < 0.01$).**

In the case of a high dose of IR (5Gy) the same change of Mg-ATPase activity is manifested as was obtained during 1Gy IR (Fig.5). Mg-ATPase activity is decreased after 1week and is increased during the second and third weeks after IR exposure.

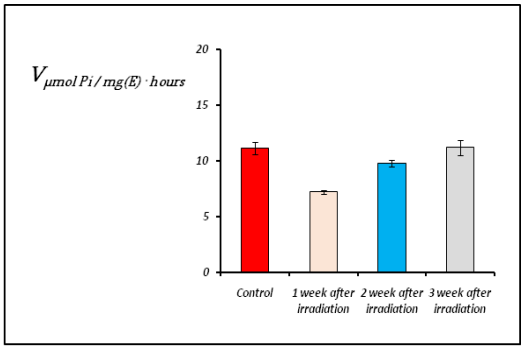


**Fig.5 Dependence of synaptic membrane Mg-ATPase activity on IR (5Gy). The reaction medium was [MgATP]=1.69mM; [$Mg_f^{2+}$]=[$ATP_f$]=0.31mM.($P < 0.01$).**

DISCUSSION

It is well established, that exposing cells to IR causes immediate free radical formation leading to ROS generation, and thus, results in cell damage. In healthy cells, ROS are serving multiple signaling functions, and the body's antioxidant systems, including thiols, control their activity by neutralizing the excessive free radicals. IR-induced increase in free radicals are known to initiate lipid peroxidation, which leads to cell membrane damage [26]. Changes in membrane lipid composition and oxidative state could have dramatic consequences for Na,K-ATPase enzymatic activity [27]. Accordingly, an increase in the concentration of lipid peroxidation products was previously correlated with inhibition of the Na,K-ATPase [27]. Elevation of endogenous ouabain upon IR treatment was also detected [28].

Ouabain is known to specifically inhibit the Na,K-ATPase, it has also been shown to activate this enzyme [29-31] at concentrations comparable to the endogenous ouabain level. Endogenous ouabain is known as a hormone synthesized in the zona glomerulosa cells of the adrenal cortex from cholesterol [28]. IR activates sympathetic nervous system and stress–hormone axis [28], which, in its in turn, regulate endogenous ouabain synthesis and release. Notably, in contrast to the suppressive action of free radicals on the Na,K-ATPase, free radicals have been suggested to be an important component of the oxidative stress amplification loop [28]. The binding of ouabain to the Na,K-ATPase has been suggested to activate multiple signaling pathways that can increase the generation of mitochondrial ROS, which, in turn, can further modify the Na,K-ATPase and potentiate this signaling [28]. Redox signaling is a result of reversible, covalent modification of specific cysteine thiol residues in active and allosteric sites of proteins, which results in the alteration of protein structure and function. ROS oxidizes cysteine residues in proteins to produce disulfides (R-S-S-R) via the formation of a sulfenic acid (R-SOH) intermediate by a biologically reversible reaction [32]. Disulfides can be formed differently; between adjacent cysteines within a protein, known as intra-protein disulfide, between two proteins (interprotein disulfide), or as a mixed-disulfide formed between a protein thiol and glutathione, termed S-glutathionylation. Thioredoxins (Trx) or glutaredoxins (Grx) protein are responsible for reversible reduction of the protein, resulting in a reversible signal transduction mechanism. Further oxidation of protein thiols by $H_2O_2$ to higher oxidation states form sulfinic (R-$SO_2H$) and sulfonic (R-$SO_3H$) acids, within an irreversible reaction [32].

The sodium potassium pump is polymer, formed by three different subunits. The largest is the 100–113 kDa catalytic α subunit, responsible for catalytic activity and ion transport; the others are regulatory subunits – the 55 kDa β subunit and the tissue-specific regulatory proteins of 7–11 kDa members of the FXYD family [33]. Each Na,K-ATPase subunit type contains cysteine residues. The only reduced thiol within the beta subunit resides at the edge of the membrane surface, immersing into and out of the membrane during the pumping cycle [33]. The FXYD subunit has two thiols [34]. The catalytic α subunit has binding sites for ATP and for ions, forms a transport pore, and 23–24 thiols are presented, depending on the isoform [34]. These thiols of different subunits are potential targets of regulatory thiol modifications. We can speculate that ROS at low concentrations reacts with thiolate (S-) from Cys, forming a sulfenate ($SO^-$) that can result in the formation of disulfide bonds (SS) along with other thiols and activation of the enzyme. Increasing ROS concentration oxidizes the sulfenate to sulfinate ($SO_2^-$), and finely to sulfonate ($SO_3^-$), resulting in the irreversible oxidation of Na,K-ATPase and ROS-mediated toxicity. So, from our experimental results we can say, that at the beginning stage, after 1Gy and 5Gy treatment IR stimulate ROS formation and increases Ouabain level. Reversible modification of regulatory thiols of all subunits of Na,K-ATPase by ROS and its signaling pathway stimulates Na,K-ATPase and increase its activity (Fig.1; Fig.2); Further elevated ouabain binds to the Na,K-ATPase activates pathways that can increase the generation of mitochondrial ROS, by Na,K-

ATPase oxidant amplification loop, which, in turn, irreversibly modify enzyme thiols and cause Na,K-ATPase inhibition (Fig.1). In case of Mg-ATPase, elevated ROS levels are not sufficient to irreversibly modify enzyme, and there is only activation of the enzyme system (Fig4; Fig.5).

From our experimental results, we can ascertain that IR treatment of mice results in the alteration of the Na,K-ATPase and Mg-ATPase activity. Na,K-ATPase activity is increased during the initial 3 weeks after IR, after 3 weeks enzyme activity is decreased, while Mg-ATPase activity is increased during observation.

REFERENCES

[1] Kennedy, A.R. (2014). Biological effects of space radiation and development of effective countermeasures. *Life Sci. Space Res*., 1, 10–43.
[2] Ryan, J.L.(2012). Ionizing radiation: The good, the bad, and the ugly. *J. Investig. Dermatol.*,132, 985–993.
[3] Zhou, T.; Lu, L.; Wu, S.; Zuo, L. (2017). Effects of Ionizing Irradiation on Mouse Diaphragmatic Skeletal Muscle. *Front. Physiol.*, 8, 506.
[4] Biau, J.; Chautard, E.; Verrelle, P.; Dutreix, M. (2019). Altering DNA Repair to Improve Radiation Therapy: Specific and Multiple Pathway Targeting. *Front. Oncol.*, 9, 1009.
[5] Kaloˇcayová, B.; Kovaˇciˇcová, I.; Radošinská, J.; Tóthová, L.; Jagmaševiˇc-Mézešová, L.; Fülöp, M.; Slezák, J.; Babál, P.; Janega, P.; Vrbjar, N. (2019). Alteration of renal Na,K-ATPase in rats following the mediastinal γ-irradiation. *Physiol. Rep.*, 7, 13969.
[6] Wang, L.Y.; Yang, P.Y.; Chen, Y.J.; Wu, H.D.; Huang, Y.H.; Hsieh, C.H.(2019). Inspiratory muscle training attenuates irradiation-induced diaphragm dysfunction. Am. *J. Transl. Res.*, 11, 5599–5610.
[7] Russell, J.A.; Connor, N.P. (2014). Effects of age and radiation treatment on function of extrinsic tongue muscles. *Radiat. Oncol.*, 9, 1–15.
[8] D'Souza, D.; Roubos, S.; Larkin, J.; Lloyd, J.; Emmons, R.; Chen, H.; De Lisio, M. (2019). The Late Effects of Radiation Therapy on Skeletal Muscle Morphology and Progenitor Cell Content are Influenced by Diet-Induced Obesity and Exercise Training in Male Mice. *Sci. Rep.*, 9, 6691.
[9] Huber, S.M.; Butz, L.; Stegen, B.; Klumpp, D.; Braun, N.; Ruth, P.; Eckert, F. (2013). Ionizing radiation, ion transports, and radioresistance of cancer cells. *Front. Physiol.*, 4, 212.
[10] Matsuda, H.; Giblin, F.J.; Reddy, V.N. (1982). The effect of X-irradiation on Na-K-ATPase and cation distribution in rabbit lens. *Investig. Ophthalmol. Vis. Sci.*, 22, 180–185.
[11] Hitschke, K.; Buhler, R.; Apell, H.J.; Stark, G. (1994). Inactivation of the Na,K-ATPase by radiation-induced free radicals. *Evidence for a radical-chain mechanism. FEBS Lett.*, 353, 297–300.
[12] Skou J. (1957). Influence of some cations on an adenosine triphosphatase from peripheral nerves. *Biochemistry Biophysics Acta*, 23, 394-401. https://doi.org/10.1016/0006-3002(57)90343-8.
[13] Blanco G. & Mercer R.W. (1998). Isozymes of the Na-K-ATPase: heterogeneity in structure, diversity in function. *Am. J. Physiol*. 275, F633–F650 doi: 10.1152/ajprenal.1998.275.5.F633.
[14] Chkadua G., Nozadze E., Tsakadze L., Shioshvili L., Leladze M., Arutinova N., Dzneladze S., Javakhishvili M., & Kupradze S. (2022). Some Kinetic Features of Na,K-ATPase and Sensitivity to Noradrenalione. *Cell Biochemistry and Biophysics*, V. 80, issue 1, 23-29. doi:10.1007/s12013-021-01032-6.
[15] Hernandez J. (1992). Na,K-ATPase regulation by neurotransmitters. *Neurochemistry Int.*, 20 (1), 1-10. doi: 10.1016/0197-0186(92)90119-c.
[16] Vague P., Coste T.C., Jannot M.F., Raccah D., & Tsimaratos M. (2004). C-peptide, Na,K-ATPase and diabetes. *Exp. Diabesity Research*, 5, 37-50. doi: 10.1080/15438600490424514.
[17] Vizi A. & Seregi A. (1982). Receptor independent stimulatory effect of noradrenaline on Na,K-ATPase in rat brain homogenate. Role of lipid peroxadation. *Biochemisry Pharmacology*, 31(13), 2231-2236. doi: 10.1016/0006-2952(82)90106-x.
[18] Stadtman E.R. (1992). Protein oxidation and aging. *Science*. 257,1220–1224.doi: 10.1126/science.1355616.
[19] Finkel T. (2011). Signal transduction by reactive oxygen species. *J. Cell Biol.*, 194, 7–15

doi: 10.1083/jcb.201102095.
[20] Rhee S.G., Kang S.W., Jeong W., Chang T.S., Yang K.S.,& Woo H.A. (2005). Intracellular messenger function of hydrogen peroxide and its regulation by peroxiredoxins. *Curr. Opin, Cell Biol.*, 17,183–189 doi: 10.1016/j.ceb.2005.02.004.
[21] Liu J., Kennedy D.J, Yan Y., & Shapiro J.I. (2012). Reactive Oxygen Species Modulation of Na/K-ATPase Regulates Fibrosis and Renal Proximal Tubular Sodium Handling. *International Journal of Nephrology 3:* ID381320 doi:10.1155/2012/381320
[22] De Robertis E. (1969). Structural components of the synaptic region. *Structural Neurochemistry,* 2,365-380 doi: 10.1007/978-1-4615-7157-5_15.
[23] Fiske G.H. &Subbarow Y. (1925). The colorimetric determination of phosphorus. *Biological Chemistry*, 66, 375-400. https://doi.org/10.1016/S0021-9258(18)84756-1.
[24] Kazanov A. & Maslova M. (1984). The investigation of activation of Na,K-ATPase in the red blood cells of mammals. *Journal of Evol. Biochemistry and Physiology*, 16 (5), 81-87.
[25] Lowry O., Rosenbrough N., & Randall R. (1951). Protein measurement with the folin phenol reagent. *Journal of Biological Chemistry*, 193 (1), 265-275. doi:10.1016/S0021-9258(19)52451-6.
[26] Purohit, S.C.; Bisby, R.H.; Cundall, R.B. (1980). Chemical damage in gamma-irradiated human erythrocyte membranes. *Int. J. Radiat. Biol. Relat. Stud. Phys. Chem. Med.*, 38, 159–166.
[27] Cornelius, F.; Habeck, M.; Kanai, R.; Toyoshima, C.; Karlish, S.J. General and specific lipid-protein interactions in Na,K-ATPase. *Biochim. Biophys. Acta*, 2015, 1848, 1729–1743.
[28] Violetta V. Kravtsova, Arina A. Fedorova, Maria V. Tishkova, Alexandra A. Livanova, Oleg V. Vetrovoy, Alexander G. Markov, Vladimir V. Matchkov and Igor I. Krivoi (2022). Chronic Ouabain Prevents Radiation-Induced Reduction in the α2 Na,K-ATPase Function in the Rat Diaphragm Muscle; *Int. J. Mol. Sci.*, 23, 10921
[29] Holthouser, K.A., Mandal, A., Merchant, M.L., Schelling, J.R., Delamere, N.A., Valdes, R.R. Jr., Tyagi, S.C., Lederer, E.D., Khundmiri, S.J.(2010). Ouabain stimulates Na-K-ATPase through a sodium/hydrogen exchanger-1 (NHE-1)-dependent mechanism in human kidney proximal tubule cells. Am. *J. Physiol. Ren. Physiol.*, 299, F77–F90.
[30] Ketchem, C.J., Conner, C.D., Murray, R.D., Du Plessis, M., Lederer, E.D., Wilkey, D., Merchant, M., Khundmiri, S.J. (2016). Low dose ouabain stimulates Na-K ATPase α1 subunit association with angiotensin II type 1 receptor in renal proximal tubule cells. *Biochim. Biophys. Acta*, 1863, 2624–2636.
[31] Klimanova, E.A., Tverskoi, A.M., Koltsova, S.V., Sidorenko, S.V., Lopina, O.D., Tremblay, J.m, Hamet, P., Kapilevich, L.V., Orlov, S.N. (2017). Time- and dose-dependent actions of cardiotonic steroids on transcriptome and intracellular content of Na+ and K+: A comparative analysis. *Sci. Rep.*, 7, 45403.
[32] Cremers C.M. & JakobU. (2013). Oxidant sensing by reversible disulfide bond formation. *Biol.Chem.,* 288 (37), 26489-26496. doi: 10.1074/jbc.R113.462929.
[33] Toyoshima C., Kanai R., & Cornelius F. (2011). First crystal structures of Na+,K+-ATPase: new light on the oldest ion pump. *Structure*, 19, 1732–1738. doi:10.1016/j.str.2011.10.016.
[34] Bogdanova A., Petrushanko I., Boldyrev A., & Gassmann M. (2006). Oxygen- and Redox-Induced Regulation of the Na/K ATPase. *Curr. Enzyme Inhibit.*, 2, 37–59. doi:10.2174/157340806775473490.

# EVALUATION OF DIFFERENTLY EXPRESSED GENES IN IRRADIATED AND INTACT MICE TO STUDY RADIOACTIVE AGING PHENOMENON

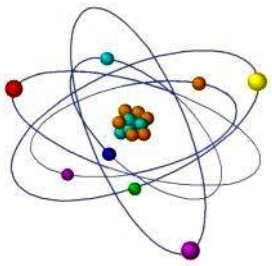

**[1,] Ioramashvili I.V.*, [2]Gogebashvili .M,E.,**
**[1]Sujashvili R.Sh, [2]Ivanishvili N.I.**
[1]Laboratory of Biophysics, I.Beritashvili Center of Experimental Biomedicine, Georgia
[2]Laboratory of Radiation Safety Problems, I. Beritashvili Center of Experimental Biomedicine, Georgia
*Corresponding author: i.ioramashvili@biomedicine.org.ge

ABSTRACT: *The question about processes which lie behind aging of organisms still does not have an unambiguous answer. The main reason of this uncertainty are numerous manifestation forms and effects participating in this process at various structural and functional levels of the organization of living organisms. In order to specify the processes involved in the aging effect, we used two methodological stages: 1. we analyzed RNA sequences from publicly available databases to find differently expressed genes in old and young mice and mice after radiation exposure; 2. compared obtained set of genes with genes recognized as age related. If we take into the account that we can possibly dose the acceleration of aging process by varying radiation exposure, then the identification of specific genes can significantly narrow the genetic spectrum which is most important for the aging of organisms. Given the high degree of similarity of the investigated mice genes with the human genome, this methodological approach can lead us towards unification of integrative mechanisms of aging, and the development of methods for biomedical monitoring of this process.*

**Key words:** aging, longevity, genes, bioinformatics, RNA-sequence, irradiation

## INTRODUCTION

According to the World Health Organization (WHO), age-related diseases are currently leading among the main causes of death: coronary heart disease (CHD), stroke, cancer, and diabetes. Aging is the main risk factor for these and many other socially significant chronic neurodegenerative disorders such as dementia, Alzheimer's and Parkinson's diseases [1]. Such a variety of ailments increasingly dictates the need to study more general mechanisms underlying the aging process, without focusing only on individual specific cases. Accumulation of mutations and antagonistic pleiotropy, oxidative effects of free radicals, self-destruction of cells (apoptosis), telomeres shortening, neuroendocrine theory and other popular hypotheses are currently discussed in scientific publications regarding aging theories [2].

Thus a large number of different versions create a necessity to study adequate methods to trigger the aging process. Ionizing radiation, which is capable of dosing the influence on the regulatory mechanisms of aging, favorably differs from other methodologies. An assessment of the aging associated biological processes reveals the acceleration of normal aging by ionizing radiation [3].

Analyzing this phenomenon, we should mention that radiation has pluripotent effects, including such fundamental processes as DNA repair and blocking of proliferative activity. At the same time, the postradiational fate of cellular populations, including aging and apoptosis, mainly depends on the accuracy of implementation of reparation processes [4]. Obviously, that there is regularity associated with different levels of high doses of radiation, because of an increasing probability of DNA double-strand breaks. In this case, active induction of cellular aging processes is observed [5]. Thus, radiation aging can be considered as more general form of premature decrease of vital activity of organisms,

here caused by radiation exposure [6]. Aging is defined as the age-related deterioration of biological functions necessary for life [7]. In other words, ionizing radiation affects aging through molecular and cellular mechanisms on the various structural and functional levels of biological objects.

Experiments on irradiated (5Gy) mice of different age groups confirmed that the cognitive abilities for spatial learning were markedly reduced in groups of 3-month-old mice, while 1-year-old mice did not show a very noticeable deterioration in cognitive abilities [8]. These observations lead us to the question about genetic nature of radiosensitivity of older mice to compare with younger mice.

Genetic variability of longevity may be observed due to the fact that genes that influence lifespan represent various molecular functions but may be involved in similar biological processes and health disorders, which could contribute to genetic heterogeneity of longevity and the lack of replication in genetic association studies [9]. It is very important that the inheritance of longevity is still poorly understood. There are several controversial opinions about it [10,11]. So the question of the genetic inheritance of longevity is still open for study.

The process of gene expression is responsible for using the information from gene to synthesize a functional product, which can result in proteins production. In the case when the level of gene expression in different conditions of organism is statistically different, then the study of these differences gives us the possibilities to understand the biological difference between these conditions [12]. To provide us with right direction for further investigations, ascertain the genetic nature of changes in the body caused by radiation, and identify genes that are radiosensitive and specific to the aging organism, we used Publicly available database and analyzed differently expressed mouse genes (Mus Musculus C57Bl/6J SPF) of irradiated organism and young (7-12 weeks) and old (12-19 months) non-irradiated mice.

## MATERIALS AND METHODS

In this work the RNA - seq study identified differently expressed genes between irradiated and not irradiated conditions in mice. The main steps of the analysis was performed on Galaxy web platform - free, open source software, which provides necessary tools for step-by-step analysis of different expressed genes [13].

We used RNA sequence from Publicly available data from European Nucleotide Archive (ENA) which provides a comprehensive record of the world's nucleotide sequencing information, covering raw sequencing data, sequence assembly information and functional annotation. Data was obtained from project: PRJEB38394, from ENA archive. Referenced investigation was created by Service Laboratory of Functional Genomics and Bioinformatics Institute of Molecular Genetics of the ASCR, RNA sequences were obtained by NextSeq 500 sequencing, the name of study is "Comparison of CD8+ T-cell sub-types from peripheral lymph nodes and spleen from Balb/c or C57Bl/6J SPF mice mice by transcription profiling".

For our purposes RNA sequencing data from C57Bl/6J SPF mice (10-12 weeks) who were irradiated with 4 Gy and sacrificed 16 days after irradiation and young (7-12 weeks) and old (12-19 months) non-irradiated mice were studied. According to published data each sample consisted of a pool of lymphocytes originating from 2-5 mice. For each population, data were obtained from 3 independent biological triplicates [14].

On Galaxy server we analyzed 6 irradiated with 4Gy samples - ERR4164688, ERR4164689, ERR4164690, ERR4164691, ERR4164692, ERR4164693, and 4 not irradiated samples ERR4164694, ERR4164695, ERR4164696, ERR4164697.

We started from quality control of the reads using FastQC and Cutadapt Galaxy tools. Reads mapping to a reference genome was made by STAR tool. Referenced genome file was taken from ZENODO

database [15]. The number of reads from the mapped sequences per annotated genes were counted using featureCounts tool. For each step, Quality reports of each step were aggregated using MultiQC. DESeq2 tool was used on the read counts to normalize them and extract the differentially expressed genes. DeSeq2 results for different expressed (DE) genes were visualized by variance plot, heatmap and Volcano Plot (Fig.1).

Analysis revealed 322 differently expressed genes of irradiated and not - irradiated young mice, and 658 differently expressed genes of irradiated and not – irradiated old mice. We considered only those genes where expression differences (2FoldChange) exceeded 1, and the level of statistical significance was p.value > 0.05.

## RESULTS AND DISCUSSION

We can see (Fig.1, Fig.2) that irradiation quite strongly affects the expression of many genes in both young and old mice. But as the aim of the study was to identify the genes that are supposedly responsible for the process of radioactive aging, we compared differently expressed genes under the influence of radiation in young and old mice separately Fig.3. All further calculations were made by seaborn and pandas packages, in python.

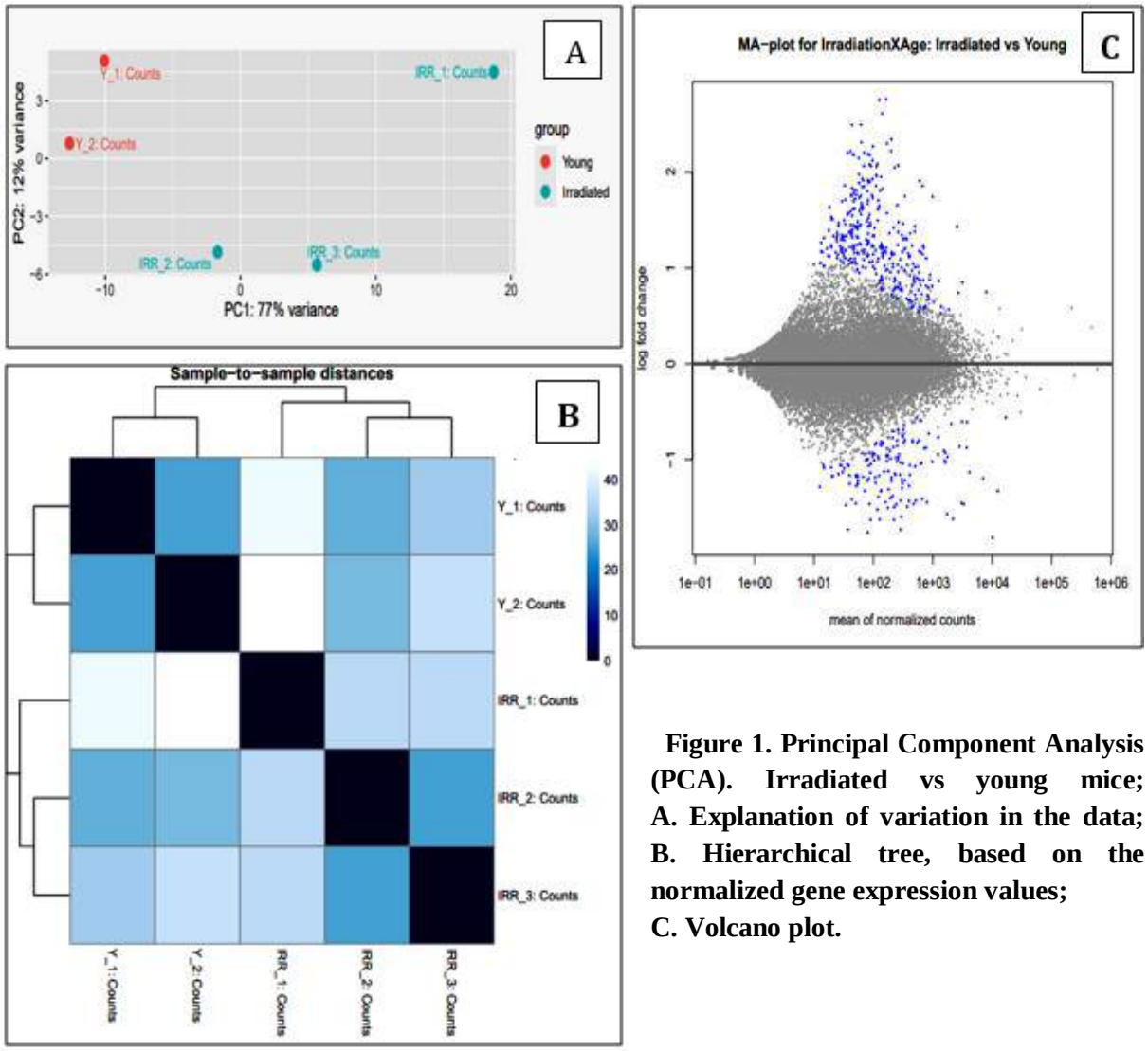


**Figure 1. Principal Component Analysis (PCA). Irradiated vs young mice; A. Explanation of variation in the data; B. Hierarchical tree, based on the normalized gene expression values; C. Volcano plot.**

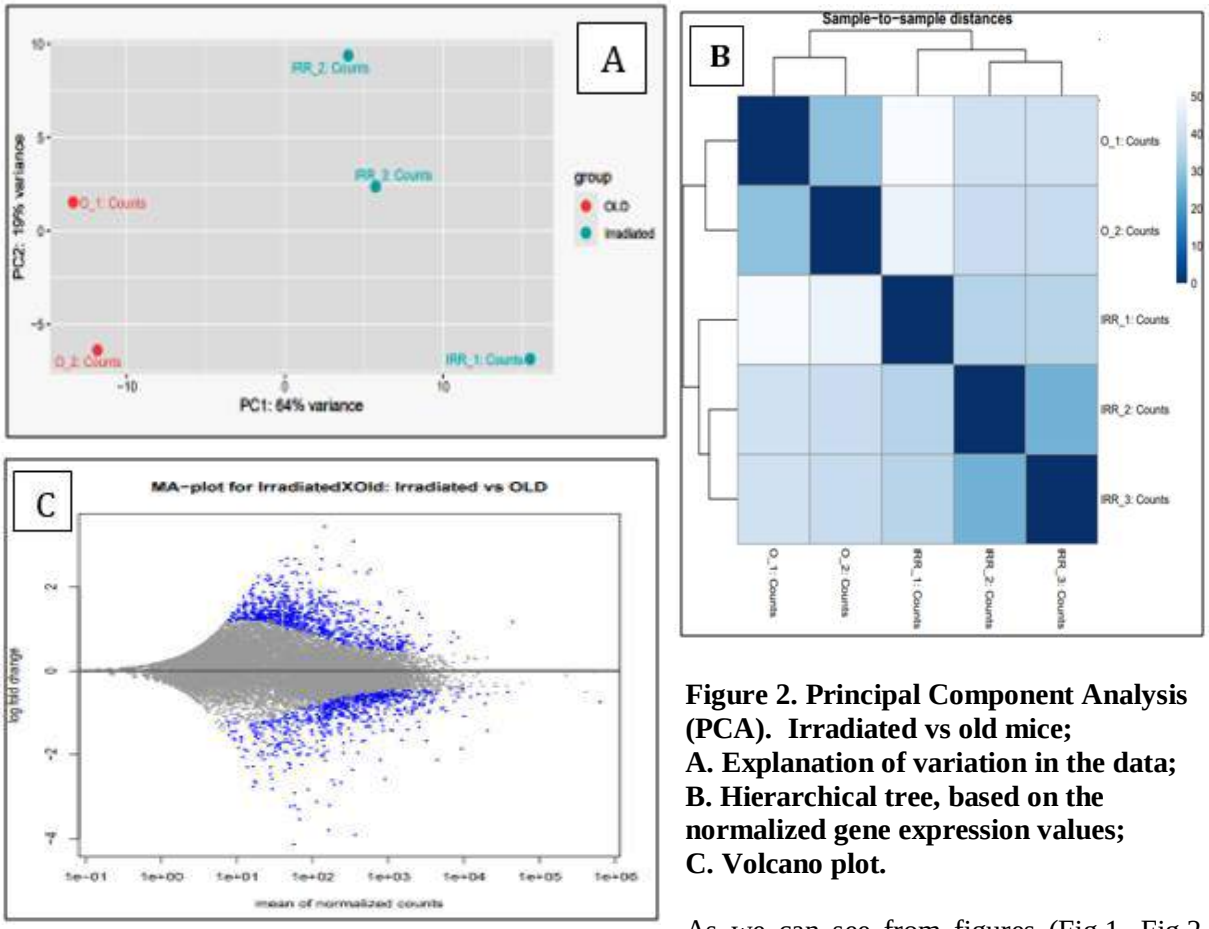


**Figure 2. Principal Component Analysis (PCA). Irradiated vs old mice;**
**A. Explanation of variation in the data;**
**B. Hierarchical tree, based on the normalized gene expression values;**
**C. Volcano plot.**

As we can see from figures (Fig.1, Fig.2, Fig.3), the comparison of differences in gene expression under the influence of radiation in young and old mice indicates that older mice have more genes with different level of expression. There are almost twice more genes with low expression level in the group of old mice, than in group of young mice.

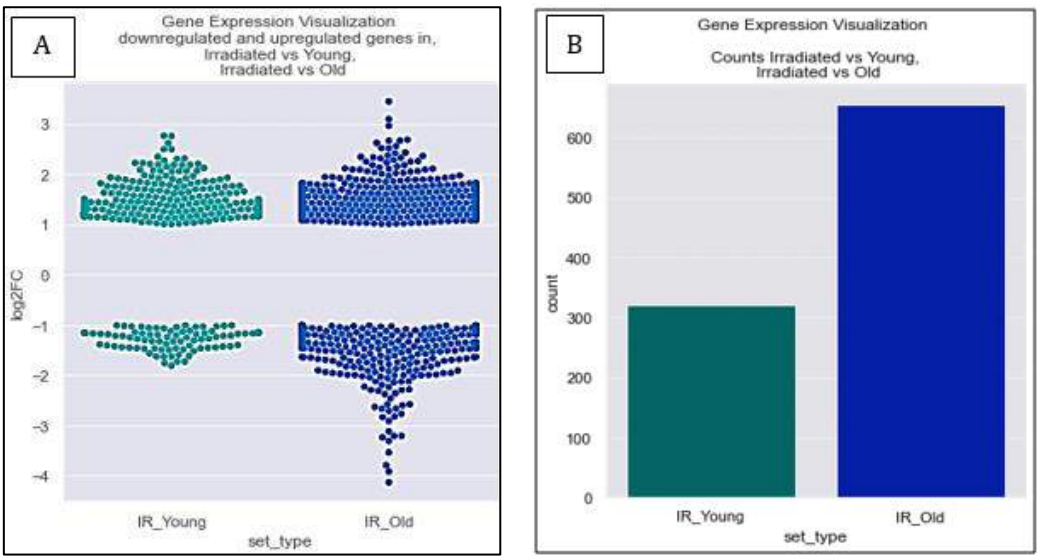


**Figure 3. Visualization of gene expression differences (Log2Fold Change) between Irradiated against young and irradiated against old groups of mice.**
**A. visualization of downregulated and upregulated genes in two groups;**
**B. Amount of differently expressed genes.**

Also in the group of older mice are more upregulated and downregulated genes with high range of changes (abs(Log2(FC) )≥2) than in young mice. But absolute level of expression mostly is lower than 2 (abs(Log2(FC) ) < 2)(Fig.3) in both cases. If we subset only data with high level of expression, we can indicate that more than 3 genes at once are changed in 2, 10, 11 and 13 chromosomes in case of young mice and more than 5 genes in chromosomes 1, 2, 3, 4, 5, 6, 7, 8, 9, 10, 11, 13, 14, 16, 19 and X in case of old mice (Tab.2). It indicates that old mice have more valuably changed genes and more chromosomes are affected by the influence of radiation.

**Table 2. Most differently expressed genes in young and old mice groups**

| Chromosome | Old mice genes (\|Log2(FC)\| >= 2) | Young mice genes (\|Log2(FC)\| >= 2) |
|---|---|---|
| chr1 | Fcgr2b ; Slamf6 ; Atp1b1 ; Ramp1 ; Gm38204 ; Gm10522 | Kif14 ; Nuf2 ; |
| chr10 | Myb ; Tet1 ; Lrrc75b ; Adamts14 ; Slc41a2 ; | Cdk1 ; Lilr4b ; Lilrb4 ; |
| chr11 | Ccl5 ; Eml6 ; Tanc2 ; Alox8 ; Dusp3 ; 2010300F17Rik ; | Mpo ; Aurkb ; Spag5 ; |
| chr12 | Ifi27l2a ; | Rrm2 ; Ncapg2 ; |
| chr13 | Itga1 ; C130051F05Rik ; Tppp ; Gm48624 ; Cenpk ; Gcm2 | Hist1h3b ; Hist1h2bb ; Hist1h4f ; |
| chr14 | Bmpr1a ; Spry2 ; Nt5dc2 ; Esco2 ; | /---/ |
| chr15 | Rbfox2 ; | Espl1 ; |
| chr16 | Pros1 ; Mx2 ; App ; Cd86 ; Fstl1 ; | /---/ |
| chr17 | Afdn ; H2-Eb1 ; | Ccnf ; Uhrf1 ; |
| chr18 | Dsg2 ; | /---/ |
| chr19 | Gm6545 ; Anxa1 ; Gm47242 ; | /---/ |
| chr2 | Olfm1 ; Ptprj ; Kif5c ; Dapl1 ; Slc43a3 ; Gm44027 ; Nr4a2 ; Sulf2 ; | Tpx2 ; Mcm10 ; Ube2c ; Nusap1 ; |
| chr3 | Gm37589 ; Kcna2 ; A930002I21Rik ; | /---/ |
| chr4 | Dmrta1 ; Camk2n1 ; Phf13 ; Id3 ; Adgrb2 ; | Clspn ; |
| chr5 | Oas2 ; Gbp10 ; Drc1 ; Gm42986 ; | Ncapg ; |
| chr6 | Kcnj8 ; Klra9 ; Igkv4-55 ; Igkv5-39 ; Trbv29 ; | /---/ |
| chr7 | Fcgrt ; Dennd5a ; Sbf2 ; Tspan32 ; Sox6 ; Trpm1 ; | Sox6 ; Cd22 ; |
| chr8 | Gypa ; Nr3c2 ; | Neil3 ; |
| chr9 | S1pr5 ; Izumo1r ; Phxr4 ; Gm48114 ; Gm38111 ; | |
| chrX | Tsc22d3 ; Gm5124 ; Cenpi ; Gata1 ; | Kif4 ; |

This finding can be explained by superimposing of certain number of genetic mutations (errors) associated with aging, on the effect of radiation-induced damages. This fact manifests itself as high expression levels of differently expressed genes corresponding with level of damage, while the radiosensitivity of young organisms determined by radiosensitivity of critical systems.

We carried out comparative analysis of radiation-induced changes in gene expression of young and old mice with genes associated with the aging process in mice (the database published in the GenAge Database of Aging-Related Genes from Human Aging Genomic Resources). Fig.6.

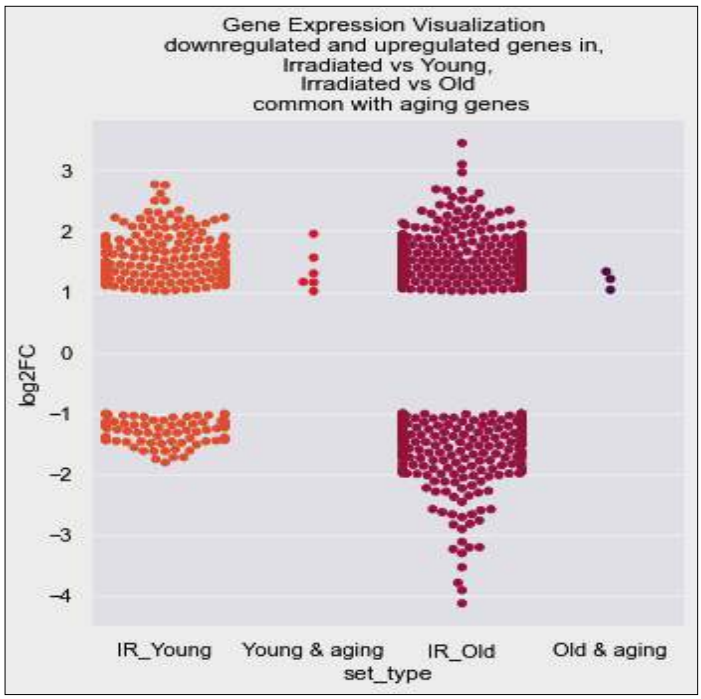


**Figure 6. Differently expressed genes in irradiated and young mice, irradiated and old mice, and genes from both groups, which are common with aging associated genes database.**

Despite the greater number of differently expressed genes in group of old mice, they have only three genes, common with genes from the database associated with aging. In young mice, there are six common genes. The table (Tab. 1.) represents these proteins with their expression levels and type of impact on the lifespan according to the database.

**Table 1. Differently expressed genes from old and young groups, common with aging associated genes.**

| **Group type (Research)** | **Gene name** | **Chromosome (Research)** | **log2FC (Research)** | **Description (Web database information)** | **lifespan effect (Web database information)** | **longevity influence (Web database information)** |
|---|---|---|---|---|---|---|
| Young & aging | Bub1b | chr2 | 1.9509 | Budding uninhibited by benzimidazoles 1 homolog, beta (S. cerevisiae) | Increase and Decrease | Pro-Longevity |
| Old & aging | Bub1b | chr2 | 1.331002 | Budding uninhibited by benzimidazoles 1 homolog, beta (S. cerevisiae) | Increase and Decrease | Pro-Longevity |
| Young & aging | Hells | chr19 | 1.1492015 | Proliferation associated SNF-2-like gene | Decrease | Pro-Longevity |
| Old & aging | Hells | chr19 | 1.0283135 | Proliferation associated SNF-2-like gene | Decrease | Pro-Longevity |
| Young & aging | Lmna | chr3 | 1.5582066 | lamin A | Increase and Decrease | Unclear |
| Young & aging | Foxm1 | chr6 | 1.297876 | Forkhead box M1 | Decrease | Pro-Longevity |
| Young & aging | Txn1 | chr4 | 1.0061757 | Thioredoxin 1 | Increase | Pro-Longevity |
| Young & aging | Brca1 | chr11 | 1.1598353 | Breast cancer 1 | Decrease | Pro-Longevity |
| Old & aging | Brca1 | chr11 | 1.2083834 | Breast cancer 1 | Decrease | Pro-Longevity |

Indicated genes are in more or less degree responsible for organism development and changes in their expression can cause serious pathologies. *Bub1b* gene is encoding spindle assembly checkpoint protein BubR1, the reduction of BubR1 expression in mouse is associated with increased aneuploidy, senescence and infertility [16]. In human low expression of BUB1B contributes to initiation and progression of human colon adenocarcinomas and lung cancer [17]. In our case we can see slight growth of expression in irradiated animals compared to old and young mice. Lymphoid-specific helicase – HELLS is an important component of chromatin remodeling, which takes part in DNA remodeling [18]. Increased expression of HELLS, as in our case is regulated by the oncogenic transcriptional regulator YAP1 downstream of Smoothened, the positive transducer of SHH signaling [19]. A-type lamins are encoded by the lamin A gene (*LMNA*), mutations in *Lmna* is linked to progeroid diseases Hutchinson-Gilford progeria and atypical Werner's syndromes, striated muscle diseases, muscular dystrophies and dilated cardiomyopathies, lipodystrophies affecting adipose tissue deposition, diseases affecting skeletal development, and a peripheral neuropathy. Nuclear lamina has important roles in regulating DNA synthesis, RNA transcription, and in the organization of chromatin [20]. FoxM1 is a member of the forkhead family of transcription factors [21]. In human overexpression of Forkhead Box M1 (FoxM1 or FoxM1b) transcription factor is observed in a number of aggressive carcinomas [22]. Thioredoxin (TXN), encoded by *Txn1* is a critical antioxidant in the defense against oxidative stress, and regulates dithiol/disulfide balance of interacting proteins. Development of the midbrain in juvenile rats critically needs *Txn1* [23]. Early embryonic lethality can be caused by disruption of *Txn1* gene [24]. Mutations in *Brca1* are causing genome abnormalities and instabilities towards cancer, and affecting many oncogenic genes and pathways including DNA damage repair and oncogenesis [25].

We have a suggestion that this set of genes is most vulnerable to radiation in terms of the effect of radiation-induced aging and requires more sophisticated investigation.

## CONCLUSIONS

The investigation of radiobiological effect of ionizing radiation exposure in mice by means of bioinformatics approach based on the criterion of different gene expression, makes it possible to identify a set of genes where visible changes in the level of expression was observed under the influence of radiation. This information may allow us to identify the specific gene set responsible for the radiological regulation of life longevity for inherited aging model.

With a high degree of probability our results may allow us to develop an effective predictive model of aging in mice, to facilitate study of inherited age-related changes. Taking into the account the commonality of investigated genes with human gene analogues, our studies can acquire valuable practical application along with the theoretical significance in the field of biomedicine.

## REFERENCES:

[1]. Tinetti ME, McAvay GJ, Murphy TE, Gross CP, Lin H, Allore HG. Contribution of individual diseases to death in older adults with multiple diseases. J Am Geriatr Soc. 2012 Aug;60(8):1448-56. doi: 10.1111/j.1532-5415.2012.04077x. Epub 2012 Jun 26. PMID: 22734792; PMCID: PMC3419332.

[2]. Jian Tong, Tom K. Hei. Aging and age-related health effects of ionizing Radiation Radiation Medicine and Protection, 2020, Volume 1, Issue 1 (Cover date: March 2020) Pages 15-23

[3]. Mohammed Al-Jumayli, Stephen L. Brown, Indrin J Chetty, Martine, Benjamin. The Biological Process of Aging and the Impact of Ionizing Radiation

[4]. Noda A, et al: Unrepairable DNA double-strand breaks that are generated

by ionising radiation determine the fate of normal human cells. J Cell Sci 125:5280-5287, 2012

[5]. Rossiello F, et al: Irreparable telomeric DNA damage and persistent DDR signalling as a shared causative mechanism of cellular senescence and ageing. Curr Opin Genet Dev 26:89-95, 2014

[6.] Suzuki M, Boothman DA: Stress-induced premature senescence (SIPS)-influence of SIPS on radiotherapy. J Radiat Res 2008. 0801220010-0801220010

[7]. Gilbert SF: Developmental Biology. Sunderland, MA: Sinauer Associates, 2014.

[8]. Kalmakhelidze, Sophio & Museridze, D & Gogebashvili, Mikheil & Lomauri, K & Gabunia, T & Sanikidze, Tamara. (2022). Effects of ionizing radiation on cognitive parameters in white mice. Georgian medical news. 187-192.

[9]. Yashin Anatoliy I., Wu Deqing, Arbeeva Liubov S., Arbeev Konstantin G., Kulminski Alexander M., Akushevich Igor, Kovtun Mikhail, Culminskaya Irina, Stallard Eric, Li Miaozhu, Ukraintseva Svetlana V., Genetics of aging, health, and survival: dynamic regulation of human longevity related traits, Frontiers in Genetics, V-6,2015, https://www.frontiersin.org/articles/ 10.3389/fgene.2015.00122, DOI=10.3389/fgene.2015.00122, ISSN=1664-8021

[10]. Paulo MC de Oliveira, Suzana Moss de Oliveira, Americo T Bernardes, Dietrich Stauffer, Siblings of centenarians live longer: a computer simulation, The Lancet Journal, Published: September 12, 1998DOI:https://doi.org/10.1016/S0140-6736(05)60056-6

[11]. Ruby, J. G., Wright, K. M., Rand, K. A., Kermany, A., Noto, K., Curtis, D., Varner, N., Garrigan, D., Slinkov, D., Dorfman, I., Granka, J. M., Byrnes, J., Myres, N., & Ball, C. (2018). Estimates of the Heritability of Human Longevity Are Substantially Inflated due to Assortative Mating. *Genetics*, *210*(3), 1109–1124. https://doi.org/10.1534/ genetics.118.301613

[12]. Anjum A, Jaggi S, Varghese E, Lall S, Bhowmik A, Rai A. Identification of Differentially Expressed Genes in RNA-seq Data of Arabidopsis thaliana: A Compound Distribution Approach. J Comput Biol. 2016 Apr;23(4): 239-47 doi: 10.1089/cmb.2015.0205 Epub 2016 Mar 7. PMID: 26949988; PMCID: PMC4827276

[13]. https://link.springer.com/protocol/10.1007/978-1-0716-1307-8_20

[14]. https://www.ebi.ac.uk/ena/browser/view/PRJEB38394

[15]. Lucille Lopez-Delisle, Customized gtf file from Ensembl version 92 mm10, ZENODO, OpenAIRE, May 14, 2020, DOI: 10.5281/zenodo.3827120

[16]. Baker, D., Jeganathan, K., Cameron, J. *et al.* BubR1 insufficiency causes early onset of aging-associated phenotypes and infertility in mice. *Nat Genet* 36, 744–749 (2004). https://doi.org/10.1038/ng1382

[17]. Fu X, Chen G, Cai ZD, Wang C, Liu ZZ, Lin ZY, Wu YD, Liang YX, Han ZD, Liu JC, Zhong WD. Overexpression of BUB1B contributes to progression of prostate cancer and predicts poor outcome in patients with prostate cancer. Onco Targets Ther. 2016 Apr 15;9:2211-20. doi: 10.2147/OTT.S101994. PMID: 27143916; PMCID: PMC4844448

[18]. Liang Xiao, Li Linji, Fan Yuchao, "Diagnostic, Prognostic, and Immunological Roles of HELLS in Pan-Cancer: A Bioinformatics Analysis", Frontiers in Immunology, V.13, 2022, https://www.frontiersin.org/articles/10.3389/fimmu.2022.870726,
DOI:10.3389/fimmu.2022.870726, ISSN1664-3224

[19]. Robinson MH, Maximov V, Lallani S, Farooq H, Taylor MD, Read RD, Kenney AM. Upregulation of the chromatin remodeler HELLS is mediated by YAP1 in Sonic Hedgehog Medulloblastoma. Sci Rep. 2019 Sep 20;9(1):13611. doi: 10.1038/s41598-019-50088-1. PMID: 31541170; PMCID: PMC6754407

[20]. Stewart CL, Kozlov S, Fong LG, Young SG. Mouse models of the laminopathies. Exp Cell Res. 2007 Jun 10;313(10):2144-56. doi: 10.1016/j.yexcr.2007.03.026. Epub 2007 Mar 31. PMID: 17493612; PMCID: PMC1949387

[21]. Mónica Alvarez-Fernández and René H. Medema, "Novel functions of FoxM1: from molecular mechanisms to cancer therapy", MINI REVIEW article, Front. Oncol., 05 March 2013, Sec. Molecular and Cellular Oncology, https://doi.org/10.3389/fonc.2013.00030

[22]. Tanya V. Kalin, I-Ching Wang, Timothy J. Ackerson, Michael L. Major, Carol J. Detrisac, Vladimir V. Kalinichenko, Alexander Lyubimov, Robert H. Costa, "Increased Levels of the FoxM1 Transcription Factor Accelerate Development and Progression of Prostate Carcinomas in both TRAMP and LADY Transgenic Mice", Cancer Res (2006) 66 (3): 1712–1720. https://doi.org/10.1158/0008-5472.CAN-05-3138

[23].Iori Ohmori, Mamoru Ouchida, Hirohiko Imai, Saeko Ishida, Shinya Toyokuni, Tomoji Mash imo, “Txn1 mutation causes epilepsy associated with vacuolar degeneration in the midbrain”, bioRxiv 2021.10.07.463470; doi: https://doi.org/10.1101/2021.10.07.463470

[24]. Bondareva AA, Capecchi MR, Iverson SV, Li Y, Lopez NI, Lucas O, Merrill GF, Prigge JR, Siders AM, Wakamiya M, Wallin SL, Schmidt EE. Effects of thioredoxin reductase-1 deletion on embryogenesis and transcriptome. Free Radic Biol Med. 2007 Sep 15;43(6):911-23. doi: 10.1016/j.freeradbiomed.2007.05.026. Epub 2007 May 31. PMID: 17697936; PMCID: PMC2099259.

[25]. Wu, X., Guo, M., Cui, J. *et al.* Heterozygotic *Brca1* mutation initiates mouse genome instability at embryonic stage. *Oncogenesis* 11, 41 (2022). https://doi.org/10.1038/s41389-022-00417-3

# ACCESSORY SPLEEN CYST: A CASE REPORT

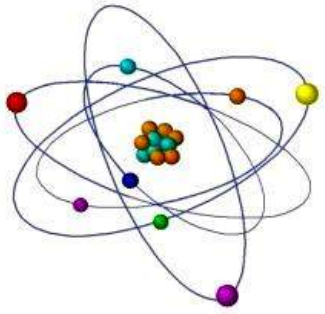

**Urushadze O.P., Tortladze I.M., Karanadze K.M., Labuchidze M.R., Goletiani T.G.**

Radiology Department, The First University Clinic, Tbilisi State Medical University

*Corresponding author: iraklitortladze@yahoo.com

**ABSTRACT:** *Cystic disease of the spleen is a relatively rare disease. It is classified either as a true primary cyst or as a secondary pseudocyst. Most splenic cysts are pseudocysts, which have non-epithelial lining, and are caused by previous abdominal blunt trauma. Conversely, primary splenic cysts have epithelial lining and are subdivided into parasitic and non-parasitic cysts. The non-parasitic primary splenic cyst is considered congenital and comprises about 10% of all splenic cysts. Total or partial splenectomy is the treatment of choice, but parasitic infection must be excluded prior to an operation. In this present report, we described a symptomatic and managed non-parasitic extra splenic cyst.*

**Key words:** accessory spleen cyst, rare radiological diagnosis, computed tomography

## INTRODUCTION

Cystic disease of the spleen is relatively rare, with an incidence of 0.07% [1,2]. The splenic cysts are categorized either as primary (true cysts) or as secondary (pseudocysts). The latter is mostly caused by abdominal trauma and has no epithelial lining in the cystic lumen. Conversely, a primary splenic cyst has an epithelial lining of the lumen.

Additionally, primary splenic cysts are further subdivided into parasitic and non-parasitic cysts. The non-parasitic primary splenic cyst is considered congenital and comprises about 10% of all splenic cysts. An accessory spleen is identical to a normal spleen in terms of function and structure. It is formed by a developmental defect, in the 5th week of embryogenesis [1,2,3,6]. Accessory spleens are found in approximately 10 – 15 % of the general population [4,5,6]. They may be found anywhere along splenic vessels, 1-2% pancreatic tail, the great omentum, the mesentery, or the gonads, most commonly: splenic hilum [3]. We present here a rare case of accessory primary non-parasitic splenic cyst that is confirmed by pathologic diagnosis after partial splenectomy. The combination of these two conditions is very rare in clinical practice.

## CASE REPORT

A 22-year-old female with dull abdominal pain of several days duration was referred to our hospital from a local clinic, where abdominal ultrasonography (US) revealed a large cystic mass in the spleen (Fig.1).

On abdominal examination, a soft non-tender mass was palpable in the left upper quadrant. Her medical history was notable only for an appendectomy performed several years ago. She had no other traumatic event in the abdomen. Her vital signs were stable and all laboratory findings were within the normal range. Abdominal computed tomography (CT) scan revealed the splenic cyst to measure 14 cm in diameter with scoliosis most likely due to mass effect.

**Fig.1. Ultrasound-US accessory spleen cyst Abdominal ultrasound revealed round, avascular, non-homogenous patterns of a cyst mass(25x28mm) in the left upper abdominal quadrant.**

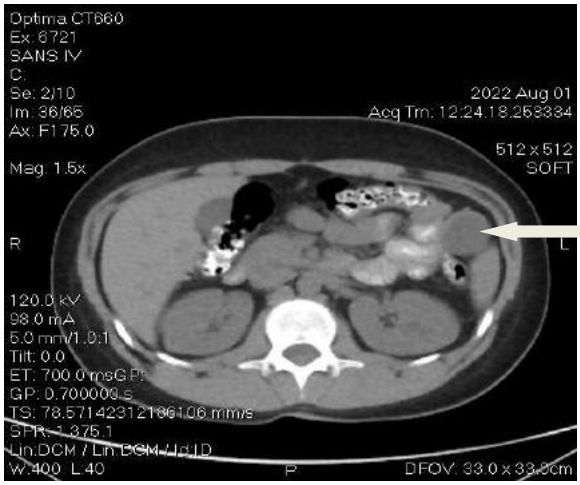


**Fig. 2. Abdominal CT, accessory spleen cyst**

**On the abdominal CT scan, a round-shaped, non-homogenous growth with straight edges was detected at the edge of the spleen. The inside of the growth contained fluid. With contrast enhancement, the cystic formation has its own blood supply. It is a branch of the splenic artery.**

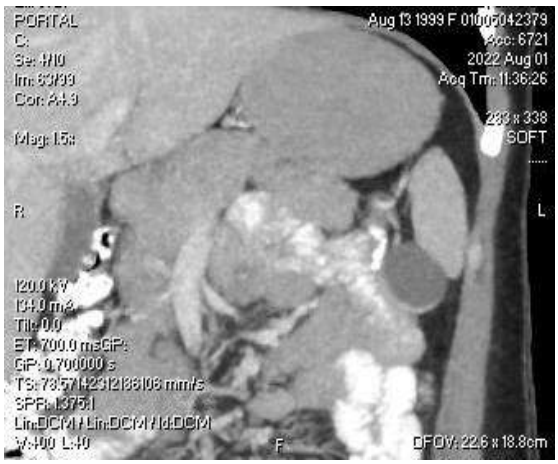


**Fig. 3. Abdominal CT, Accessory spleen cyst, branch of the splenic artery.**

The patient was offered open or laparoscopic partial resection of the spleen, and the patient opted for open surgery for financial reasons. On laparotomy, the cyst was found to arise from the spleen. It was adhered to the left lateral side of the liver and left stomach wall. The cystic fluid was carefully aspirated to avoid rupture into the operation field. After this, the whole cyst was excised in a partial splenectomy. A closed drain was left near the splenectomy site. The result of the serologic hydatid antibody test had been notified several days after the operation and was negative. Both carbohydronic antigen 19-9 (CA 19-9) and carcinoembryonic antigen (CEA) of the cystic fluid were over 1,000 U/ml respectively. The pathologic report indicated a primary splenic cyst with cyst walls containing stratified squamous epithelial cells. The patient was discharged on the 10th postoperative day without complications.

## DISCUSSION

Accessory spleens are found in approximately 10 – 15 % of the general population. They may be found anywhere along splenic vessels, 1-2% pancreatic tail, The great omentum, the mesentery, or the gonads, most commonly: splenic hilum. [1,2,4,5]. Cystic disease of the spleen is relatively rare, with an incidence of 0.07%.1 The splenic cysts are categorized either as primary (true cysts) or as secondary (pseudocysts). The latter is mostly caused by abdominal trauma and has no epithelial lining in the cystic lumen. Conversely, a primary splenic cyst has an epithelial lining of the lumen.
Additionally, primary splenic cysts are further subdivided into parasitic and non-parasitic cysts [7,8]. The non-parasitic primary splenic cyst is considered congenital and comprises about 10% of all splenic cysts. Total or partial splenectomy is the treatment of choice, but parasitic infection must be excluded prior to an operation. In this case, abdominal ultrasonography (US) had revealed a large cystic mass in the spleen, and abdominal ultrasound revealed round, avascular, non-homogenous patterns of a cyst mass (25x28mm) in the left upper abdominal quadrant. Abdominal computed tomography (CT) scan revealed the splenic cyst to measure 14 cm in diameter with scoliosis most likely due to mass effect, on abdominal CT scan a round-shaped, non-homogenous growth with straight edges was detected at the edge of the spleen. The inside of the growth contained fluid, and with contrast enhancement, the cystic formation has its own blood supply. It is a branch of the splenic artery, the tissue is painted as the spleen parenchyma, and the density of the remaining hypodense area does not change.

Radiological diagnosis: Accessory Spleen Cyst

Surgery and the morphological study of the obtained material confirmed the radiological diagnosis. Accessory splenic tissue is identical to the splenic tissue by histomorphological examination, with typical red and white pulp. The result of the serologic hydatid antibody test had been notified several days after the operation and was negative. Both carbohydronic antigen 19-9 (CA 19-9) and carcinoembryonic antigen (CEA) of the cystic fluid were over 1,000 U/ml respectively. The pathologic report indicated a primary splenic cyst with cyst walls containing stratified squamous epithelial cells.

## CONCLUSION

The accessory splenic cyst is very rare in clinical practice. Accurate diagnosis derives from pathological examination after surgical removal. Radiological findings and the features of contrast-enhanced CT are very important to make a correct preoperative diagnosis.

REFERENCES

[1]. Kang, S. I., & Jeon, S. Y. (2013, August). Primary non-parasitic splenic cyst: a case report. Korean J Hepatobiliary Pancreat Surg 17(3), pp. 139-141.
[2]. Zavras, N., Machairas, N., Foukas, P., Lazaris, A., Patapis, P., &Machairas, A. (2014, April). Epidermoid cyst of an intrapancreatic accessory spleen: a case report and literature review. World J Surg Oncol, p. 92.
[3]. Mohammadi S, Hedjazi A, Sajjadian M, Ghrobi N, Moghadam MD, Mohammadi M. Accessory Spleen in the Splenic Hilum: a Cadaveric Study with Clinical Significance. Med Arch. 2016 Oct;70(5):389-391
[4]. Hyo Jung Ko, Jae Ryong Shim, Tae Beom Lee, Byung Hyun Choi, Jung-Hee Lee, Je Ho Ryu Kwangho Yang Epidermoid cyst in an intrapancreatic accessory spleen in the pancreashead: a case report. BMC Gastroenterology, 392 (2020)
[5]. Zhuo Zhang, Jian Cheng Wang. An Epithelial Splenic Cyst in an Intrapancreatic Accessory Spleen. A Case Report.Department of Surgery, Rui Jin Hospital Medical College Jiao Tong University. Shanghai, PR China2009.
[6]. Akkaflo¤lu S, Çelebio¤lu EC, Çal›flkan S, Sancak ‹T. Retrospective radiologic analysis of accessory spleen by computed tomography. Anatomy 2019;13(2):87–91.
[7]. Epidermoid Cyst in a Pancreatic Accessory Spleen Mimicking an Infected Abdominal Cyst in a Child A. M. Fink, S. Kulkarni, P. Crowley, J. A. Crameri
[8]. Intrapancreatic accessory spleen with an epidermoid cyst: a malignant mimicry, JiaJia Wee, Charles K F Vu and Vishal G Shelat.

# EFFECT OF ACUTE GAMMA IRRADIATION ON THE BEHAVIORAL PARAMETERS IN WHITE MICE

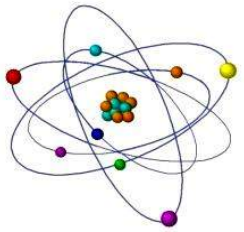

**[1,2]Kalmakhelidze S.L., [1]Museridze D.P., [2]Sanikidze T.V.**

[1]Laboratory of Neurotoxicology, I.Beritashvili Center of Experimental Biomedicine, Georgia
[2]Department of Medical Physics and Biophysics, Tbilisi State Medical University, Georgia

*Corresponding author: sofokalmakhelidze@gmail.com

ABSTRACT: *High doses of ionizing radiation exposure have been shown to induce impairments in the limbic system. As hippocampal abnormalities have been linked to an impairment of behavioral functions, the present work aimed to investigate whether exposure to 5Gy of ionizing radiation can develop behavioral deficits in adult mice. White mice (Mus musculus) were irradiated with $^{137}Cs$. Experimental animals were tested in an open field maze over a period of 30 days after irradiation. A study of open-field parameters revealed that gamma irradiation can be considered a radiobiological factor inducing anxiety and emotionality in mice.*

**Key words:** Gamma irradiation, white mice behavior, open field test

## INTRODUCTION

Radiation-induced brain injury is a long-term and dynamic process. Post-radiation brain injury results in neurobehavioral disorders as a consequence of functional and anatomic deficits [1]. Radiation-induced cognitive impairments are related to the hippocampus, a key subcortical structure in the mammalian brain, involved in three primary functions: the formation of new memories, spatial learning, and emotions. Increasing evidence indicates that radiation-induced early cerebral changes may be determining factors of behavioral and emotional impairments [2,3]. The *Cornu Ammonis* (CA) is a seahorse-like structure that describes the different layers of the hippocampus. There are four hippocampal regions CA1, CA2, CA3, and CA4. CA3 receives fibers from the dentate gyrus granule cells. The entorhinal cortex–hippocampal neuron network plays a major role in episodic memory and spatial information about the occurrence of former events [4,5,6]. Pathophysiological responses to radiation-induced brain injury include the following changes increased numbers of apoptotic cells, reduced neurogenesis in the subgranular zone (SGZ), demyelination, or blood-brain barrier (BBB) disruption [7,8,9]. Stem cells in SGZ of the hippocampal Dentata Gyrus and the SVZ along the lateral ventricles have special sensitivity to ionizing radiation [10,11]. There is growing evidence of significant cognitive impairment during the post-irradiation period when there are no expressed histological abnormalities. Elevated zero maze, the Open Field test, the elevated plus maze, the Morris water maze, and the elevated-type multi-way maze are the most commonly used tests to measure behavior in animal models [12]. High doses of gamma irradiation significantly increase impairment in short-term memory, decreases the spatial learning process, and cause radiation-induced aging [13]. Though the mechanisms involved in this process are still the subject of study.

This study aimed to determine the influence of acute gamma irradiation on behavioral parameters using an open-field maze.

## MATERIAL AND METHODS

The experimental protocol was by the guidelines for the care and use of laboratory animals as adopted by the Ethics Committee of the Tbilisi State Medical University (TSMU). Animal care and maintenance: 3-month-old male mice (Mus musculus), were obtained from the Vivarium of Tbilisi State Medical University. They were housed in animal cages, with room temperature maintained at 200 -220C and relative humidity of 50-70%. Also, a time-controlled system provided 08:00-20:00 h of light and 20:00-08:00 h dark cycles. All mice were given a standard rodent chow diet and water from sanitized bottle fitted with stopper and sipper tubes.

Experimental design.

After acclimatization for a week to laboratory conditions, the mice were divided into two groups. The I control group of 3-month-old not irradiated mice, II experimental group of 3-month-old irradiated mice. Mice whole-body irradiation with $^{137}$Cs was performed at a dose rate of 1,1Gy/min for a total dose of 5Gy with the equipment "Gamma-capsule-2".

Anxiety-like behavior and exploratory activity were estimated in the open field. The open field consists of a Plexiglas enclosure (40×40 cm) placed in the center of a normally lit experimental room. Mice were placed in the left corner of the enclosure; head facing an open space, their anxiety-like and exploratory behaviors were recorded for 5 min across the area divided into 16 squares. The parameters measured were the time spent in the center of the arena (four central squares), the total time spent near the walls, the number of rearing, and defecation. Tests were performed on days 2, 4, 6, 8, 10, 12, 14, and 30 after irradiation.

## RESULTS AND DISCUSSION

Our study aimed to evaluate radiation-induced behavioral changes using an open-field test. The open field test is often used to assess anxiety and locomotor activity; The main variables recorded during the test period are the time taken to leave the starting square, time spent in the center of the arena rearing, grooming frequency, and several defecation boli [15,16].

Less time spent in the central area of the box, increased rearing, grooming, and defecation frequency demonstrates anxiety-like behavior in rodents. Furthermore, thigmotaxis refers to the specific behavior of animals (staying close to walls in the open field), which is a well-established indicator of animal anxiety and fear [17, 18].

In this study, we assessed four parameters of the Open field test (OFT) to evaluate the anxiety and emotionality of experimental animals. As shown in Fig.1 compared to the control group rearing behavior increases on the 2$^{nd}$, 4$^{th}$, 6$^{th}$, 14$^{th,}$ and 30$^{th}$ days after irradiation (5Gy). On the 8$^{th}$, 10$^{th}$, and 12$^{th}$ days after irradiation, the difference from the control group was not statistically significant. Rearing behaviors could be considered as an additional measurement of anxiety in rodents and may be used in the repeated testing process [19,20]. Anxiety-like behavior conditions are thought to be mediated by the hippocampal formation which is a key target of the stress response [21]. Recently, oxidative stress has also been implicated in high anxiety levels. The formation of reactive oxygen species after irradiation could cause hippocampal impairments resulting in behavioral changes [22].

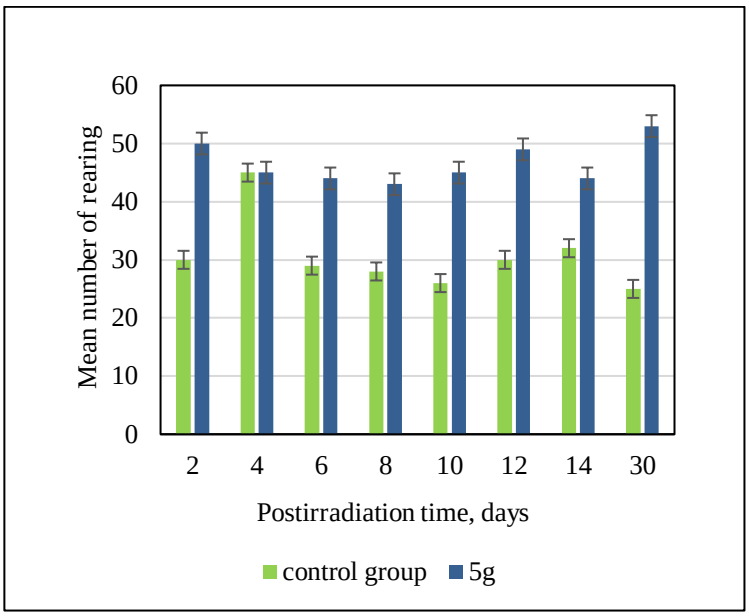


**Fig.1. Mean number of rearing in experimental animals during the post-radiation period**

Thigmotaxis or wall-hugging behavior is observed in experimental mice and is in relation to anxiety-related behaviors. Increased time spent in the outer zones of the maze is linked to thigmotaxis [23,24]. In our study on the 2nd, 4th, 12th, 14th, and 30th days of irradiation time spent in the center is less than time spent at the walls of the maze (approximately 1 minute). Animals of the experimental group showed increased thigmotaxis compared to the control group (Fig.3,4).

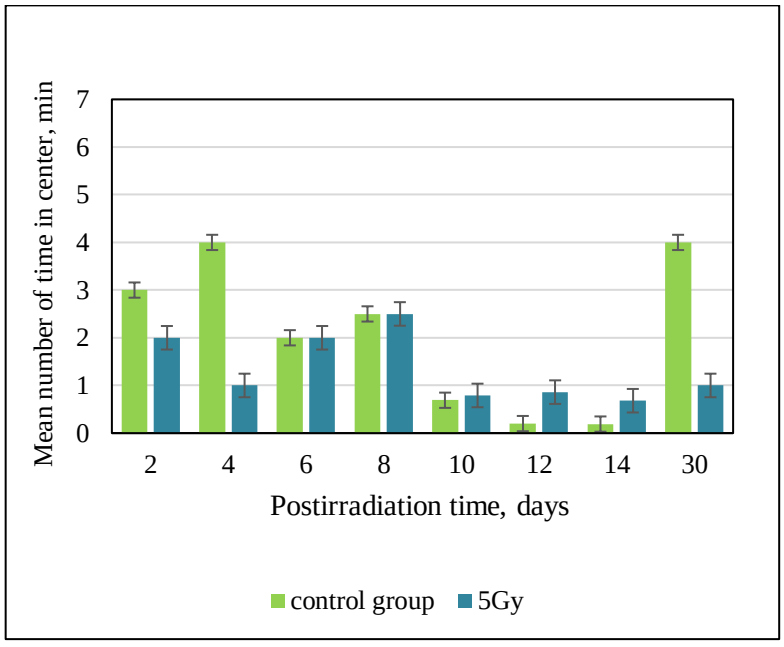


**Fig 2. Mean number of time spent in the center of open field in experimental animals during the post-radiation period**

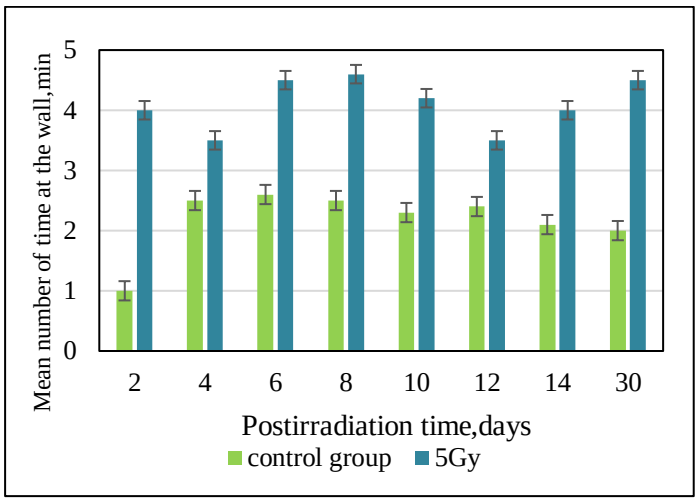


**Fig 3. Mean number of time spent at the walls of open field in experimental animals during the post-radiation period**

The fourth parameter assessed in the open field was the number of defecations as an increased number of boli can be indicative of anxiety and emotionality in the mice (the amount of the boli was calculated after a testing period) Fig. 4 shows a mean number of the bolus according to post-radiation period. On the 2nd, 4th, 6th, 8th, and 30th days of irradiation amount of bolus increases in comparison with control group animals. On the 10th 12th and 14th days, the number of defecations is approximately the same as in the control group.

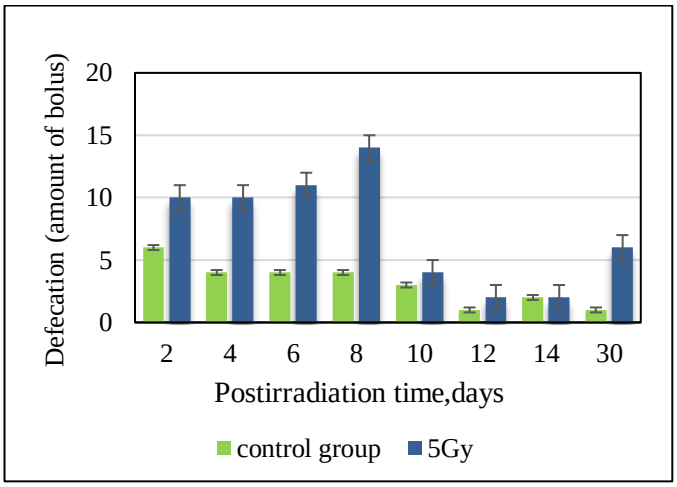


**Fig. 4. Defecation: number of fecal boluses during the post-radiation period**

CONCLUSION

Using a laboratory white mouse model, we showed that ionizing radiation exposure could lead to increased anxiety-like behavior. A study of open-field parameters revealed that gamma irradiation can be considered a radiobiological factor inducing anxiety and emotionality in mice. Behavior changes can be considered as an integrated radiobiological effect, which includes both injury of the central nervous system, as well as implications for other organ systems in this process.

REFERENCES

[1]. Calvo W, Hopewell JW, Reinhold HS, Yeung TK. Time and dose-related changes in the white matter of the rat brain after single doses of X-rays. Br J Radiol.1988; 61:1043–1052

[2]. Rola R, Raber J, Rizk A, Otsuka S, Vanden Berg SR, Morhardt DR, Fike JR. Radiation-induced impairment of hippocampal neurogenesis is associated with cognitive deficits in young mice. Exp Neurol. 2004;188(2):316-30.

[3]. Winocur G, Wojtowicz JM, Sekeres M, Snyder JS, Wang S.Inhibition of neurogenesis interferes with hippocampus-dependent memory function. Hippocampus.2006;16:296–304

[4]. Daugherty AM, Bender AR, Raz N, Ofen N. Age differences in hippocampal subfield volumes from childhood to late adulthood. Hippocampus. 2016;26(2):220-8.

[5]. Kitamura T, Macdonald CJ, Tonegawa S. Entorhinal-hippocampal neuronal circuits bridge temporally discontiguous events. Learn Mem. 2015; 18;22(9):438-43.

[6]. Moser MB, Rowland DC, Moser EI. Place cells, grid cells, and memory. Cold Spring HarbPerspect Biol. 2015; 2;7(2):a 021808.

[7]. Lianhong Y, Jianhua Y, Guoqian L, Yi L, Rong W, Jinping C, Yamei T. Pathophysiological Responses in Rat and Mouse Models of Radiation-Induced Brain Injury. Mol Neurobiol 2017;54(2):1022-1032

[8]. Mizumatsu S, Monje ML, Morhardt DR, Rola R, Palmer TD, Fike JR. Extreme sensitivity of adult neurogenesis to low doses of X-irradiation. Cancer Res 2003; 63:4021–4027

[9]. Belarbi K, Jopson T, Arellano C, Fike JR, Rosi S. CCR2 deficiency prevents neuronal dysfunction and cognitive impairments induced by cranial irradiation. Cancer Res. 2013;73:1201–1210.

[10]. Rao AA, Ye H, Decker PA, Howe CL, Wetmore C. Therapeutic doses of cranial irradiation induce hippocampus-dependent cognitive deficits in young mice. J Neuro Oncol. 2011;105:191–198.

[11]. Tada E, Parent JM, Lowenstein DH, Fike JR. X-irradiation causes a prolonged reduction in cell proliferation in the dentate gyrus of adult rats. Neuroscience. 2000; 99:33–41

[12]. Seibenhener ML, Wooten MC. Use of the Open Field Maze to measure locomotor and anxiety-like behavior in mice. J Vis Exp. 2015; 6:(96):e52434.

[13]. Kalmakhelidze, S., Museridze, D., Sanikidze, T., Gogebashvili, M., Tophuria, D., Ivanishvili, N., &Ormotsadze, G. (2021). Study of Cognitive Parameters in Postradiation Period in White Mice. Radiobiology and Radiation Safety, Vol.1, #1, 57–62.

[14]. Alexander TC, Butcher H, Krager K, Kiffer F, Groves T, Wang J, Carter G, Allen AR. Behavioral Effects of Focal Irradiation in a Juvenile Murine Model. Radiat Res. 2018 Jun;189(6):605-617

[15]. Jänicke B, Coper H. Tests in Rodents for Assessing Sensorimotor Performance During Aging Advances in Psychology. 1996; Vol.114:201-233

[16]. Valvassori SS, Budni J, Varela RB, Quevedo J. Contributions of animal models to the study of mood disorders. Braz J Psychiatry. 2013;35 Suppl 2:S121-31.

[17]. Walz N, Mühlberger A, Pauli P. A Human Open Field Test Reveals Thigmotaxis Related to Agoraphobic Fear. Biol Psychiatry. 2016 Sep 1;80(5):390-7.

[18]. Seibenhener ML, Wooten MC. Use of the Open Field Maze to measure locomotor and anxiety-like behavior in mice. J Vis Exp. 2015 Feb 6;(96):e52434.
[19]. Fritz, A.K., Amrein, I., & Wolfer, D.P. (2017). Similar reliability and equivalent performance of female and male mice in the open field and water-maze place navigation task. American Journal of Medical Genetics, Part C: Seminars in Medical Genetics, 175, 380–391. doi:10.1002/ajmg.c.31565
[20]. Oliver Sturman, Pierre-Luc Germain & Johannes Bohacek (2018) Exploratory rearing: a context- and stress-sensitive behavior recorded in the open-field test, Stress, 21:5, 443-452
[21]. Lawrence, Y.R., Li, X.A., el Naqa, I., Hahn, C.A., Marks, L.B., Merchant, T.E., Dicker, A.P.Radiation dose-volume effects in the brain. Int. J. Radiat. Oncol. Biol. Phys. 2010; 76, S20–S27
[22]. Bouayed J, Rammal H, Soulimani R. Oxidative stress and anxiety: relationship and cellular pathways. Oxid Med Cell Longev. 2009;2(2):63-7.
[23]. Tye, K. M., Prakash, R., Kim, S. Y., Fenno, L. E., Grosenick, L., Zarabi, H., et al. Amygdala circuitry mediating reversible and bidirectional control of anxiety. Nature.2010; 471, 358–362.
[24]. Makale, M.T., McDonald, C.R., Hattangadi-Gluth, J., Kesari, S. Brain irradiation and long-term cognitive disability: current concepts. Nat. Rev. Neurol.2017; 52–64.

# MEGAKARYOBLASTS AND ERYTHROBLASTS IN MICE BONE MARROW AFTER GAMMA-IRRADIATION WITH SUBLETHAL DOSES. EXTRACELLULAR UBIQUITIN EFFECT

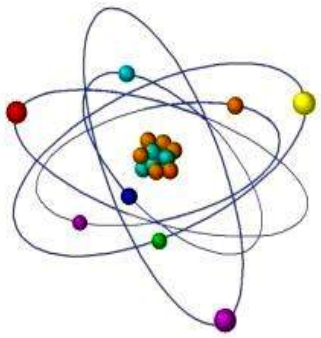

***Sujashvili R.Sh, Ioramashvili I.V.**
Laboratory of Biophysics, I.Beritashvili Center of Experimental Biomedicine, Georgia

*Corresponding author: sujaruss@gmail.com

ABSTRACT**:** *Studies show that erythropoiesis and thrombopoiesis are interrelated. We provided cytological and statistical analyses of elevation-depletion picks for megakaryocytes and erythroblasts in bone marrow (BM) and the passage of mature cells into the bloodstream (PB) of irradiated mice.*
*The source of radiation was $^{137}Cs$ with dose rate 1Gy/min., due exposure 5min. Nonlinear white mice of 23±2gr. were used for tests. Animals were divided into three groups: the first control group of intact mice; the second test group of mice irradiated with the dose of $LD_{50}$ 5Gy; the third test group of mice irradiated with 5Gy intraperitoneally injected with ubiquitin at the 72-hour point after irradiation. PB and BM samples from the control group and the test groups of mice have been taken every 24 hours after irradiation for 7 days. Microscopy and statistical methods have been used for calculation of cell count of PB and BM.*
*Analysis of the most active periods of bone marrow spontaneous regeneration - 3-5$^{th}$ days – showed us that intraperitoneally injected ubiquitin modulates the ratio of erythroblast/megakaryocytesand descends pick sizes during proliferative activity in BM. Thrombocytosis detected in the second groupcounterbalanced by ubiquitin in the third group. Erythrocyte's count remained almost unchanged. One can assume that Platelet count increase in PB is associated with passage of both megakaryocytes and morphologically transformed erythroblasts. Further investigation with appliance of more sophisticated technics is necessary to evince feasibility of ubiquitin involvement in erythroblast/platelet transition. Probability of prevention of thrombocytosis by extracellular ubiquitin is high. More so as ubiquitins ability to moderate leukocyte regeneration picks was corroborated by our previous works.*

**Key words:** Erythroblasts, megakaryocytes, irradiation, platelet regeneration

## INTRODUCTION

Today, more than ever, the threat of radiation pollution is relevant. Radiation can be non-ionizing, that is, safe, but usually when we talk about radiation, we mean ionizing radiation that is dangerous to health. Types of ionizing radiation are high-frequency ultraviolet waves, gamma rays, X-rays, alpha and beta particle radiation [1]. The primary causes of radiation disease are radiation contamination of the environment, natural radiation sources, inadequate management of radiodiagnosis and radiotherapy. Radiation disease classically considered a blood disease, can develop when the body is irradiated with a single high dose or with a low dose for a long time [2].

Ionizing radiation can damage the human body at the molecular, cellular or organ level. The subsequent life cycle of a damaged cell can develop in three ways: the cell dies immediately, the cell can repair the damage in the DNA structure, or the cell enters a dormant state. A dormant cell, if not provoked, may remain in the body for a lifetime and not develop into a tumor.

The very first effect of irradiation is cellular depletion in bone marrow causing immunological problems during regeneration due to release of nonfunctional cells into the bloodstream.

Although high-dose chemotherapy and radiotherapy prolong survival in cancer patients, the side effects of these therapies, including pancytopenia, remain serious concerns [3,4].

Recent studies have shown that stimulation of erythroid cells with erythropoietin (Epo) leads to a decrease in the number of megakaryocytes and following thrombocytopenia. Conversely, both

endogenous and exogenous sources of thrombopoietin induce activation of thrombocytopoiesis and anemia in mice [5,6].

It should also be noted that megakaryocytes and erythrocytes have certain biochemical similarities, and various clinical conditions indicate a feedback relationship between the production of red blood cells and platelets. This hypothesis is confirmed by several studies. The discovery of agents that affect such transformation may be useful both for the regulation of malignant transformation of blood and protecting cancer patients from therapy-induced thrombosis [7].

After administration of a megakaryocyte differentiation stimulating agent phorbol 12-myristate 13-acetate (PMA)-into erythroleukemic cell culture, 4 Gy X-ray irradiation significantly increased the expression of CD41 antigens within 72 hours. Hence, radiation enhances the differentiation of erythroleukemic cells towards the megakaryocyte cell line [8,9].

Severe thrombocytopenia may result in spontaneous bleeding. In radiation injured patients, bleeding and thrombocytopenia are directly responsible for significant mortality.

The protein ubiquitin has been recognized for the last two decades as one of the main regulators of cellular processes.Our recent experimental results confirmed that extracellular ubiquitin has the ability to regulate the spontaneous regeneration of bone marrow cells [10,11].Hence,we speculated it probably shows effect on changes of ratio of erythroblasts and platelets and could serve as a regulator of thrombocytopenias caused by the posttherapeutic treatment of cancer patients.

## MATERIAL AND METHODS

Non-linear white mice MUS MUSCULUS were used for study. Blood was obtained after decapitation of anesthetized animals. Bone marrow samples collected from femora and samples prepared immediately. Femoral marrow content was expelled by syringe containing 0.5 ml of saline. Clots of bone marrow were homogenized by agitation through the syringe. 5.000 cells per Azur-eosin-stained samples were counted. Animals were anesthetized by ether before decapitation. Statistical analyses were performed by RStudio software.

Treatment of animals performed in accordance with regulations established by the animal's ethic committee of Iv. Beritashvili Center of Experimental Biomedicine (Protocol N06/13.10.2020).

## RESULTS AND DISCUSSION

We provided cytological and statistical analyses of alterations of elevation-depletion picks for megakaryocytes and erythroblasts in bone marrow (BM) and the passage of mature cells into the bloodstream (PB) of irradiated mice.

$^{137}$Cs was used as a source of radiation with dose rate 1Gy/min., due exposure 5min. Nonlinear white mice Mus Musculus of weight of 23±2gr. were used for tests. Animals were divided into three groups: the first control group of intact mice; the second test group of mice irradiated by the dose of $LD_{50}$5Gy; the third test group of mice irradiated by $LD_{50}$ 5Gy intraperitoneally injected by 20μg/mlof ubiquitin at the 72-hour point after irradiation. PB and BM samples from the control group and the test groups of mice have been taken every 24 hours after irradiation for 7-8 days [Fig.1., Tab.1,2].

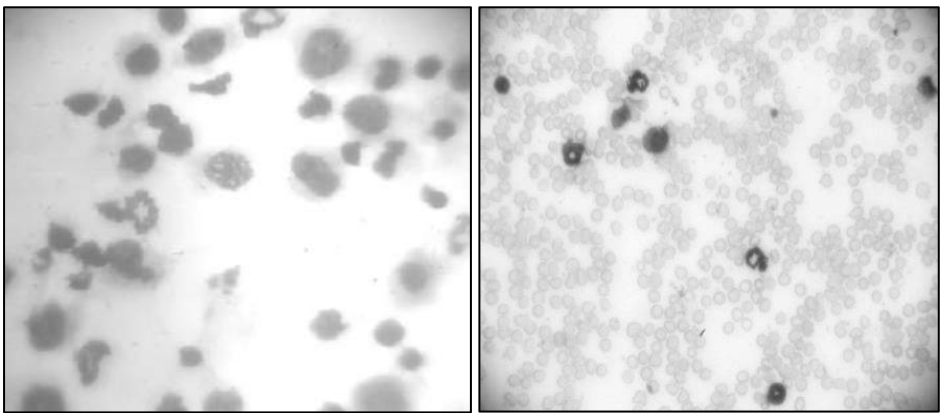

**Fig. 1. Samples of microscopy figures of blood and bone marrow smears for mice of control group Azur-eosin staining. Magnification 1000X.**

Count of erythroblasts and megakaryocytes decrease within 24 hours after irradiation. Elevation begins in 48 hours, followed by a depletion. The number of erythrocytes in the blood is practically unchanged. The number of platelets increases dramatically in 3-5 days, which probably occurs at the expense of both erythroid and thrombotic precursors as it is seen that both counts decline [Tab.1, Fig.2].

**Tab. 1. Total amount of cells per group. The results expressed as means±SD.RStudio packages "gtsummary", "tidyverse", flextable" are used for calculation of the esults**

| **Days/N-total counted cells** | **1/ N = 30[1]** | **2/ N = 30** | **3/ N = 30** | **4/ N = 30** | **5/ N = 30** | **6/N = 30** | **7/ N = 30** | **8/ N = 30** | **control, N = 60[1]** | **p-value [2]** |
|---|---|---|---|---|---|---|---|---|---|---|
| Erythrocytes PB | 632.3 (±37.4) | 610.2 (±28.4) | 620.3 (±37.0) | 588.0 (±40.6) | 619.0 (±49.3) | 617.3 (±30.1) | 622.5 (±31.3) | 601.8 (±35.4) | 635.8 (±38.2) | <0.001 |
| ThrombocytesPB | 8.6 (±1.9) | 10.3 (±2.5) | 18.4 (±2.9) | 20.1 (±3.0) | 21.7 (±2.7) | 10.7 (±2.9) | 9.7 (±2.7) | 10.8 (±3.0) | 15.5 (±4.2) | <0.001 |
| Megakaryocytes BM | 10.9 (±2.9) | 12.1 (±3.3) | 10.0 (±2.3) | 5.9 (±1.1) | 8.2 (±2.0) | 9.0 (±2.0) | 9.9 (±1.8) | 8.4 (±1.7) | 15.7 (±5.4) | <0.001 |
| Erythroblast BM | 52.3 (±19.1) | 76.1 (±19.5) | 44.2 (±9.0) | 35.9 (±10.6) | 54.7 (±11.6) | 51.6 (±12.5) | 55.7 (±10.5) | 57.3 (±8.2) | 101.0 (±24.4) | <0.001 |
| [1]Mean (SD) | | | | | | | | | | |
| [2]Kruskal-Wallis rank sum test | | | | | | | | | | |

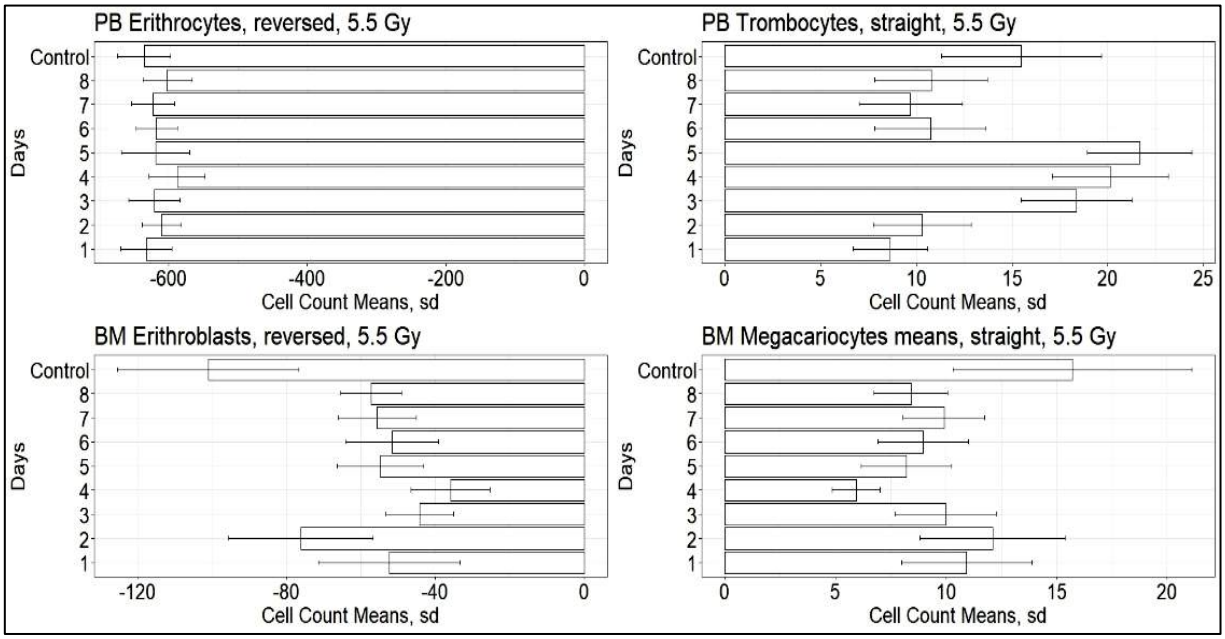


**Fig. 2. Statistical analyses of PB and BM cells of irradiated mice. Source of radiation $^{137}$Cs. The results expressed as means±SD. Control group presents intact animals, test group – irradiated mice 5Gy, due 1Gy/min. RStudio packages"ggplot2", "cowplot", "tidyverse" used for demonstration the results.**

In ubiquitin injected groups we observed strict elevation of platelets in 6 hours due corresponding 78 hours after irradiation followed by diminish of cell number next 3 days, unlike previous irradiated groups. Erythroblast and megakaryocyte count moderated, whilst erythrocyte count remained unchanged [Tab.2, Fig.3].

**Tab. 2. Total amount of cells per group. The results expressed as means±SD.RStudio packages "gtsummary", "tidyverse", flextable" are used for calculation of the results.**

| Day/ N- total counted samples after ubiquitin injection | 3/N = 30[1] | 4/N = 30 | 5/N = 30 | 6/N = 30 | 7/N = 30 | Control N = 60[1] | p-value[2] |
|---|---|---|---|---|---|---|---|
| ErythrocytesPB | 611.7 (±23.6) | 622.8 (±31.3) | 619.3 (±30.6) | 613.8 (±33.9) | 619.0 (±41.2) | 635.8 (±38.2) | 0.057 |
| Thrombocytes PB | 24.8 (±5.7) | 20.2 (±3.5) | 12.4 (±2.4) | 9.2 (±2.6) | 8.9 (±2.2) | 15.5 (±4.2) | <0.001 |
| Megakaryocytes BM | 9.2 (±1.7) | 9.8 (±2.0) | 7.3 (±1.9) | 9.7 (±2.2) | 9.2 (±1.7) | 15.7 (±5.4) | <0.001 |
| Erythroblasts BM | 31.4 (±11.8) | 58.8 (±16.0) | 46.1 (±15.4) | 50.6 (±10.1) | 50.4 (±12.6) | 101.0 (±24.4) | <0.001 |
| [1]Mean (SD) | | | | | | | |
| [2]Kruskal-Wallis rank sum test | | | | | | | |

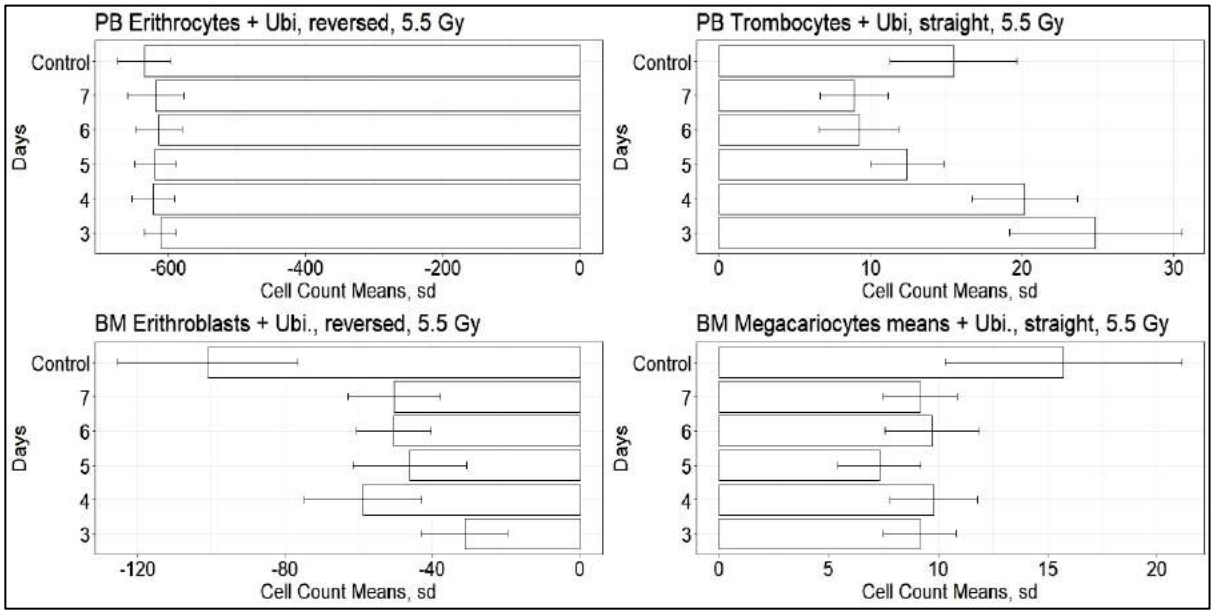


**Fig. 3. Statistical analyses of PB and BM cells of irradiated mice. Source of radiation $^{137}$Cs. The results expressed as means±SD. Control group presents intact animals, test group – irradiated mice 5Gy, due 1Gy/min.20µg/mlof ubiquitin at the 72-hour point after irradiation. RSudio packages "ggplot2", "cowplot", "tidyverse" are used for demonstration the results [12,13,14].**

Analysis of the most active periods of bone marrow spontaneous regeneration - 3-5$^{th}$ days – showed us that intraperitoneally injected ubiquitin modulates the ratio of erythroblast/megakaryocytes and descends pick sizes during proliferative activity in BM. Thrombocytosis detected in the second group counterbalanced by ubiquitin in the third group. Erythrocyte's count remained almost unchanged. One can assume that Platelet count increase in PB is associated with passage of both megakaryocytes and morphologically transformed erythroblasts. Probability of prevention of thrombocytosis by extracellular ubiquitin is high. More so as ubiquitin ability to moderate leukocyte regeneration picks was corroborated by our previous works [10,11]. Ubiquitinis evidently involved in regulation of transformation of bone marrow cells and regulates platelet count, hencemay be useful for the regulation of malignant transformation of blood and protecting cancer patients from therapy-induced thrombosis. Further investigation with appliance of more sophisticated technics is necessary to evince feasibility of ubiquitin involvement in erythroblast/platelet transition.

REFERENCES

[1] Pawel, D. J., &Puskin, J. S. (2012). U.S. Environmental Protection Agency Radiogenic Risk Models and projections for the U.S. population. *Health Physics*, *102*(6), 646–656. https://doi.org/10.1097/hp.0b013e318242794c

[2] Brenner, D. J., et al. (2003). Cancer risks attributable to low doses of ionizing radiation: Assessing what we really know. *Proceedings of the National Academy of Sciences*, *100*(24), 13761–13766. https://doi.org/10.1073/pnas.2235592100

[3] Elting, L. S., et al. (2001). Incidence, cost, and outcomes of bleeding and chemotherapy dose modification among solid tumor patients with chemotherapy-induced thrombocytopenia. *Journal of Clinical Oncology*, *19*(4), 1137–1146. https://doi.org/10.1200/jco.2001.19.4.1137

[4] Dardis, C., Milton, K., & Patel, N. (2017). Thrombopoietin receptor agonists are effective in treating chemotherapy-induced thrombocytopenia in patients with gliomas undergoing myelotoxic treatment. *Oncomedicine*, *2*, 37–41. https://doi.org/10.7150/oncm.17909

[5] Antonchuk, J. *et al.* (2004) "Synergistic effects on erythropoiesis, thrombopoiesis, and stem cell competitiveness in mice deficient in thrombopoietin and steel factor receptors," *Blood*, 104(5), pp. 1306–1313. Available at: https://doi.org/10.1182/blood-2004-04-1522.

[6] Shiozawa, Y. *et al.* (2013) "Erythropoietin supports the survival of prostate cancer, but not growth and bone metastasis," *Journal of Cellular Biochemistry*, 114(11), pp. 2471–2478. Available at: https://doi.org/10.1002/jcb.24592

[7] Hacein-Bey-Abina, S. *et al.* (2020) "Erythropoietin is a major regulator of thrombopoiesis in thrombopoietin-dependent and -independent contexts," *Experimental Hematology*, 88, pp. 15–27. Available at: https://doi.org/10.1016/j.exphem.2020.07.006

[8] BİRİKEN, D., YAZIHAN, N. and YILMAZ, Ş. (2018) "Investigation of cytokine and Midkine responses of human THP-1 leukemia cells induced by PHORBOL-12-MYRISTATE-13- acetate (PMA) at different concentrations and Times," *MikrobiyolojiBulteni*, 2018(2), pp. 147–155. Available at: https://doi.org/10.5578/mb.66745.

[9] YANG, J. *et al.* (2010) "Shp1 gene induces apoptosis and erythroid differentiation in human erythromyeloblastoid leukemia cell line K562," *Academic Journal of Second Military Medical University*, 30(6), pp. 653–656. Available at: https://doi.org/10.3724/sp.j.1008.2010.00653

[10] Rusudan Sujashvili, *et al*. (2020) "Moderation of quantitative changes of regenerating erythropoietic cells by extracellular ubiquitin "*Georgian Medical News*,292-293, pp. 87-92;https://www.researchgate.net/publication/336125050

[11] Sujashvili, R., et al. (2016). "Regulation of leucogenesis by extracellular ubiquitin in rodents after chemically induced inhibition," J. Cytology and Genetics, 50(5), pp. 334–338, SpringerLink. https://link.springer.com/article/10.3103/S0095452716050133

[12] Wickham, H., & Sievert, C. (2016). *GGPLOT2: Elegant graphics for data analysis*. Amazon. Retrieved February 7, 2023, from https://www.amazon.com/ggplot2-Elegant-Graphics-Data-Analysis/dp/331924275X

[13] Wickham, H., et al. (2019). "Welcome to the Tidyverse". *Journal of Open Source Software, 4*(43), 1686. https://doi.org/10.21105/joss.01686

[14] Sjoberg D, Whiting K, Curry M, Lavery J, Larmarange J (2021). "Reproducible Summary Tables with the gtsummary Package." *The R Journal*, 13, 570-580. doi:10.32614/RJ-2021-053, https://doi.org/10.32614/RJ-2021-053

# RADIOBIOLOGICAL HYPOTHESIS OF THE EVOLUTION OF GEORGIAN WHEAT

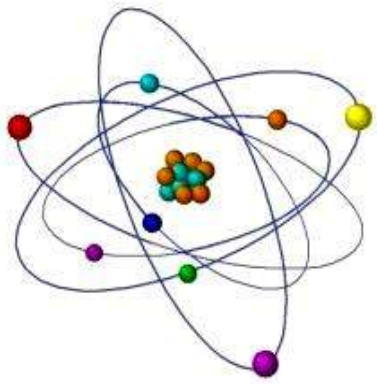

**[1]Gogebashvili M.E*, [1]Ivanishvili N.I, [2]Chokheli M.I., [1]Shubitidze M.N, [2]Chxutiashvili G.A, [2]Samadashvili C.Z.**

[1]I.Beritashvili Center of Experimental Biomedicine, Laboratory of Radiation Safety Problems, Georgia.
[2]Scientist-Research Center of Agriculture, Georgia

*Corresponding author: gogebashvili@gmail.com

ABSTRACT: *The efficiency of research on the origin and evolution of crop species is largely determined by the development of multidisciplinary theoretical and methodological approaches. Modern molecular genetics and archaeological techniques have revealed new aspects of the theory of centers of the origin of crop species. Based on this, the issue of the evolution of Georgian wheat landraces is one of the most important scientific tasks for understanding the processes of unique gene centers formation outside the known boundaries of the spreading cultural zones. In thisaspect, the search for factors of the possible effect on the evolution of specific species can significantly advance us in understanding the formation of isolated groups of the genus Triticum L. Despite many years of study on this issue, the absence of a definitive, generally accepted pattern of the origin of all species of wheat makes it difficult to ascertain the exact phylogeny of both ancestors and the genus as a whole. In our studies, we considered the possibility that radiation factor may be involved in the evolution of Georgian landraces. It is shown that in the case of the radiation effect, conditions are created for evolutionary changes towardthe polyploidization of species.The use of endemic species: Triticum monococcum L- 2n = 14, Triticum timopheevii (Zhuk) Zhuk.-2n=28, Triticum macha Dekapr. & Menabde - 2n=42, Triticum zhukovskyi Menabde & Ericzjan- 2n=42, Triticum dicoccum Schrank ex Schübler - 2n = 28, Triticum aestivum 2n = 42. Revealed clear dependence of radioresistance on the level of their ploidy. Having examined the places where endemic wheat species were found and matched them tothe background radiation of this zone, the conclusion is made about the possibility of the impact of the radiation factor on the evolutionary process of Georgian wheat landraces.*

**Key words**: wheat, radiation, ploidy, evolution.

## INTRODUCTION

Georgia's wheat, as well as grape vines, have great historical and cultural significance, in addition to their agricultural purpose. This is the reason for the great interest in scientific research on the origin and distribution of wheat. Based on the use of molecular-genetic, biochemical, botanical, cytological, immunological, geographical, archeological and other methods, as a result of many years of research on various types of wheat, a hypothesis was formed about the possible course of evolution of the genus Triticum [1,2,3,4]. As early as the end of the 18th century, the first hypotheses appeared that indicated the existence of parallelism in the localization of wild and cultivated plants [5]. The abundance of hypotheses led to the revelation of mutually contradictory results. Vavilov made a significant contribution to the formation of views on the centers of origin of cultivated plants [6,7,8,9,10]. He was the first one to show that cultivated plants developed not

only limited distribution boundaries but also a specific area. Despite its small area, Georgia is the only country in the world where 15 types of wheat are recorded. Out of 15 types of wheat, 5 of them are endemic to Georgia. The mountainous regions of Racha-Lechkhumi are considered to be the place of origin of endemic Georgian wheat. [11,12.] Based on expedition materials and theoretical conclusions, Vavilov unequivocally showed that the centers of origin of cultural plants are located in the zones of optimal climatic conditions of the earth, and what is especially noteworthy, these "centers" are mainly located in mountain ecosystems. There is an abundance of evidence in favor of the assumption that the first foci of cultivation of such plants were mountain ecosystems and from there spread to the surrounding bar areas [13]. According to the natural parameters, the mentioned zones differ in temperature, soil moisture, relief diversity, which created favorable conditions for the geographical isolation of species. At the same time, if we take into account the differences of evolutionarily established forms, we can assume that genetically diverse centers should be characterized by some additional natural conditions, under the influence of which it would be possible to cause intense mutational processes. In mountainous regions - high radiation background can be considered as such condition.

As is known, the natural radiation background is determined by the mountain deposits, soil and water, as well as space radiation. An important component of the radiation background is the natural radioactivity of mountain rocks and soil, which is mainly represented by radioactive potassium, uranium, thorium and their decay products. No less noteworthy is the fact that, unlike the modern radiation background, radiation exposure reached a significant level in the past geological eras. [14] The evolution of Georgian wheat provides an opportunity to obtain a rather wide range of genetic material [15], the results of research conducted in this direction can be used as a model for explaining the evolutionary processes of the relatively closed zones of mountainous regions. Based on the above-mentioned factors, the aim of our research was to study the possible influence of ionizing radiation on the course of evolutionary processes of endemic Georgian wheat, as well as on the formation of phylogenetic processes in specific mountainous regions of Georgia.

## MATERIAL AND METHODS

Wheat plants with different genomic indicators were used as the object of research: *Triticum monococcum.L, Triticum timopheevii (Zhuk) Zhuk, Triticum dicoccum Schrank ex Schübler, Triticum macha Dekapr. & Menabde, Triticum zhukovskyi Menabde & Ericzjan, and Triticum aestivum*. The modeling factor of radiation exposure was gamma radiation, which allows for determining the level of radioresistance of genotypes of researched plants. Pre-sowing irradiation of wheat seeds was carried out on a gamma-device (irradiation source $^{137}$Cs, dose rate – 1,1 Gy/min).

## RESULTS AND DISCUSSION

As can be seen from fig.1, the selected varieties of wheat differ from each other in the level of radioresistance. Because of this, it was not difficult to separate three groups according to radioresistance: I-2n=14- is characterized by low radioresistance; II-2n=28- group with medium radioresistance; III-2n=42- the most radiostable group.

Such a clear dependence between ploidy and the level of radioresistance is a theoretical basis for the conclusion that in the presence of radiation factor in the environment, the directed formation

of mechanisms of adaptive effects is taking place. In particular, the process of polyploidization of many plant organisms during radiation exposure creates a prerequisite for the formation of a genotype with high radioresistance. This phenomenon is confirmed by studies of polyploidization processes of Georgian wheat varieties [16]. It is clear that the realization of these forms of natural selection requires long-term, chronic exposure to the selection factor. By comparing the Vavilovian picture of the centers of origin of cultivated plants and the zones of uranium deposits, it can be confirmed that many centers of intense speciation exactly correspond to the zone of uranium deposits, which is characterized by an anomalously high natural radiation background on the Earth's surface [17].

All of this confirms the correspondence of the location of almost all the centers of intensive speciation of cultural plants investigated by Vavilov [18] and many micro-centers of the origin of narrow-endemic species of related crops identified by Zhukovsky [19] with uranium accumulation zones, which are characterized by high natural radioactivity of the environment, which is completely understandable from the point of view of modern radiobiology; That is, it is possible that the main mutagenic factor is a highly radioactive environment, which has the ability to affect the entire complex of plants at the same time. Presumably, the latter circumstance can explain the parallelism in the variation of the inheritance of related organisms. Those natural circumstances (optimal climatic zones, differences in the microclimate of mountainous regions, temperature, soil, amount of precipitation, conditions of geographical isolation), which, according to Vavilov, determined the localization of the centers of form formation, probably also influenced the origin of species.

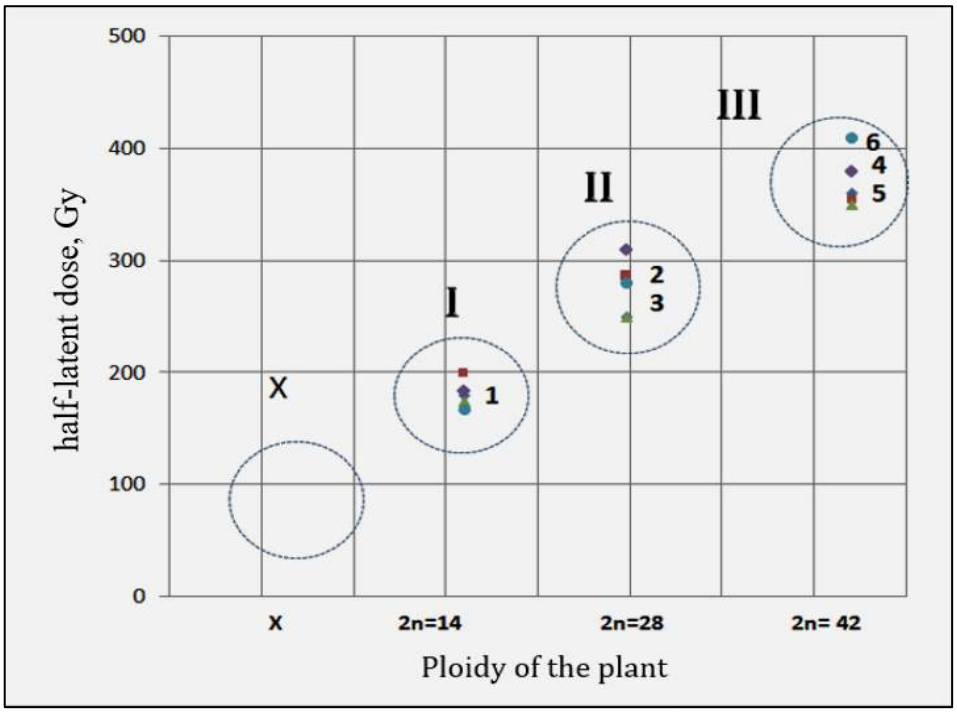


**Fig. 1. Ranked groups of radioresistance of test plants**

1-*Triticum monococcum.L,* 2-*Triticum timopheevii (Zhuk) Zhuk.,*
3-*Triticum dicoccum Schrank ex Schübler,* 4-*Triticum macha Dekapr. & Menabde.,*
5-*Triticum zhukovskyi Menabde & Ericzjan.,* 6-*Triticum aestivum L.*
Conditional groups of I-III radioresistance, X-hypothetical zone of radioresistance.

Of particular importance are studies showing that intense radiation exposure appears to be the most powerful and major factor in induced mutagenesis. During the long geological effects, the impact of the mentioned factor ensured intensive speciation processes and active natural selection.Therefore, the study of the radiological state of endemic areas can significantly strengthen the position in the assessment of the role of ionizing radiation in the evolution of local wheat species.

For the reliability of the model of the effect of radiation on the formation of endemics, we carried out an analysis of the zones in which the main endemic kinds of wheat were found for a certain period of time. This zone was mainly represented by the Racha-Lechkhumi region [20,21].Geographically, this zone is located on the northern borderline: Tsageri-Orbeli-Lailashi-Patara Oni; Eastern border: Khvanchkara-Dgnorisa; South and West: Tamakoni-Gordi-Mkewana (fig. 2).As can be seen from the presented picture, this area is characterized by a highdegree of isolation of landscapes, as well as a high rate of radioactivity. The study of the radionuclide content of the mentioned zone showed the presence of radioactive elements of uranium, thorium, and potassium in the soil [22]. Taking into account the physical characteristics of these natural radionuclides (for example, the half-life of uranium - 4.4 billion years), we can assume the radioactivity of this zone for many geological periods.


**Fig. 2. The landscape zone of Racha-Lechkhumi, where several types of Georgian endemic wheats have been recorded.**

CONCLUSIONS

Thus, as a result of the analysis of the radiobiological parameters of the detection zone of Georgian wheat species (Racha-Lchkhumi), a conclusion can be made with great probability about the participation of radiation in the formation of genotypes within the given zone. Radiation is such an influencial factor that has the ability to cause polyploidization processes in wheat species, which, in turn, leads to an increase in their radioresistance. It is on the basis of this last statement that we tried to formulate the radiation-local hypothesis of the evolution of Georgian

wheat varieties, in favor of which Vavilov's phrase - "the zones of the maximum variety of cultural plants, are also the centers of their origin" [8].The paleobotanical data obtained in recent years about the development of agriculture in specific areas are noteworthy, which indicates the polycentric origin of this field [23].Naturally, the radiation-local hypothesis offered by us does not provide a concrete answer to the question of the evolution of Georgian wheat. However, the radiobiological approach indicates a lack of defined evolutionary links (Fig, 1) both at the level of the organism and the origin of specific genes. It is known that in the ecological zones of isolated landscapes, there is a high probability of the disappearance of certain forms of organisms, which is why the study of intermediate genetic links (due to their existence) creates great difficulties, and molecular-genetic studies are carried out only on the basis of existing genetic lines. In our opinion, further study of the detailed issues related to thepeculiarities of the evolutionary processes of isolated mountain ecosystems requires multidisciplinary approaches.

REFERENCES

[1]. T. Beridze, The “Wheat Puzzle” and Kartvelins Route to the Caucasus, International Scientific Conference, Wheat In European Countries and Georgian as of the Origin of Wheat, October 02-04, 2019, Tbilisi Georgi, pages 83-92
[2]. AnnedeVareilles, Ruth Pelling, Jessie Woodbridge, Ralph Fyfe. Archeology and agriculture: plants, people, and past land-use. Volume 36, Issue 10, 2021, Pages 943-954.
[3]. Pengzheng Lei Xiulan Wei RuitingGaoFulinHuoXiaojunNie Wei Tong Weining Song. Genome-wide identification and characterization of SRO gene family in wheat: Molecular evolution and expression profiles during different stresses. Plant Physiology and Biochemistry, Volume 154, September 2020, Pages 590-611.
[4]. KishkAbdelmageed, Xu-hong Chang, Zhi-Qiang Tao. Evolution of varieties and development of production technology in Egypt wheat: A review. Journal of Integrative Agriculture. Volume 18, Issue 3, March 2019, Pages 483-495.
[5]. Stromeyer F. CommentatioinauguralissistensHistoriaeVegetabiliumGeographicæ specimen. Göttingae: H. Dieterich, 1800.-80p.
[6]. Wagner M. Die Darvin'scheTheorie und das Migrationsgesetz der Organismen. Leipzig: Duncker and Humblot, 1868. 62 s.
[7]. Vavilov N.I. On the Eastern Centers of Origin of Cultivated Plants // Novy Vostok. 1924. No. 6. S. 291–305.
[8]. Vavilov N.I. Centers of origin of cultivated plants//Works on applied botany and breeding. 1926, v.16, No. 2, -248s.
[9]. Vavilov N.I. World centers of varietal wealth (genes) of cultivated plants//Izvestiya GIOA, 1927, v.5, No. 5, p.339-351.
[10]. Vavilov N.I. Estudiosorbeel origin de las plantascultivatas // Buenos Aires: Acmé Agency. 1951a. 192 p.
[11]. Sinskaya E.N. Historical geography of cultural flora (At the dawn of agriculture). Publishing house "Kolos", 1969, 480s.
[12]. Neruchev S.G. Uranus and life in the history of the Earth. Publishing house 2nd VNIIGRI, 2007, -326s.
[13]. M. Mosulishvili, D. Bedoshvili, I. Maisaia. A consolidated list of Triticum species and varieties of Georgia to promote the repatriation of local diversity from foreign genebanks. Annals of Agrarian Science 15 (2017) 61-70.

[14]. Marine Mosulishvili, David Bedoshvili, InezaMaisaia, Nana Rusisshvili, GulnariChkhutiashvili, The ancient, traditional Georgian wheat species and their role in wheat evolution, Wheat In European Countries and Georgian as of the Origin of Wheat, October 02-04, 2019, Tbilisi Georgi, pages 232-239.
[15]. Samadashvili Tsotne, Chkhutiashvili Gulnari, Endemic species and varieties of the Georgian wheat and their value, Wheat In European Countries and Georgian as of the Origin of Wheat, October 02-04, 2019, Tbilisi Georgi, pages 92-98.
[16]. Gorgidze A.D. Phylogenetics of Georgian endemic wheats. Metzniereba, 1977, - 218p.
[17]. Laverov N.P. Foreign deposits of uranium. M.1983.-320s.
[18]. Vavilov N.I. Origin and geography of cultivated plants. L.1987, -438s.
[19]. Zhukovsky P.M. The world gene pool of plants for breeding. Megagencentres and endemic microgencentres.L. "Science", 1970, -88s.
[20]. L. Menabde Wheat of Georgia 1948.
[21]. P. Naskyashvili, M. Sikharulidze, E. in Chernihiv. Wheat selection in Georgia 1983. [22]. Nacvaladze D. at al. Establishment exposure doses of ground radioactivity in the territory of Georgia, Radiation research, Tbilisi, 1998, v.VIII, p.243-259.
[23]. Smith B.D. Eastern North America as an independent center of plant domestication//Proc/Natl Acad/Sci.USA.2006, V.103.N33. p.12223-12228.

# HEALTH PECULIARITIES OF THE EMPLOYEES IN INTERVENTIONAL MEDICAL CARE

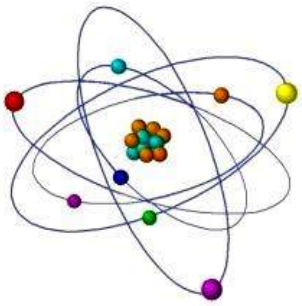

**Tsimakuridze M. P*., Giorgadze N.G., Tsimakuridze M.P., Topuria D.Z., Matoshvili M.T.**

Tbilisi State Medical University, Tbilisi, Georgia

*Corresponding author: mtsimakuridze98@yahoo.com

ABSTRACT: *According to the prognosis of WHO experts, ischemic heart diseases as well as cerebrovascular diseases in the world will occupy a prominent place among the ten leading causes of disease burden by 2030, which will further increase the number of people involved in the management of these pathologies as well as the number of employees in this field. Among the modern methods of the treatment of cardiovascular pathologies, interventional cardio therapy has achieved significant advancement in recent years. The purpose of the study was to determine the characteristics of health disorders of medical personnel employed in specialized procedures (coronary interventional cardiology). The objects of the research were: medical personnel working in coronary interventional cardiology and workers of cardiac catheterization laboratories of medical centers. The criteria for the inclusion of clinics in the study were: the presence of an interventional cardiology department, the smooth operation of the mentioned department during the last 3 years and involvement in the General Healthcare Programme with the emergency inpatient service. 56 employees of the catheterization laboratory were interviewed with the questionnaire prepared by us. Among them, 21 were interventional medical workers (all males), 11 were interventional assistants (all males), and 24 were catheterization laboratory nurses (9 females and 15 males). Factors of the work environment and work mode affect the health status of the employees. Among the interviewees, there was a high level of evidence of sensitization of the body, which was manifested in an increase in cases of the respiratory system and skin allergies (40% of the men (interventional workers: 58% 37-55-year-old; assistants: 26% 29-34-year-old; nurses: 16% 24-26-year-old age group representatives) and 48% of the women (interventional workers: 0%; assistant 0%; nurse 100% 28-35-year-old age group representatives). An increase in allergic reactions was noted (skin rashes in the form of small petechiae, burning and itching of the eyes, increased skin pigmentation, and allergic rhinitis were detected).*

**Key words**: interventional workers, factors of the work environment, allergic health effects

According to the frequency of development, diseases of the cardiovascular system have been in first place in the list of non-communicable diseases (NCDs) for years. Cardiovascular diseases are one of the main causes of death in all the countries of the world and account for about half of the deaths caused by noncommunicable diseases. According to experts, this number will reach 23.6 million by 2030 (Figure 1) [1].

More than 80% of these cases occur in middle- and low-income countries, where human and financial resources for healthcare are limited. According to the prognosis of WHO experts, ischemic heart disease will occupy a prominent place among the ten leading causes of disease burden in the world by 2030 (Figure 2) [1, 2]. In the structure of incidence of ischemic heart diseases in Georgia, angina pectoris accounts for almost half of the cases accounts for angina pectoris, the share of which has increased from 38.4% to 49.3%, while the rate of the share of myocardial infarction: 2.9% to 7.0% [5, 7].

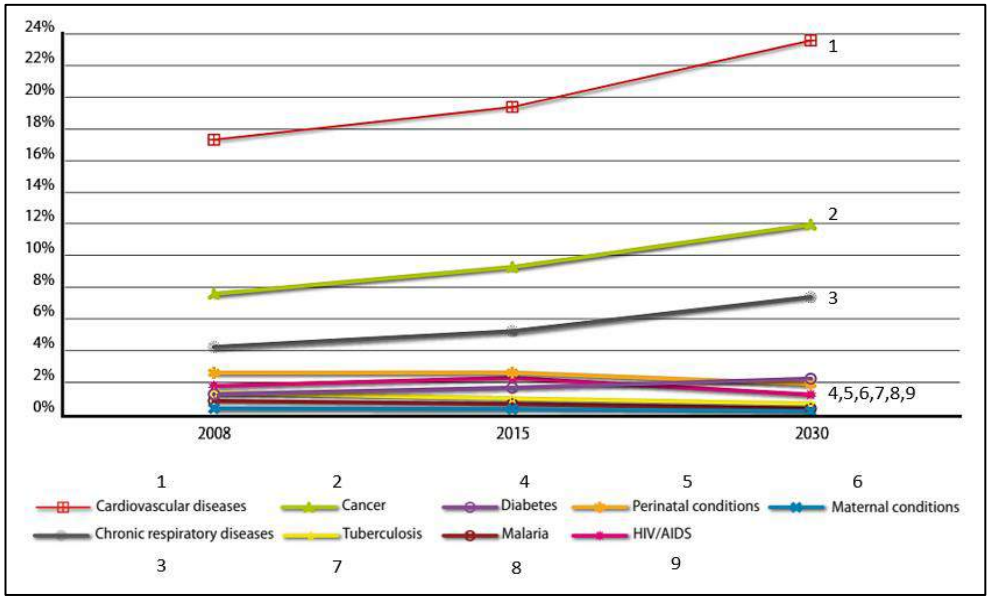


**Fig.1. The projected mortality trends from 2008 to 2030 for NCDs, CVDs and communicable diseases (Global Atlas on Cardiovascular Disease Prevention and Control WHO)**

| 2004 Disease or injury | As % of total DALYs | Rank | Rank | As % of total DALYs | 2030 Disease or injury |
|---|---|---|---|---|---|
| Lower respiratory infections | 6.2 | | | 6.2 | Unipolar depressive disorders |
| Diarrheal diseases | 4.8 | | | 5.5 | Ischaemic heart disease |
| Unipolar depressive disorder | 4.3 | | | 4.9 | Road traffic accidents |
| Ischaemic heart disease | 4.1 | | | 4.3 | Cerebrovascular disease |
| HIV/AIDS | 3.8 | | | 3.8 | COPD |
| Cerebrovascular disease | 3.1 | | | 3.2 | Lower respiratory infections |
| Prematurity and low birth weight | 2.9 | | | 2.9 | Hearing loss, adult onset |
| Birth asphyxia and birth trauma | 2.7 | | | 2.7 | Refractive errors |
| Road traffic accidents | 2.7 | | | 2.5 | HIV/AIDS |
| Neonatal infections and other | 2.7 | | | 2.3 | Diabetes mellitus |
| COPD | 2.0 | | | 1.9 | Neonatal infections and other |
| Refractive errors | 1.8 | | | 1.9 | Prematurity and low birth weight |
| Hearing loss, adult onset | 1.8 | | | 1.6 | Birth asphyxia and birth trauma |
| Diabetes mellitus | 1.3 | | | 1.6 | Diarrheal diseases |

**Fig.2 Tenleadingcausesofburdenofdisease,world,2004and2030 (Global Atlas on Cardiovascular Disease Prevention and Control WHO)**

In order to avoid the forecast made by WHO experts for 2030, in September 2015, the United Nations adopted the Sustainable Development Goals for 2016-2030, the third goal of which is related to health: "Ensure healthy lives and promote well-being for all age groups". Among the defined sub-goals, two are quantitative in nature, and one of them envisages a 1/3 reduction in mortality from non-communicable diseases [2, 3].

According to the prognosis of WHO experts, ischemic heart diseases as well as cerebrovascular diseases in the world will occupy a prominent place among the ten leading causes of disease burden by 2030, which will further increase the number of people involved in the management of these pathologies as well as the number of employees in this field. This implies the management of the working conditions as well as the work process of the employees and the detection of their possible health effects [2, 3, 9].

Among the modern methods of the treatment of cardiovascular pathologies, interventional cardio therapy has achieved significant advancement in recent years [4, 6, 8]. The main achievement of interventional cardio therapy is to reduce the period of post-procedural rehabilitation and to avoid the development of post-operative discomforts, such as pains and surgery scars as much as possible. Interventional cardio therapy is the "gold standard" for the treatment of acute myocardial pathology [6].

A coronary intervention involves restoring the patency of stenosed (narrowed) or occluded (clogged) blood vessels with a special endoprosthesis (stent). This procedure has significantly improved the condition of the patients. If years ago, heart surgery was often perceived as a process far more serious than the disease itself, today it is considered a simple and easy intervention. Stenting is not performed without a coronary angiography, because it depends on the findings of this study, whether the stent can be implanted in the stenosed or occluded section of the blood vessel or not. According to WHO recommendations, angiography of coronary arteries is recommended for patients with ischemic heart disease (IHD) [8].

With the improvement of cardiac catheterization techniques (which implies better radiographic equipment, a contrast with fewer side effects) and the introduction of effective methods of coronary artery disease treatment (coronary stenting, aortocoronary shunting (CABG)), diagnostic coronary angiography has become one of the most important components of cardiac catheterization. Every year, several million coronary angiograms are performed worldwide, and procedural lethality is only 0.1% [6, 7, 8].

The purpose of the study was to determine the characteristics of health disorders of medical personnel employed in specialized procedures (coronary interventional cardiology). The objects of the research were: medical personnel working in coronary interventional cardiology and workers of cardiac catheterization laboratories of medical centers. Adequate selection of medical centers was carried out at the initial stage in accordance with the aim and objectives of the research. The criteria for the inclusion of clinics in the study were: the presence of an interventional cardiology department, the smooth operation of the mentioned department during the last 3 years, and involvement in the General Healthcare Programme with the emergency inpatient service.

Taking into account the listed criteria, 14 medical centers were selected for the study (9 of them were multi-professional, and 5 were mono-professional), where sanitary-technical and sanitary-hygienic indicators were evaluated, which were compared with the relevant normative acts, and a survey of the working staff was conducted with a specially designed questionnaire.

Based on the timing of interventional medical workers' activities, it was revealed that one cycle of intervention lasts 45 minutes. From individual operations, the maximum time (10-10 min) is spent on antiseptics and anesthesia, as well as on hemostasis (by applying dressing and bandages), which is 22.2-22.2% of the total work cycle.

The average duration of coronary angiography takes 20 minutes, coronary stenting takes 30 minutes (the duration of the procedure depends on the anatomical features of the patient's coronary arteries and the number of stents required for placement). On average, 7 procedures are performed during a day: 4 coronary angiography and 3 stenting procedures.

Implantation of a pacemaker and a cardioverter-defibrillator (ICD) lasts 2 hours, the average number of which is 3-5 during a month (often a patient refrains from such intervention due to financial problems).

During the month, there were 5-6 calls to the interventional medical worker at night for the procedure. During the timing of the labor process, it was determined that the coronary study actually takes 20-40 minutes, and the stenting takes 40-50 minutes.

It is known that 0.05% of the patient's radiation dose is irradiated to medical personnel (exposed parts of the body) when wearing protective clothing. And the dosimeter, inside the lead jacket, records an additional 10% of 0.05%. The interventionist's assistant and support staff are irradiated with 30% of the amount of radiation of the operator [8].

During a study to find out if the medical personnel usually use personal protective equipment (to reduce radiation), it was determined that 98% of catheterization laboratory personnel do not use protective glasses; 67% of medical personnel do not attach the dosimeter to their body during the procedure; in most cases, it is not possible to determine closeness to the upper limit of radiation during the day, and subsequently, 98% of the personnel do not use a special radiation reducing shield during the procedure.

Factors of the work environment and work mode affect the health status of the employees. 56 employees of the catheterization laboratory were interviewed with the questionnaire prepared by us. Among them, 21 were interventional medical workers (all males), 11 were interventional assistants (all males), and 24 were catheterization laboratory nurses (9 females and 15 males). The average age was distributed as follows: interventional workers - 40.3 years, assistants - 32.1 years, catheterization laboratory female nurses - 28.5 years, and male nurses - 25 years. The average work experience in the interventional sphere of interventional workers was 10.3 years, interventionist assistants – 3.1 years, and catheterization laboratory nurses – 1 year.

To the question - "Has your health condition changed during the period of work in interventional medicine?" in 55% of cases the answer was negative, and in 45% of cases, we received a positive answer (diagram 1).

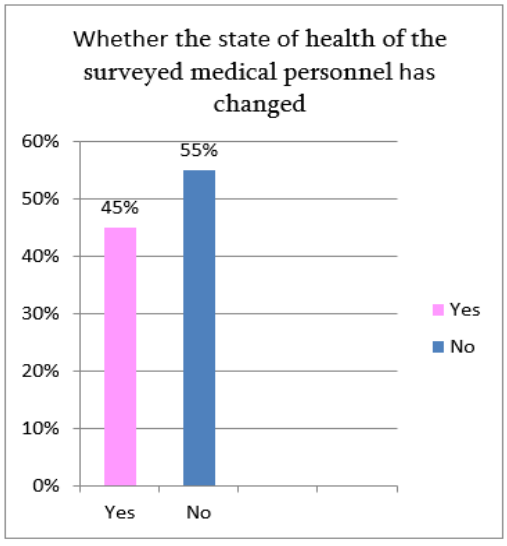


**Diagram 1**

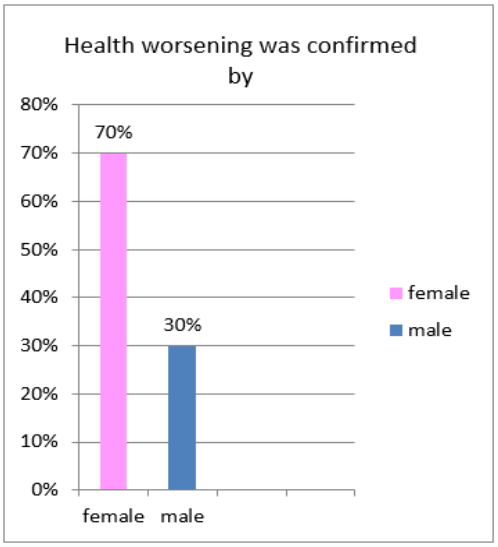


**Diagram 2**

Of 56 interviewed persons who reported deterioration of their health 70% were women, and 30% were men (diagram 2).

Further analysis of the data was conducted in the group of individuals with health effects.

Among the interviewees, there was a high level of evidence of sensitization of the body, which was manifested by an increase in cases of the respiratory system and skin allergies (40% of the men (interventional workers: 58% 37-55-year-old; assistants: 26% 29-34-year-old; nurses: 16% 24-26-year-old age group representatives) and 48% of the women (interventional workers: 0%; assistant 0%; nurse 100% 28-35-year-old age group representatives). It should be noted that depending on the

specifics of the professionals the correctness of the diagnoses recorded by the interviewees hardly raises any doubts.

An increase in the allergic reactions was noted (skin rashes in the form of small petechiae, burning and itching of the eyes, increased skin pigmentation, and allergic rhinitis were detected), which, in turn, was aggravated by the disorders of the ventilation system in 7-8% of the investigated clinics, the use of contrast substances during the procedures, the lack of adequate ventilation of the room. Also, the interior decoration of the clinic, made with low-quality building materials, created conditions for the sensitization of the body.

In general, clinic employees, not only catheterization laboratory staff, reported allergic reactions when they were in the clinic, while leaving the building the complaints were resolved. A positive exposure and elimination test was recorded, indicating the action of allergens in the workplace. It should be noted that there was no strict control over disinfectant solutions, which should have hypoallergenic ingredients.

We think that the complaints regarding immune system disorders were caused by the peculiarity of the interviewed medical personnel's activities. In particular, stress, irrationally distributed work process, disordered biorhythm (an average of 5-6 - night calls during a month), and presence of haptens/allergens in the workplace.

REFERENCES

[1]. Global Atlas on cardiovascular disease prevention and control (WHO)

[2]. Global status report on noncommunicable diseases 2014 “Attaining the nine global non-communicable diseasestarget: a shared responsibility” WHO

[3]. Contribution of six risk factors to achieving 25x25 non-communicable disease mortality reduction target:modellingstudy www.the lancet.com.2014

[4]. Grossman & Baim's Cardiac Catheterization, Angiography, and Intervention Eighth Edition

[5]. Peculiarities of the Spread of Cardiovascular Diseases - National Center for Disease Control and Public Health (Georgian)

[6]. Practical Handbook of Advanced Interventional Cardiology: Tips and Tricks4th Edition, Kindle EditionHealthcare / Brief Statistical Review 2016 -National Center for Disease Control and Public Health (Georgian)

[7]. Oxford Textbook of Interventional Cardiology – Edited by Simon Redwood, Nick Curzen, Martyn Thomas, Oxford University Press

[8]. Shaburishvili T., Khabeishvili G., Amaglobeli L., Wann L.S.et all., Interventional Cardiology for Coronary Diseases, Tbilisi Cardiovascular Clinic Publishing House, Tbilisi 2010 (Georgian)

[9]. Tsimakuridze M., Giorgadze N., Tsimakuridze M, Hygienic Assessment of the Working Environment of Employees in Interventional Medicine, J. Radiology and Radiation Safety, Vol.1, N2, 2021, p.93-100

# A RETROSPECTIVE ANALYSIS OF CT COLONOSCOPY OF 7 YEARS EXPERIENCE IN A CLINICAL PRACTICE

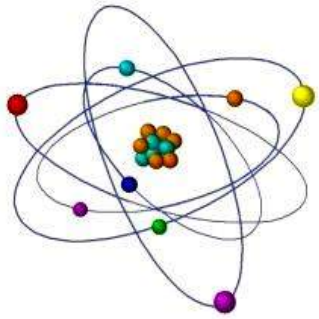

***Tandilava I.I.[1,2,3], Urushadze O.P.[2], Tsetskhladze D.SH.[1,3], Kashibadze K.N.[1,3], Phutkaradze S.I.[1], Meskhi N.E.[1], Berodze M.R.[1]**

Batumi Referral Hospital[1], Georgia
Tbilisi State Medical University[2], Georgia
Batumi Shota Rustaveli State University[3] Georgia

*Corresponding author: iatandilava@gmail.com

ABSTRACT*: Timely diagnosis of cancerous and non-cancerous colon diseases is one of the pressing issues of modern medicine. Colorectal cancer is a significant problem for the world population due to its high prevalence and mortality rates and the considerable financial costs associated with this disease, and its possible complications. CT colonography is a highly informative and less invasive imaging method of the large intestine. Despite worldwide implementation into clinical practice, especially in the USA and Western European countries, it is rarely used in Georgia. The study aims to increase the effectiveness of diagnosing pathologies of the large intestine in our country by promoting the widespread implementation of the CT colonography method in clinical practice and improving the techniques of conducting the study and interpreting the results. The study took place in the Batumi referral hospital, where CT colonography was introduced into clinical practice in 2015, after which it has been actively used and becoming more popular daily. The material was collected from May 15, 2015, to October 31, 2022. A total of 352 CT colonography were performed in the mentioned period. By analyzing the data of our examined patients and statistical processing, we obtained the following results: sensitivity of CT colonography in the diagnosis of congenital anomalies of the colon is 98.0%, specificity - 100%, diagnostic accuracy - 98.2%; in the diagnosis of diverticula, respectively: 92.3%, 95.1%, 92.7%; In the diagnosis of polyps: 87.3%, 85.6%, 85.9%. Based on the obtained results, it can be concluded that CT colonography is an accurate, highly informative, and less invasive method of colon examination; Colorectal cancer screening performed with it is less invasive, less time-consuming, and as effective as optical colonoscopy; one of the most prominent advantages of CT colonography is the ability to detect non-intestinal pathologies. Improving the technical parameters of CT colonography will allow us to reduce radiation exposure levels for patients while maintaining image quality.*

**Key words:** Virtual CT Colonoscopy, Virtual Colonoscopy, CT Colonography

## INTRODUCTION

Timely diagnosis of cancerous and non-cancerous colon diseases is one of the important issues of modern medicine. According to the statistics of the International Agency for Research on Cancer (IARC) in 2020, colorectal cancer is the third most common malignant tumor in the world and the second most common cause of cancer-related deaths (Fig. 1) [1]. Colorectal cancer is a big problem for the world population due to its prevalence, high mortality rate, and the significant financial costs associated with this disease and its possible complications [2,3].

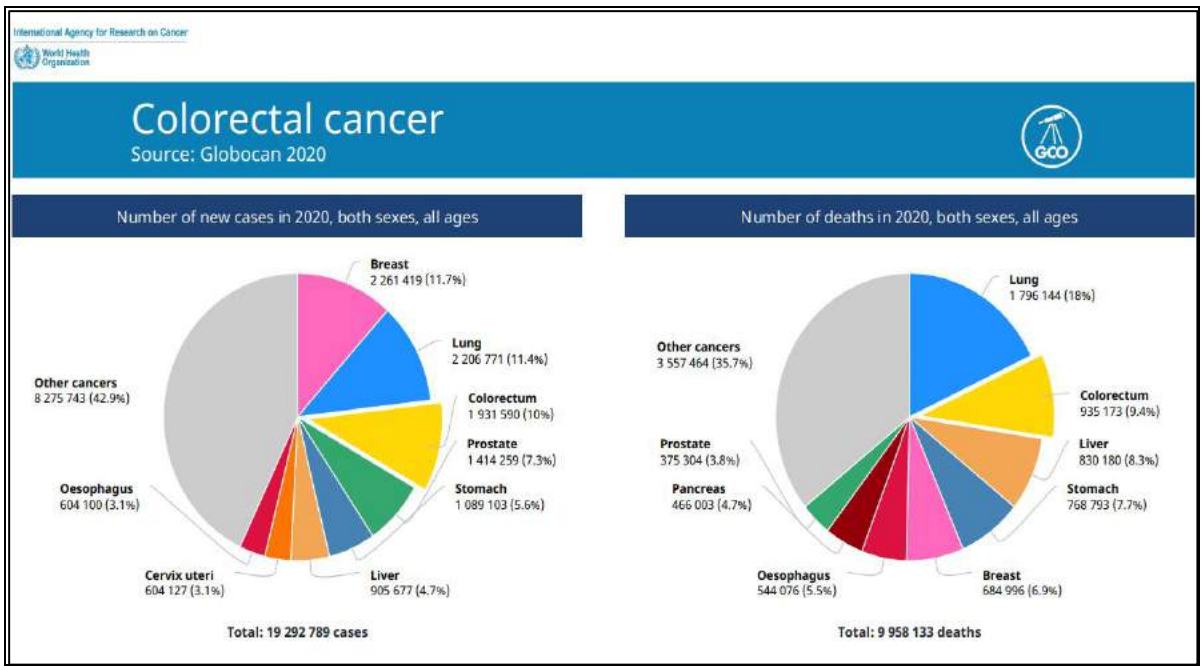


**Figure 1. International Agency for Research on Cancer (IARC) 2020 statistics.**

In addition, it should be noted that the number of patients with colorectal cancer and other various pathologies of the large intestine (Crohn's disease, diverticulosis complications) is increasing irreversibly. Despite the above, the number of deaths caused by colorectal cancer in recent decades has also decreased, which is a direct result of the improvement of its screening, treatment, and diagnostic methods [1,4,5,6,7].

Nowadays, the primary methods for diagnosing pathologies of the large intestine are irrigoscopy-irrigography, optical colonoscopy, computer tomography, and CT colonography; In recent years, colon ultrasound and MRI-colonography have been actively used in clinical practice [8,9]. Each method has its advantages and disadvantages, but none of them can provide a complete study of the large intestine.

CT colonography is a highly informative and less invasive diagnostic method, detecting pathological changes in the colon wall and diagnosing cancer at an early stage [7,10,11,12,13]. With its help, a qualified and experienced radiologist can assess the shape, location, contours, haustration, folds, lumen, wall thickness, and the surface of the colon, detect the pathological area and determine its exact location, assess the degree of tumor invasion, the condition of surrounding tissues and lymph nodes, identify regional and distant metastases, assess the state of other organs in the abdomen [3,6]. Compared to colonoscopy, the examination is quicker and less invasive, it is elegant and comfortable, does not require sedatives and analgesics, and has a lower probability of complications, including a small risk of perforation (1-2:20,000); Due to these properties, unlike optical colonoscopy, its repeated use does not represent significant discomfort for the patient [2,3,4,5,14].

CT colonography is currently one of the main methods of diagnosing colon diseases in the USA and Western European countries; In addition, in some advanced countries, it is included in the colorectal cancer screening program; For example, CT colonography is supported by the US Preventive Services Task Force (USPSTF) as one of the main methods of colorectal cancer screening for medium-risk patients [5,15,16].

Despite the widespread implementation of CT colonography in clinical practices worldwide, especially in the USA and Western European countries, and its high diagnostic capabilities, the method is rarely used in Georgia. The study aims to increase the effectiveness of the diagnostics of large intestine pathologies in our country by promoting the widespread implementation of CT colonography in medical practices and improving the methodology and interpretation of the results.

## MATERIALS AND METHODS

The study was conducted based on the Batumi referral hospital, where CT colonography was introduced into clinical practice in 2015, after which it was actively used and becoming more popular by the day. The materials were collected from May 15, 2015, to October 31, 2022. A total of 352 CT colonography were performed in the mentioned period.

In all cases, the patient was familiarized with the necessary information about the procedure and signed the voluntary informed consent to participate in the study, following the form developed by us based on literary material, which was approved by the Biomedical Research Ethics Committee of Tbilisi State Medical University on October 15, 2017 (committee meeting N4-2017/64, 15th October 2017). During the clinical study, the patient's complaints, disease anamnesis, and clinical examination data were studied in detail. Among the instrumental methods, CT colonography, optical colonoscopy, irrigography-irigoscopy, gastrointestinal kinetic radiography, colon ultrasound, and MRI examination were performed.

CT colonographic studies were performed on a GE Brivo CT 385 16 Slice machine according to the following steps:

- Determination of examination indication,
- Intestinal preparation,
- Insufflation,
- Receiving images,
- Image processing and interpretation.

CT colonography indications are patients over 50, positive fecal occult blood test (FOBT), anemia of unknown origin, constipation for more than 72 hours, and others; it is especially the method of choice, in cases of contraindications to optical colonoscopy, the patient's fear or refusal of it, during unsuccessful or incomplete optical colonoscopy, for studying the prestenotic part of the large intestine inaccessible to optical colonoscopy, for patients with a history of allergic reactions associated to optical colonoscopy (for example, to sedatives and analgetics), cardiovascular system pathologies and diverticulitis (due to the risk of intestinal perforation).

Bowel preparation involves following a specific diet, taking laxatives, and contrast for marking fecal masses. A part of the researchers believe that adherence to the diet does not have a significant impact on bowel preparation and that the reduction of the dose of laxatives does not reduce the informativeness of the research due to the contrast marking of fecal masses and the use of the digital erasure function; According to their data, the use of the mentioned method together with the optimal efficiency of bowel preparation significantly reduces the discomfort of patients concerning CT colonography [14,17,18]. Despite the above, since we did not have any previous experience using CT colonography in our clinic, we gave priority to the more common method of bowel preparation, although we provided information to the patients about the simplified methods of bowel preparation and gave them a choice. It should be noted that the vast majority of patients chose the classical method of preparation due to the higher probability of obtaining higher-quality CT images.

According to the more common method of preparation of the bowel, patients refrained from eating vegetable food for 2-3 days before the examination; the day before the study, only liquid foods were allowed, for example, filtered meat broth, clear fruit juice without pulp, jelly and only until 13:00.

As a laxative, we used Fortrans (polyethylglycogen), which, along with the complete cleaning of the intestinal lumen, provides its optimal expansion at the expense of reducing the release of electrolytes. It is taken the day before the examination between 15:00 and 19:00 with the following dose: 1 package for every 15-20 kg of body weight dissolved in 1 liter of water. The patient takes the solution by sipping it gradually for 1 hour.

We used Omnipack (350 mg iodine/ml) for fecal mass contrast marking, 50 ml of which was diluted by the patient in 250 ml of cold water, and the resulting 300 ml aqueous solution was taken gradually per os the day before the examination between 21:00 and 22:00.

Before the study, we filled the colon with gas, for which we mostly used atmospheric air, rarely carbon dioxide or their mixture. Air was injected manually or with an insufflator, as well as by a mixed method. 30-45 minutes before insufflation, to relieve/prevent colon spasm, patients took 80 mg (two pills) of NO-SPA (Drotaverine) with 0.5 L of water, and another 0.5 L of water immediately before the start of the scan (water should be taken to better visualize the stomach and loops of the small intestine).

Out of 352 examined patients, in 332 cases - the colon was insufflated using atmospheric air manually, in 5 cases - with a $CO_2$ insufflator, and in 15 cases - using a mixed method.

Adequate distension of the colon, as well as proper bowel cleansing, is critical to the technical success of the examination, although patient safety, as well as comfort, must be considered. Because of this, in cases with patients with diverticular disease, we inflated the colon using a carbon dioxide insufflator. Continuous delivery of $CO_2$ at low pressure reduces colonic spasms, especially in segments with diverticula. Meanwhile, rapid resorption of carbon dioxide in the colonic wall results in improved comfort levels post-procedure.

For the manual method, we inflated the intestine with atmospheric air. We used relatively small flexible rectal balloon catheters and syringes with catheter tips. After inserting the rectal probe, the air was administered using a syringe; The amount of insufflated air was controlled by the patient and the medical staff (radiologist or CT operator) until the maximal tolerable limit was reached; Between insufflations, the air was blocked using a clamp. At the same time, the degree of colon distension was evaluated and controlled by CT scout images before the examination. In case of inadequate insufflation of the intestine, we performed additional air administration in agreement with the patient. With the protocol used at our institution, inadequate segmental dilation occurred in less than 1% of cases.

CT scans were performed using a pitch of 1.25 mm and slice thickness of 1.25 mm. Rotation time was set at 1.0 s, table movement speed at 27.50 mm/s, and X-ray tube potential at 100-120 kVp. Patients were scanned in both supine and prone positions in the craniocaudal direction. To obtain optimal image quality for the assessment of abdominal organs, in the supine position, scanning was performed at 120 mA, and for scanning in the prone position, 80 mA was used to reduce dose exposure; If there was a suspicion of, for example, liver metastases, we resorted to contrast enhancement, for which we used 100-130 ml of Omnipack (350 mg iodine/ml), which was injected intravenously with a delay of 60 seconds at 3.5-4.0 ml/s, during the examination with the patient supine. Before the scan, patients were instructed to take a deep breath and hold it; If they were incapable of holding their breath, they were advised to exhale slowly throughout the examination. At the end of each examination, the effective radiation dose was calculated.

Correct radiation dose management is imperative when performing CT colonography for colorectal cancer screening, as the examination may be repeated several times during an individual's lifetime. Therefore, there must be a balance between the overall benefit of screening and any theoretical risk of radiation exposure. Also, the balance between radiation dose and image quality must be maintained during the examination. Adequate preparation of patients for CT colonography and their proper positioning during the examination ensures the avoidance of repeated scans, therefore, additional radiation exposure. Currently available techniques for reducing the radiation dose during the scan include reducing the current force or voltage, automatic current modulation, and iterative reconstruction techniques.

Scans were processed and evaluated with GE AW Volume share 5 Colon VCAR EC software. Using the program Colon VCAR, parameters of the study window were automatically determined, 2D and 3D images were obtained, 120 and 360-degree panoramic images and endoluminal 3D models were formed. In case of insufficient insufflation of the large intestine, the automatic construction of the endoluminal 3D model is not possible and instead, the so-called "empty" or "blind" areas are obtained; In these cases, we formed the endoluminal 3D model manually.

We start the interpretation of the study with the 3D aerogram: we evaluated the shape, location, contours, haustration, and width of the lumen along the entire length of the colon. At this stage, we can identify anatomical variants and anomalies, diverticulum, signs of chronic inflammation, stenosis, and ileocecal (Bauhin's) valve incompetence (Fig. 2.2.2).

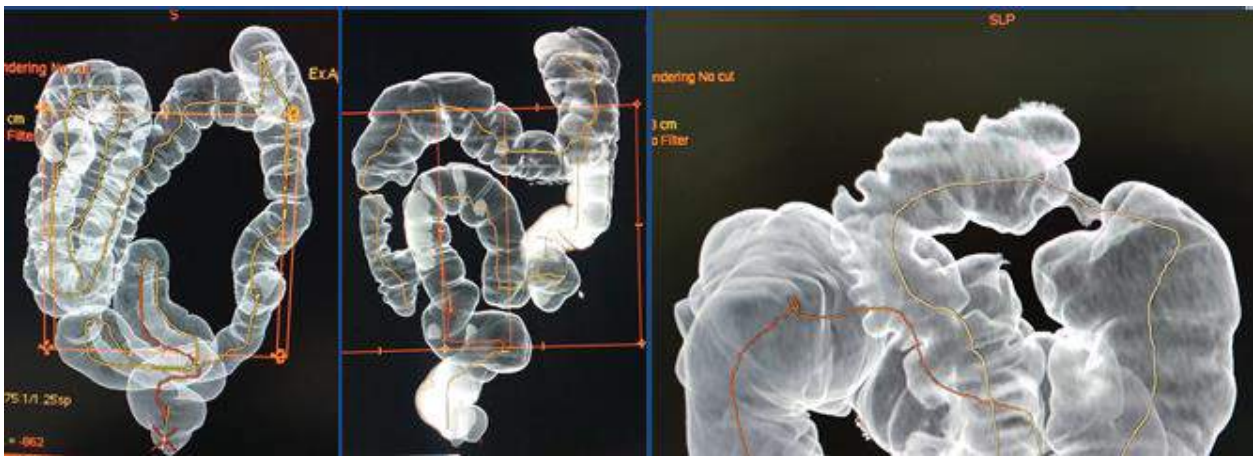

**Figure 2.2.2. CT colonography: 3D aerogram (dolichocolon, exophytic cancer, endophytic cancer)**

In the next stage, the lumen of the intestine was examined in the endoscopic window mode in the direction of the ednoluminal model, which is created either automatically or manually. The inner surface of the intestine and the nature of the folds were evaluated in order to identify lesions, stenosis, and diverticula (Fig. 2.2.3).

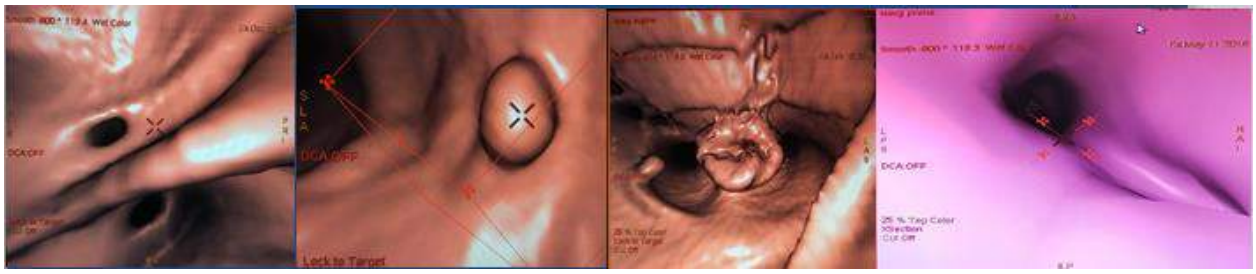

**Figure 2.2.3. CT Colonography: endoscopic window (diverticulosis, polyp, exophytic cancer, and polyp, stenosis-endophytic cancer)**

Through the virtual biopsy program, in the endoscopic window mode, it is possible to conduct differential diagnoses between different types of lesions, for example, polyps and cancer. Using the virtual biopsy (digital mapping) feature, it is possible to map the internal architecture of a polypoid lesion. Thus we can quickly and efficiently distinguish suspicious soft tissue lesions from false polyps, reducing the overall time of interpretation by reducing the number of 2D correlations required (Fig. 2.2.4).

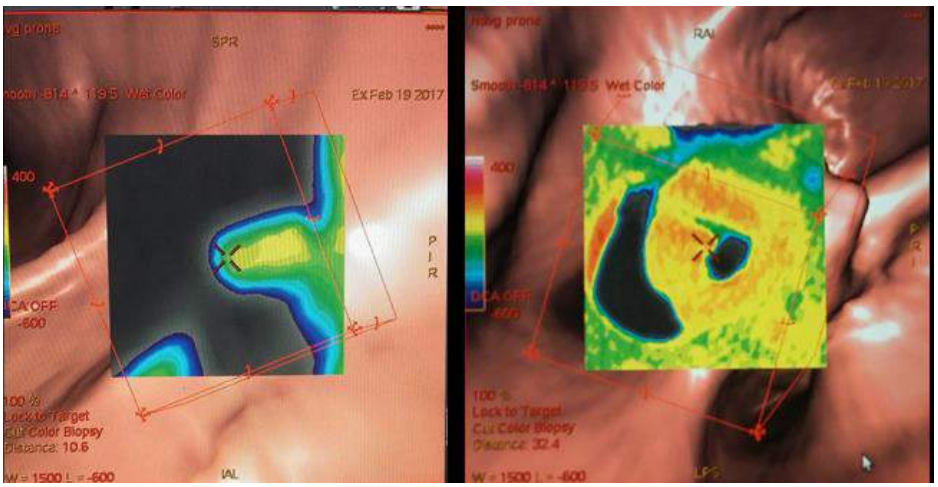

**Figure 2.2.4. CT Colonography: virtual biopsy (polyp, exophytic cancer)**

Virtual dissection mode is an innovative method in which a three-dimensional (3D) model of the large intestine is virtually opened, dissected, and displayed as a three-dimensional planar image of the mucosal surface, similar to a macroscopic pathoanatomical specimen. Evaluation of the plane image of the inner surface of the intestine obtained at this time facilitates the detection and assessment of diverticula, polyps, cancer, and other lesions, chiefly through digital labeling. Using this method, the 3D image of the colon is evaluated faster than it is possible with the endoscopic window mode, which in itself reduces the time of evaluation of the study; In addition, it is possible to increase the accuracy of the examination by minimizing the amount of the "blind zones" that accompany the endoscopic window mode (Fig. 2.2.5).

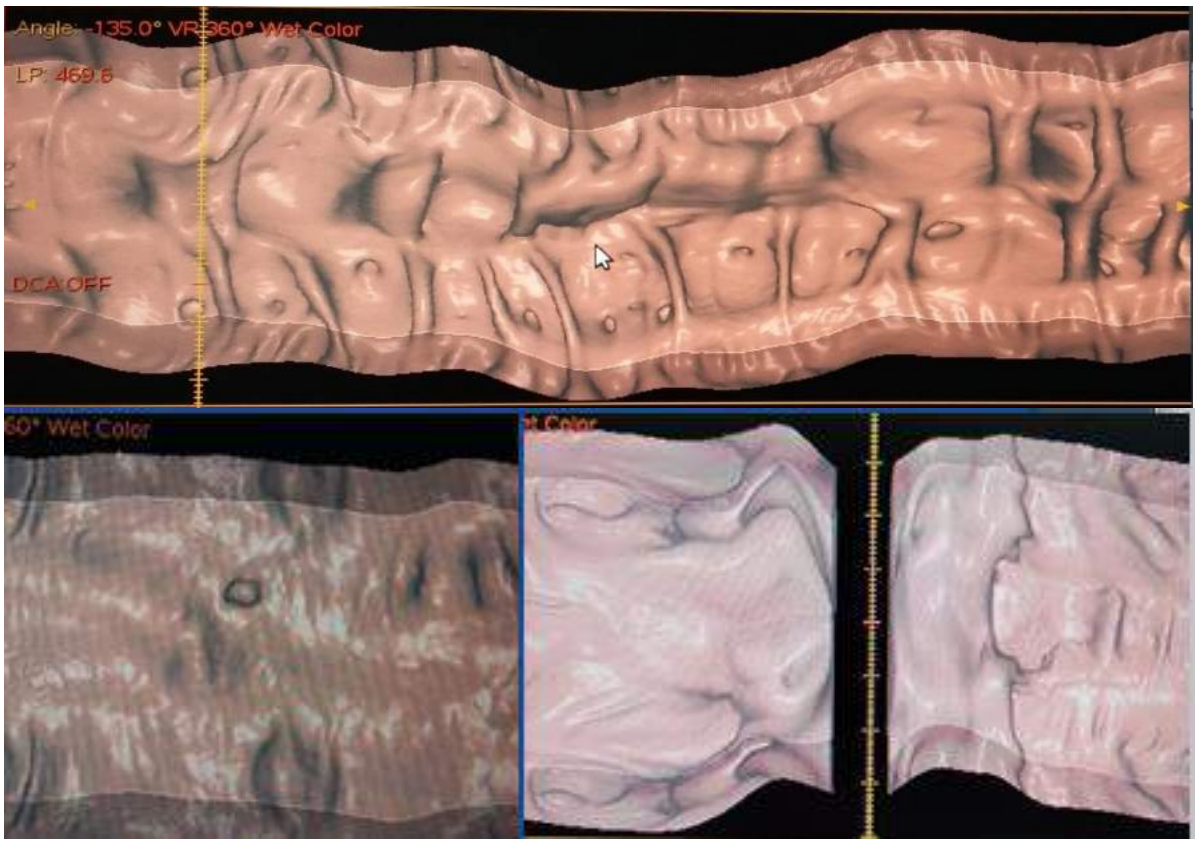


**Figure 2.2.5. CT Colonography: virtual dissection (diverticulosis, polyp, stenosis-endophytic cancer)**

Using the digital marking function, even small lesions of 2-4 mm in size, such as polyps, can be easily detected (Fig. 2.2.6).

**Figure 2.2.6.CT Colonography: digital marking (polyp, polyposis)**

Axial slices were used to assess the thickness of the intestinal wall, the degree of tumor invasion, the condition of the surrounding tissues and lymph nodes, and other abdominal organs (Fig. 2.2.7).

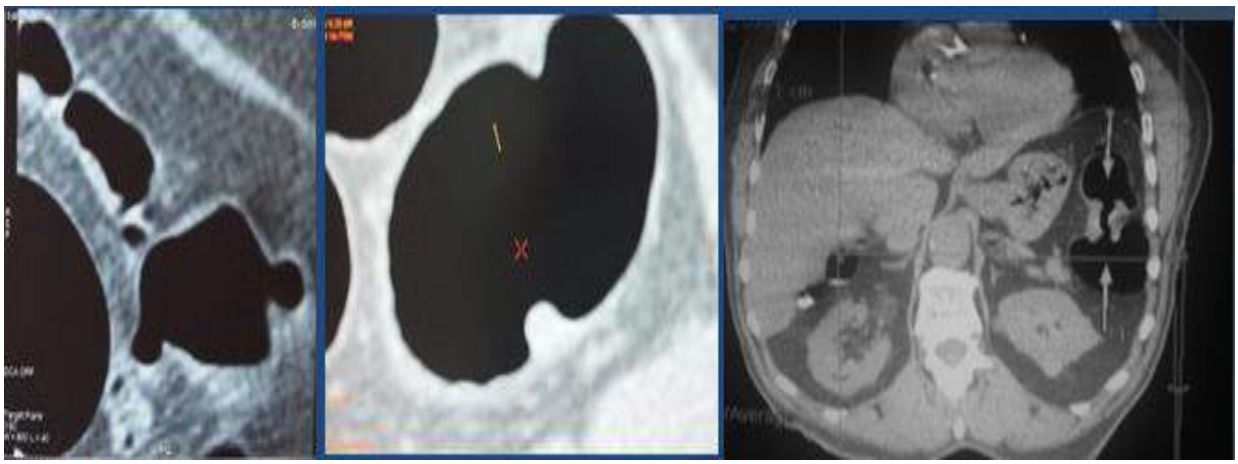

**Figure 2.2.7. Axial slices: diverticulosis, polyp, endophytic cancer**

By administering per os contrast agent and using the "digital cleaning" function of the image, it's much easier to differentiate small polyps from other types of lesions or fecal matter. (Fig. 2.2.8).

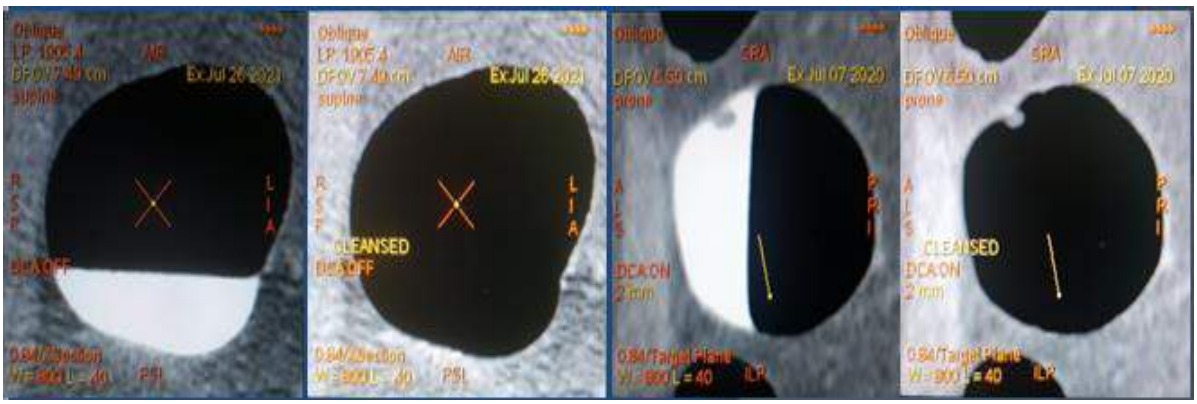


**Figure 2.2.8. CT Colonography: "digital cleaning" (norm, polyp).**

Along with many positive features, CT colonography also has some disadvantages, which, along with radiation exposure and an uncomfortable attitude towards the process of colon preparation for a large number of patients, can manifest in difficulty and sometimes impossibility of interpreting the study, which can be the result of both improper preparation of the intestine and inadequate inflation and/or collapse of its segments.

Unfortunately, cases of inadequate inflation and/or collapse of the intestine are most often found in the segments characterized by a high incidence of colorectal cancer - the rectum and sigmoid colon; Diverticular disease is also common in the sigmoid colon. Both pathologies are difficult to diagnose by CT colonography under the mentioned conditions, which makes it necessary to solve or reduce the problem created by inadequate bowel inflation, which we did by maximum air insufflation up to the limit tolerated by the patient, which was immediately followed by scanning. In this way, it was possible to obtain an image during the peak distension of the colon.

We overcome the complication of colonic evaluation by residual stool and fluid by comparing supine and abdominal images, per os contrast labeling of fecal masses, digital sweep, and digital mapping (virtual biopsy) functions (Fig. 2.2.9).


**Figure 2.2.9. inadequately insufflated sigmoid colon with fecal masses**

The vast majority of potential pitfalls in the assessment of the study can be adequately addressed if the technical requirements for performing a CT scan, including patient preparation, colonic insufflation, and scanning protocol, are handled appropriately.

Most of the patients from the main study underwent colonoscopy, as it is the "gold standard" for colonic examination. An optical colonoscopy was performed in the endoscopy department using Olympus Evis XI CV-1500. Colonoscopy and post-surgical data were used as reference methods. If necessary, a biopsy or removal of a bulky mass was performed, followed by a histological examination. Statistical data processing was carried out using the Microsoft Office Excel software package, mathematical support – SPSS.26 software package, and statistical analysis - standard methods of variational statistics; The reliability of the obtained numerical data was evaluated using Student's *t*-test. Data were considered statistically significant at $p<0.05$. The indicators of sensitivity, specificity, and diagnostic accuracy of the CT colonography method in detecting colon lesions were determined; Optical colonoscopy and results of surgical procedures were determined as reference methods.

RESULTS

Out of a total of 352 examined patients, 34(9.7%) were assigned a study after incomplete colonoscopy, 57(16.2%) - because of colonoscopy refusal, 3(0.9%) - due to colonoscopy contraindications, 230(65, 3%) - with clinical indications, 28 (7.9%) - for preventive purposes (diagram 2.1.1).

The age of the patients ranged from 17 to 91 years (average age - 56 years); 155(44%) of them were men, and 197(56%) were women (diagram 2.1.2).

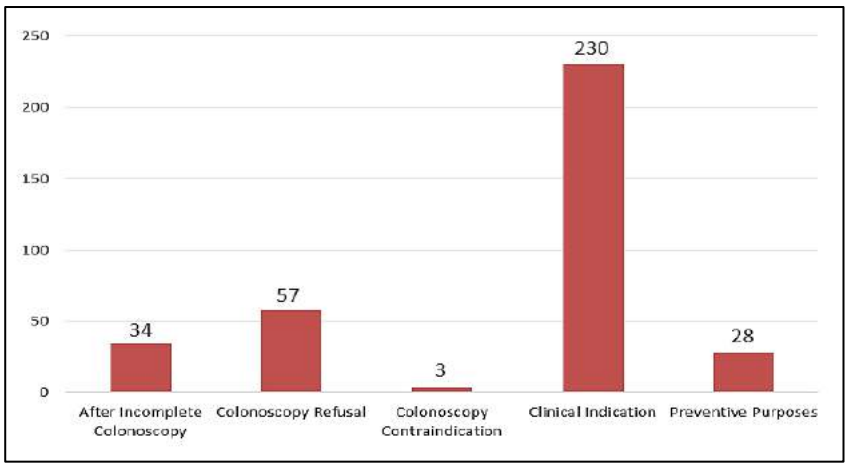


**Diagram 2.1.1. Distribution of patients according to the indication of CT colonography.**

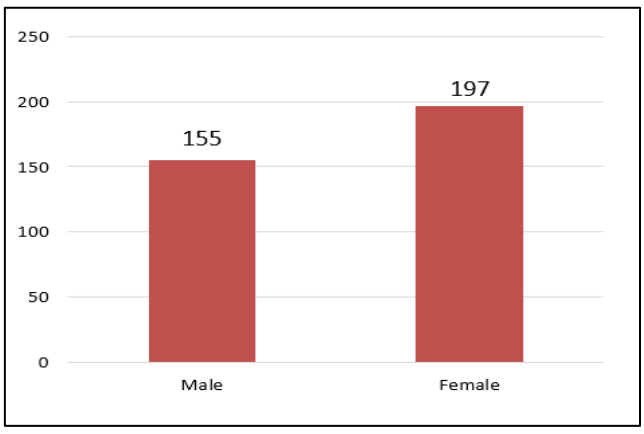


**Diagram 2.1.2. Distribution of patients by gender.**

Studying the CT colonographic research data of 352 patients, 258(73.3%) were diagnosed with dolichocolon, 24(6.8%) - only dolichotransversophtosis, 40(11.4%) - only dolichosigma, 15(4, 3%) - cecal malrotation, 1(0.3%) - megacolon. 21(6.0%) patients were found to have diverticula, 81(23.0%) - diverticulosis. A single polyp was detected in 32 (9.1%) cases and polyposis in 7 (2.0%) cases. 14 (4.0%) patients were diagnosed with colorectal cancer (diagram 2.1.3). 21 patients underwent different types of colon surgery (diagram 2.1.4).

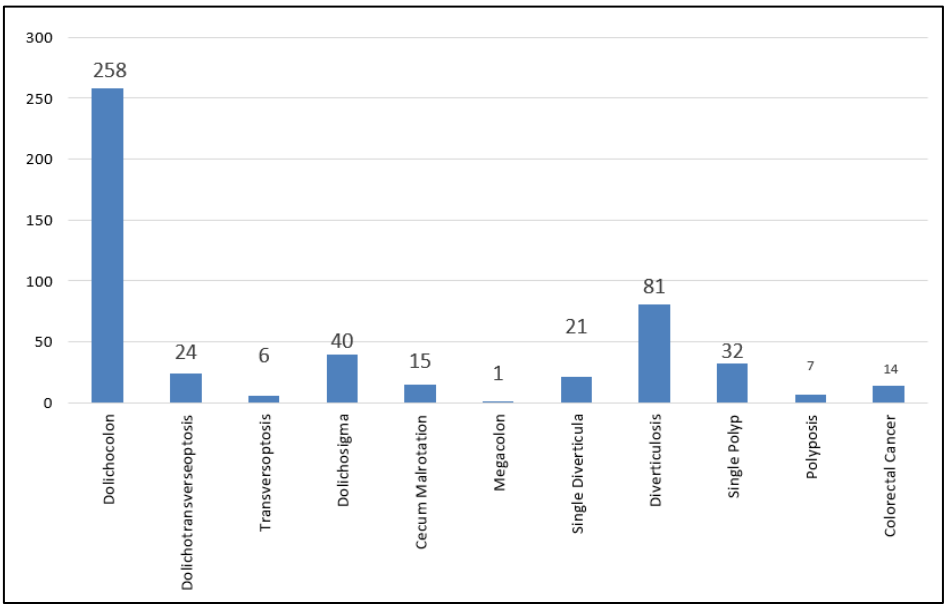


**Diagram 2.1.3. Distribution of patients according to pathologies detected by CT colonography**

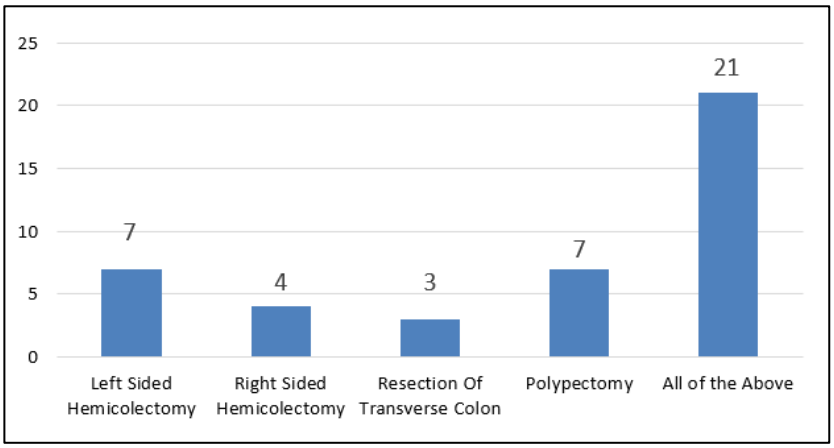


**Diagram 2.1.4. Types of surgery performed**

In addition to intestinal pathologies, extracolonic lesions were detected: 2 (0.6%) patients had peripheral lung cancer, - 1 (0.3%) sarcoidosis, - 182 (51.7%) hiatal hernia, 182 (51.7%) stomach cancer, - 2(0.6%), hepatosis - 115(32.7%), liver cyst - 17(4.8%), hepatocellular cancer - 1(0.3%), liver metastases - 5 (1.4%), gallstones - 22 (6.3%), spleen cyst - 2 (0.6%), adrenal gland adenoma - 5 (1.4%) ), single and multiple kidney cysts - 72(20.5%), urolithiasis - 29(8.2%), uterine myoma - 9(2.6%), ovarian cyst - 5(1.4%), spinal hemangioma - 12(3.4%), spinal metastasis - 1(0.3%).

By studying the data of the patients examined by us and through statistical processing, we obtained the following results: sensitivity of CT colonography in diagnosing congenital anomalies of the large intestine is 98.0%, specificity - 100%, diagnostic accuracy - 98.2%; in diagnosing of diverticula, respectively: 92.3%, 95.1%, 92.7%; for polyps: 87.3%, 85.6%, 85.9%.

## CONCLUSION

Based on the obtained results, it can be concluded that CT colonography is an accurate, highly informative, and less invasive method of colon examination; Colorectal cancer screening performed with it is less invasive, less time-consuming, and as effective as optical colonoscopy; One of the main advantages of CT colonography is the ability to detect non-intestinal pathologies. Improving the technical parameters of CT colonography will allow us to reduce radiation exposure levels of patients while maintaining image quality.

## REFERENCES

[1]. International Agency for Research on Cancer 2023. Data source: GLOBOCAN 2020. Graph production: Global Cancer Observatory.
[2]. Abraham H. Dachman, Andrea Laghi (Editors). (2011). Atlas of Virtual Colonoscopy//second Edition, Springer LLC, 307; DOI: 10.1007/978-1-4419-5852-5.
[3]. Perry J. Pickhardt. (2013). Computed tomography colonography: emerging evidence to further support clinical effectiveness// Curr Opin Gastroenterol. 29(1):55-59. doi: 10.1097/MOG.0b013e32835a3480. PMID: 23044493; PMCID: PMC4031457.
[4]. Brooks D. Cash, Mark S. Riddle, Ishan Bhattacharya, Duncan Barlow, Donald Jensen, Nicolas Moya del Pino, Perry J. Pickhardt. (2012). CT Colonography of a Medicare-Aged Population: Outcomes Observed in an Analysis of More Than 1400 Patients// American Journal of Roentgenology. 199: W27-W34. DOI:10.2214/AJR.11.7729.
[5]. Bruce Pyenson, Perry J. Pickhardt, Tia Goss Sawhney, Michele Berrios. (2015). Medicare cost of colorectal cancer screening: CT colonography vs. optical colonoscopy// Abdom Imaging. 40:2966–2976.
[6]. Cash BD, Pickhardt PJ. (2015). Defining the Risk of Small Polyps: Potential Value of CTC. // Am J Gastroenterol. 110(12):1691-3.
[7]. Cristiano Spada, Jaap Stoker, Onofre Alarcon, Federico Barbaro, Davide Bellini, Michael Bretthauer, Margriet C. De Haan, Jean-Marc Dumonceau, Monika Ferlitsch, Steve Halligan, Emma Helbren, Mikael Hellstrom, Ernst J. Kuipers, Philippe Lefere, Thomas Mang, Emanuele Neri, Lucio Petruzziello, Andrew Plumb, Daniele Regge, Stuart A. Taylor, Cesare Hassan, Andrea Laghi. Clinical indications for computed tomographic colonography: European Society of Gastrointestinal Endoscopy (ESGE) and European Society of Gastrointestinal and Abdominal Radiology (ESGAR) Guideline// Published online: 30.9.2014. Endoscopy 2014; 46: 897–908;
[8]. Fletcher, J., Luboldt, W. (2000). CT colonography and MR colonography: current status, research directions and comparison. Eur Radiol 10, 786–801.
[9]. Scardapane, A., Bettocchi, S., Lorusso, F. et al. (2011). Diagnosis of colorectal endometriosis: contribution of contrast-enhanced MR-colonography. Eur Radiol 21, 1553–1563.
[10]. Andrea Laghi, Emanuele Neri, Daniele Regge. (2015). Editorial on the European Society of Gastrointestinal Endoscopy (ESGE) and European Society of Gastrointestinal and Abdominal Radiology (ESGAR) guideline on clinical indications for CT colonography in the colorectal cancer diagnosis. // Radiol med 120:1021–1023. DOI 10.1007/s11547-015-0537-x
[11]. Jeff L. Fidler, Zheng Zhang, Benjamin A. Herman, Paul J. Limburg, J. G. Fletcher, Abraham Dachman, Jay P. Heiken, Mark D. Kuo, Christine O. Menias, Bettina Siewert, Jugesh I. Cheema, Richard G. Obregon, Peter Zimmerman, Karen M. Horton, Kevin Coakley, Revathy B. Iyer, Amy Hara, Robert A. Halvorsen, Giovanna Casola, Judy Yee, Lawrence J. Burgart, C. Daniel Johnson.

(2014). CT Colonography for the Detection of Nonpolypoid Adenomas: Sensitivity Assessed with Restricted National CT Colonography Trial Criteria. American Journal of Roentgenology. 203: W614-W622.
[12]. Mang T, et al. (2007). CT colonography: techniques, indications, findings// Eur J Radiol; 61(3):388–399.
[13]. Perry J. Pickhardt, Ifeanyi Mbah, B. Dustin Pooler, Oliver T. Chen, J. Louis Hinshaw, Jennifer M. Weiss, and David H. Kim. (2017). CT Colonographic Screening of Patients With a Family History of Colorectal Cancer: Comparison With Adults at Average Risk and Implications for Guidelines// American Journal of Roentgenology, 208:4, 794-800, DOI: 10.2214/ajr.16.16724.
[14]. Iafrate, F., Iannitti, M., Ciolina, M. *et al.* (2015) Bowel cleansing before CT colonography: comparison between two minimal-preparation regimens. *Eur Radiol* 25, 203–210.
[15]. Perry J. Pickhardt, Cesare Hassan, Steve Halligan, and Riccardo Marmo. (2011). Colorectal Cancer: CT Colonography and Colonoscopy for Detection—Systematic Review and Meta-Analysis. Radiology 259:2, 393-405.
[16]. Knudsen AB, Zauber AG, Rutter CM, et al. (2016). Estimation of Benefits, Burden, and Harms of Colorectal Cancer Screening Strategies: Modeling Study for the US Preventive Services Task Force. *JAMA.*;315(23):2595–2609. doi:10.1001/jama.2016.6828.
[17]. Bellini, D., De Santis, D., Caruso, D. *et al.* (2018) Bowel preparation in CT colonography: Is diet restriction necessary? A randomised trial (DIETSAN). *Eur Radiol* 28, 382–389.
[18]. Utano K, Takayanagi D, Nagata K, Aizawa M, Endo S, Nemoto T, Nemoto D, Isohata N, Lefor AK, Togashi K. (2019). A novel volume-reduced CT colonography regimen using hypertonic laxative (polyethylene glycol with ascorbic acid): randomized controlled trial. Eur Radiol. 2019 Oct;29(10):5236-5246. doi: 10.1007/s00330-019-06127-6. Epub 2019 Mar 22. PMID: 30903329.

# Requirements for Authors

- The article should be submitted to the A4 format in the text editor Microsoft Office Word;
- Areas: upper - 20 mm; Left - 30 mm; Right -20 mm; Bottom - 20 mm
- Font: Times New Roman. Interval -1,0
- In the article formulas must be typed in the formulas editor Equation
- Drawings and illustrative materials should be inserted in the JPEG or TIFF format
- Write the article title (14 Pt, Bold) on the first line
- Bypassing the line - the surname and first name of the author(s) (11 Pt, Bold)
- One of the authors will need to be identified as the corresponding author (*), with their full name and email address displayed.
- Full name of the organization on the next line, with indicating the country or residence (11 Pt, Bold, in case of participation of different organizations in the article should be used „1“)
- Skipping of two lines - abstract (11 Pt, Italics, not more than 500 words)
- Maximum 5 Key words (11Pt)
- Contents of the article (11Pt) by skipping the line
- Bypassing two lines – references (10 Pt). Used literature should be numbered according the sequence it is used in the main text (when citing inside the text, the number of the source should be written in square brackets). Use the following example while creating the reference list:

  [1] Author(s') surname(s) and initial(s). (Year of publication). Article name. *Journal in which the article is published, issue,* pages.

  [1] Derwing, T. M., Rossiter, M. J., & Munro, M. J. (2002). Teaching native speakers to listen to foreign-accented speech. *Journal of Multilingual and Multicultural Development*, *23*(4), 245-259.

- Electronic version of the article must be sent to the e-mail: radiobiologia2020@gmail.com
- The file must be named by the last name of the author

*The editorial board is responsible for the topics of the materials submitted for publication in the journal, and the authors' responsibility relies on the content of the article, the results and conclusions. The publisher is not responsible for possible damages, which could be a result of content derived from this publication and any liabilities arising from them remain the responsibility of the authors. Articles incompatible with the above-mentioned requirements or incompatible with the theme of the article are not considered for publication. Materials are published by the author's editorship.*

**Editorial office:** 14 Levan Gotua St, Rooms-913; 931, Tbilisi, Georgia, 0160

**Tel:** (+995) 032 237-03-00/911, **E-mail:** radiobiologia2020@gmail.com

**Website:**https://radiobiology.ge